UNIVERSITÀ
DEGLI STUDI
DI PADOVA

UNIVERSITA' DEGLI STUDI DI PADOVA

Dipartimento di Ingegneria Industriale DII

Corso di Laurea Magistrale in Ingegneria dell'Energia Elettrica

Digital Twin technology for induction motor drives

Relatore: Silverio Bolognani
Correlatore: Francesco Toso

Laureando: Flavio Stocco
1184670

Anno Accademico 2019/2020

In questo elaborato si sono valutati i possibili vantaggi nell'adottare il Digital Twin di un motore asincrono per migliorarne le dinamiche di controllo, confrontando i diversi risultati ottenuti tramite delle simulazioni realizzate con il software Matlab/Simulink.

Come suggerisce la traduzione dall'inglese "Gemello Digitale", vuole essere un sistema in grado di rappresentare il più fedelmente possibile tutte le dinamiche elettromeccaniche e termiche che ne caratterizzano il funzionamento. A differenza dei modelli FEM, in cui è necessario attendere un certo tempo prima di poter osservarne i risultati, il Digital Twin è in grado di valutare le stesse dinamiche in real-time senza alcuna perdita di precisione grazie alla tecnica di Model Order Reduction (MOR).

Nella prima parte sarà presentata una panoramica sulle possibili applicazioni del Digital Twin e sul concetto su cui si basa. Inoltre, per comprendere appieno dinamiche e risultati delle simulazioni, è presente un capitolo in cui si introducono le principali caratteristiche di un motore asincrono (induction motor) e delle relative tecniche di controllo.

Nella seconda parte sarà mostrato nel dettaglio lo schema del modello Simulink e la logica che ne descrive il suo funzionamento. Inoltre, saranno presentati obiettivi e organizzazione delle diverse simulazioni che saranno svolte successivamente.

Nelle conclusioni si valuteranno i vantaggi portati dall'adozione del Digital Twin e quale sia la strategia più conveniente per ottimizzare un azionamento di un motore asincrono secondo il metodo del Field Oriented Control (FOC).

In this paper an evaluation of the possible advantages of adopting the Digital Twin of an asynchronous motor (Induction Motor) in order to improve the control dynamics is made, comparing the different results obtained through simulations made with Matlab/Simulink software.

As the meaning of the words "Digital Twin" suggests, it is meant to be a system able to represent as faithfully as possible all the electromechanical and thermal dynamics that characterize its operation. Unlike FEM models, in which it is necessary to wait a certain amount of time before being able to observe the results, the Digital Twin is able to evaluate the same dynamics in real-time without any loss of precision, thanks to the Model Order Reduction (MOR) technique.

In the first part of the paper, an overview of the possible applications of the Digital Twin and the concept on which it is based are presented. Furthermore, in order to fully understand the dynamics and simulation results, there is a chapter in which the main features of an induction motor (IM) and its control techniques are introduced.

In the second part, the scheme of the Simulink model and the logic that describes its operation is shown in detail. Moreover, the objectives and the organization of the different simulations carried out later are presented too.

The conclusions will evaluate the advantages brought by the adoption of Digital Twin and which is the most convenient strategy to optimize an asynchronous motor drive according to the Field Oriented Control (FOC) method.

INDEX

Introduction

A Digital Twin can be easily compared to a virtual copy of a physical setup in which it responds in the same way after being given the same input of the real object; moreover, it responds in real-time or even faster, allowing to develop prediction architectures.

Digital Twining either an entire system or just a part of it, is not at all a revolutionary procedure just discovered or recently invented. For example, in the weather forecasting they utilize solid models of a region, high fidelity physics simulators and big data coming from multiple sources in order to provide both long and short weather predictions, that are communicated using a detailed rendering of the numerical results. But which are the advantages of using Digital Twin technology instead of other simulation softwares? As usually, there is not just one best solution, but it is necessary to focus on the singular different requirement.

Speaking about electric motor development, it is necessary to know in the details every behaviour and dynamic to better understand how to improve its functionality, but this requires a lot of computationally power and calculation time due to the high resolution of the results. In addition to the motor, it is equally important to develop an electric drive that can adapt its behaviour in the real different motor conditions.

In industrial applications, the electric drive is usually described by constants or by a table of pre-calculated parameters trend, trying to follow the real motor behaviour without an appropriate feedback interaction.

Thanks to the Digital Twin it is possible to evaluate the estimation of the parameters with high precision only by knowing the instantaneous currents and following the real electromechanical and thermal behaviours. In this way, the control is continuously updated with the newest motor's values, allowing to get a very reliable drive.

Another advantage of the Digital Twin technology is a bigger capability and adaptivity to perform very different kinds of work depending on the purpose for which it is designed. For example, under certain conditions, it is possible to develop a prediction of the future system trend, or to improve its behaviour by analysing the data collected by sensors or by previous simulations.

1

Digital Twin

Digital Twin can be defined as a virtual representation of a physical asset enabled through data and simulators for a real-time prediction, optimization, controlling and improved decision making. Indeed, it plays a transformative role not only in how we design and operate cyber-physical intelligent systems, but also in how we advance the modularity of multi-disciplinary systems to tackle the behaviours of ecosystems.

1.1 Digital Twin meaning and uses

Digital twin wants to be the representation of real objects with their data, functions, and behaviours in the digital word. This can help to improve not only the engineering of the singular subject, but also the whole ecosystem. For example, improving the fault detection or the loop control that often use constant or estimated values to calculate the new input control signal. Speaking about Industry 4.0, Digital Twin is the key for the future of the industrial development thanks to its reliability. With a large availability and quality of the data, it is possible to implement lots of function to improve and upgrade the different ecosystem, like Machine Learning, Data Analytics, Internet of things and functional mock-up interface. But which is the difference between a classic simulation software and the new approach with a digital twin? The most widespread software use FEM (Finite Element Method) to find all the values that describes the simulated system, but that requires a lot of time and computational power due to the high number of values. Instead, with a digital twin it is possible to evaluate all the different dynamics that describes the function of the subject in real-time or even faster. In this way it is possible to predict how the system should response before the real system, helping, for example, to improve precision and safety.
Digital twin can be applied for infinite application, but there are two main ways: it could be put beside the real object/system for monitoring and controlling all the dynamics by a digital

representation, or to replace it during the engineering of the entire ecosystem to better focus on the real behaviours. In this way it is easier to realize a real time evaluation of its conditions, especially to improve performance and safety by the estimation of the system trend and not only reading sensor data. In fact, sensors may not be enough for a correct evaluation of the true trend of the system due to maintain the price as lower is possible, or worse could be affected by disturbance conditions. Unfortunately, in the real world is not always possible realize the best solution because of the cost, that could become unsustainable. And always due to a price issue, the correct compromised may not be enough cheaper. In fact, approximations are often used to eliminate sensor's cost defining an easier control scheme. For a first overview of the Digital Twin world, it is useful take a look to a report from Oracle [5]. It presents eight possible applications of the digital twin concept:

1) *Real-time remote monitoring and control*: generally, it is almost impossible to gain a view of a very large system physically in real-time. The performance of the system can not only be monitored, but also controlled remotely using feedback mechanism.

2) *Greater efficiency and safety*: it is envisioned that digital twinning will enable greater autonomy with humans on the loop as and when required. This will ensure that the dangerous, boring and dirty jobs are allocated to robots with humans controlling them remotely.

3) *Predictive maintenance and scheduling*: a comprehensive digital twinning will ensure that multiple sensors monitoring the physical assets will be generating big data in real-time. Through a smart analysis of data, faults in the system can be detected much in advance. This will enable better scheduling of maintenance.

4) *Scenario and risk assessment*: a digital twin, or to be more precise a digital sibling of the system, will enable what-if analyses resulting in better risk assessment. It is will possible to perturb the system to synthesize unexpected scenario and study the response of the system as well as the mitigation strategies. This kind of analysis without jeopardizing the real asset is only possible via a digital twin.

5) *Better intra- and inter- synergy and collaborations*: with greater autonomy and all the information at the fingertip, teams can better utilize their time in improving synergies and collaborations leading to greater productivity.

6) *More efficient and informed decision support system*: availability of quantitative data and advanced analytics in real-time will assist in more informed and faster decision makings.

7) *Personalization of products and services*: with detailed historical requirements, preferences of various stakeholders and evolving market trend and competitors, the demand of customized products and services are bound to increase. A digital twin in the context of factories of the future will enable faster and smoother gear shifts to account for changing needs.

8) *Better documentation and communication*: readily available information in real-time combined with automated reporting will help to keep stakeholders well informed thereby improving transparency.

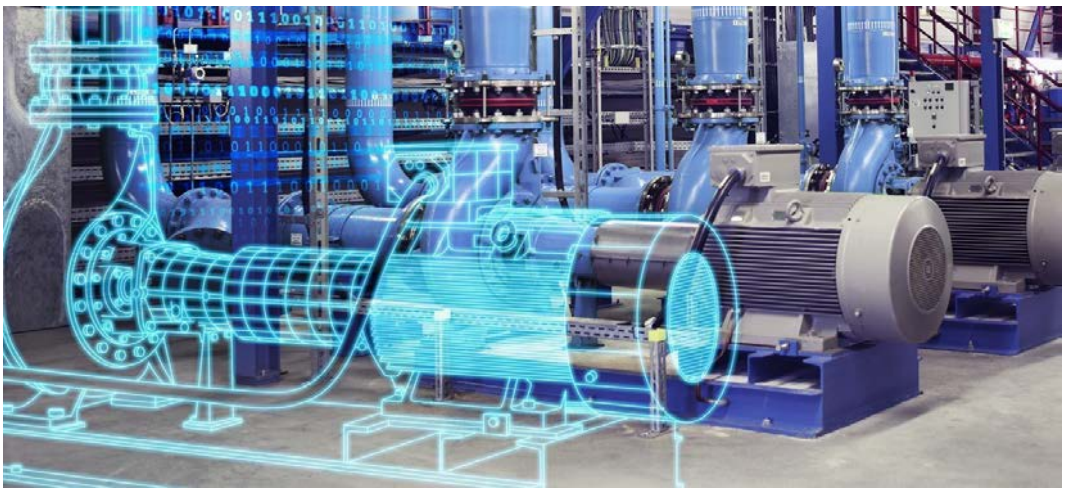

Figure 1.1: A possible graphical interpretation of Digital Twin real-time capability respect to the real physical setup

Generically, a digital twin can be realized starting from a CAD model which shows exactly the real system in all its dynamics, from its simple operations to the most complex behaviours. But a high fidelity and high-resolution model needs time and computational

power to elaborate the input data due to the FEM approach. Thanks to the Model Order Reduction (MOR), it is possible to reduce this model to a simplified and faster responsiveness, getting a real-time system reaction. Looking to the previous Oracle's report, digital twin can be developed to realize an infinite different application to improve the system. For example, according to a study made by Siemens engineers [7], a general framework for setting up a digital twin for monitoring system problematics can be:

- *Modelling*: in most cases comprehensive CAD models are available from the asst design process. These models are an assumption for setting up model-based operation support. If the diagnosis of faults is required, these faults must be included in the model too.

- *Model Order Reduction (MOR)*: the final model must run in parallel to operation and thus must be real time capable. Model order reduction techniques, which preserve important properties of the original model, need to be applied to the original model in order to achieve fast simulation models.

- *Identification*: the simulation results of the fast model must be compared to the sensor data. This allows to the identification of faults or to estimate degradation laws (for example, with machine learning).

- *Prediction of degradation*: if a fault is detected, its development needs to be predicted

- *Model Predictive Control*: based on the system prediction a control of the system performance versus early downtime may be developed.

To understand better the advantages of making the digital twin of an object, it is worth treating a practical case, which will be the main subject of this thesis. Taking an electric motor, it is not always possible insert any sensors everywhere due to the delicate balance of mechanical-electrical synergy, especially if they should be placed in the rotor (or may not be enough space to install them). Because of this, some electrical values are usually estimated, or worse, they are considered constant to their nominal working conditions even

when the electromechanical dynamics change. For example, looking to the main datasheet commercial electric engine, rotor's resistance is often given like a constant, and only rarely it is described with its law of variation with the different temperature or load condition. This disinformation cannot allow a proper control of the motor due to the impossibility of developing a precise electric drive. And this can lead to a loss off efficiency when electric engine works at different condition respect to the nominal terms, likes working with a wrong electromagnetic flux. Or could be really dangerous to the health of the different engine's elements. In particular, if the engine is made with Permanent Magnets (PM), a wrong evaluation of electric drive conditions could make the engine works at high temperature and getting an irreversibility damage due to the demagnetization of the magnets.
Thanks to digital twin it is possible to evaluate any physical value of the engine (temperature, flux, current, friction, vibration, etc.) everywhere and in real-time, developing a faithful electric drive which can fitting exactly with the real engine conditions.
After in this thesis we will study on the details some particular event to evaluate the advantages of using a digital twin on IM electric drives behaviours.

1.2 CAD/CAE model

The first step to develop a digital twin is to realize a 2D/3D model which represents the entire system or a subsystem of it. The CAD (Computer-Aided Design) software wants to realize a 3D model of the object with a high-fidelity representation. Instead, CAE (Computer-Aided Engineering) introduce physic dynamics to the 3D model to help designers and engineers to develop the product. In this way it is easier to evaluate the singular dynamic (like thermal, electrical, mechanic etc.) to improve safety and performance of the system. Given the complexity of the physical realism and the big amount of data, the equations need to be solved numerically on computers by various discretization techniques. The most widespread is FEM (Finite Element Method), a numerical method for solving partial differential equations in two or three space variables. Typically, problem areas of interest include the traditional fields of structural analysis, heat transfer, fluid flow, mass transport and electromagnetic potential. To solve a problem, the FEM subdivides a large system into smaller, simpler parts that are called finite elements. This is achieved by a particular space

discretisation in the space dimensions, which is implemented by the construction of a mesh (like a grid or a web) of the object: the numerical domain for the solution, which has a finite numbers of points. The FEM formulation of a boundary value problem results in a system of algebraic equations. These simple equations that model these finite elements are then assembled into a larger system of equations that models the entire problem. This final system could be extremely large and requires a big amount of computational power and, due to the limitation of high-performance calculator, needs a lot of time to evaluate the system evolution. During a development process, this demanding time could mainly lead to an increase of the cost due to the waiting until the end of the simulation. Around the world, the most widespread FEM software are ANSYS and COMSOL due to their high reliability and versatility.

Instead, for a real-time system monitoring and controlling is required an instantaneous, or even faster, simulation especially for a fault detection control. It is precisely in these conditions where digital twin shows its advantages through using a Reduced Order Model (ROM).

1.3 Model Order Reduction (MOR)

Model Order Reduction (MOR) is the key features to develop a digital twin being the way that allows a real-time process. This because a high-resolution approach cannot be always the best solution to evaluate system dynamics due to the computational requested power and amount of time that it requires. MOR algorithms can compress even huge 3D simulation models in such a way that the resulting reduced order models are small enough for a faster evaluation than real-time. In fact, it may not be necessary to calculate all detail, and nevertheless obtain a good understanding of the phenomena taking place. For example, a way to reduce the high quantities of data that to be evaluated is reducing the complexity of the not fundamental parts, like create a 3D model only for the most important and complex part and use 2D or 1D model for the easier one. This is one of the ways to reduce model complexity before starting calculations by an operational model order reduction to decrease its amount of data that needs to be calculated and managed.

An example of operational model order reduction is the simulation of electromagnetic effects in special situations. As is well known, electromagnetic effects can be fully described by a system of Maxwell equations. Despite the power of current computers and algorithms, solving the Maxwell equations in 3D space and time is still an extremely demanding problem, so that simplifications are being made whenever possible. An assumption that is made quite often is that of quasi-statics, which holds whenever the frequencies playing a role are low to moderate. In this case, simpler models can be used, and techniques for solving these models have been developed. Unfortunately, in many cases, it is not possible to a priori simplify the model describing the behaviour. In such cases, a procedure must be used, in which we rely on the automatic identification of potential simplifications. Designing such algorithms is, in essence, the task of the field of model order reduction.

A commercial FEM software works with a complex 3D model which is decomposed like a mesh of $10^5 – 10^9$ linear equations and/or variables. To get a steady-state and time-dependant system response, such simplification is needed in order to perform simulations within acceptable amount of time and limited storage capacity, but with reliable outcome. In some cases, we would even like to have on-line predictions of the behaviour with acceptable computational speed, in order to be able to perform optimizations of processes and product in real-time. Model Order Reduction tries to quickly capture the essential features of a structure, or rather, this means that in an early stage of the process, the most basic properties of the original model must already be present in the smaller approximation. At a certain moment, the process of reduction is stopped and, in that point, all necessary proprieties of the original model must be captured with sufficient precision.

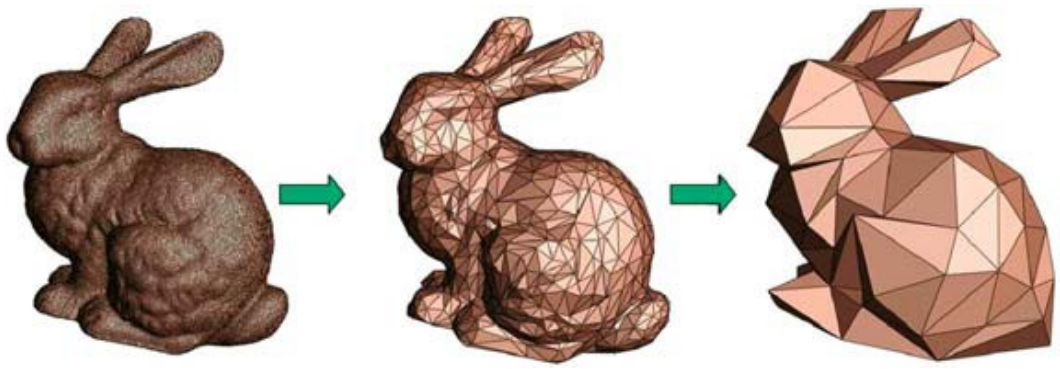

Figure 1.2: Graphical example of model order reduction

The Fig.1.2 illustrates the concept in a graphical easier way, demonstrating that sometimes very little information is needed to describe a model. This example with pictures of the bunny shows that, even with only a few facets, the rabbit can still be recognized. This is only a graphical example to explain which is the logic behind a model order reduction, but it does not want to be in any way the real mathematical approach to operate it.

Historically, the first approximation of a complicated function with a simpler formulation was made by Fourier (1768-1830) in the 1807, when he published the idea to approximate a function with a few trigonometric terms. In linear algebra, the first step in the direction of MOR came from Lanczos (1893-1974) with a way to reduce a matrix in tridiagonal form. In the same years, W.E. Arnoldi realized that a smaller matrix could be a good approximation of the original matrix. Their ideas were already based on the fact that a computer was available to do the computations, but was necessary find a way to do this approximation automatically.

The fundamental methods in the area of Model Order Reduction were published in the eighties and nineties of the past century. In more recent years such research has been done in this area, developing a large variety of methods where some are tailored to a specific application, others are more general.

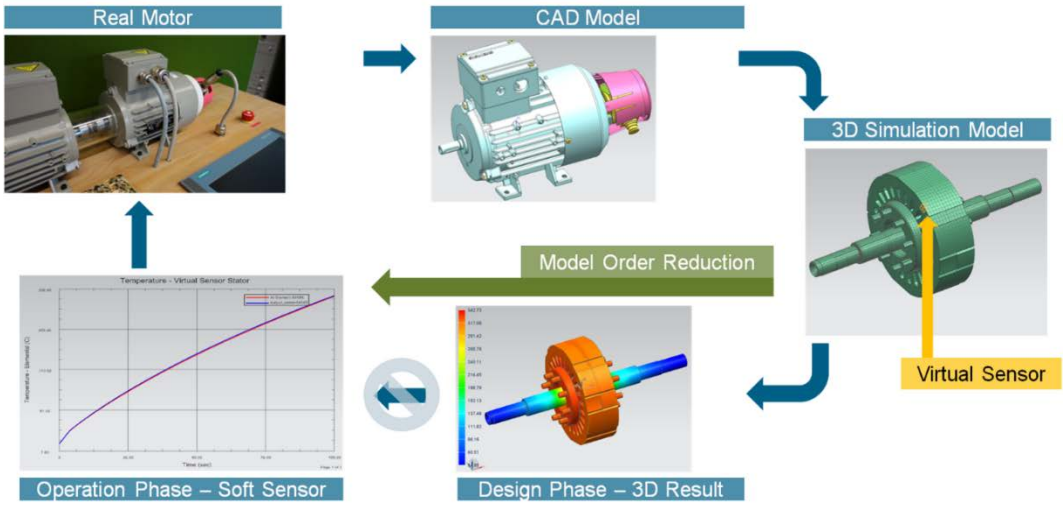

Figure 1.3: Model Order Reduction advantages on closed loop electric motor control drives

1.3.1 Dynamical Systems

To place model reduction in a mathematical context, it is necessary to realize that many models developed in computational science consist of a system of partial and/or ordinary differential equations, supplemented with boundary conditions. When partial differential equations are used to describe the behaviour, one often encounters the situation that the independent variables are space and time. Thus, after discretising in space, a system of Ordinary Differential Equations (ODE) is obtained in time. For example, considering the following explicit finite-dimensional dynamical system:

$$\frac{dx}{dt} = f(x,u), \tag{1.1}$$

$$y = g(x,u), \tag{1.2}$$

where *u* is the input of the system, *y* the output and *x* the state variable.
The complexity of the system is characterized by the number of its state variables, i.e. the dimension *n* of the state space vector *x*. Model Order Reduction can be viewed as the task of reducing the dimension of the space vector x (*n*), while preserving the character of the input-output relations. This means find a dynamical system with the form

$$\frac{d\hat{x}}{dt} = \hat{f}(\hat{x},u), \tag{1.3}$$

$$y = \hat{g}(\hat{x},u), \tag{1.4}$$

where the dimension of $\hat{x}$ is much smaller than *n.* In order to provide a good approximation of the original system, is necessary satisfying some conditions:

- Approximation error must be very small

- Preservation of the properties of the original system, such as *stability* (the output signal is limited in the time-domain) and *passivity* (not able to generate energy itself)

- The reduction procedure should be computationally efficient

1.3.2 Krylov subspace method

Most of the principal methods of Model Order Reduction are based on the Krylov subspace methods. Linear equation solvers based on Krylov subspace are heavily used today and are well established for solving 3D simulation models based on partial differential equations. Starting with a given state-space system of the form

$$E\dot{x} = Ax + Bu, \tag{1.5}$$

$$y = Zx + Du, \tag{1.6}$$

where $x \in \mathbb{R}^n$, $u \in \mathbb{R}^p$, $y \in \mathbb{R}^q$ and $E, A \in \mathbb{R}^{n\,x\,n}$, $B \in \mathbb{R}^{n\,x\,p}$, $Z \in \mathbb{R}^{q\,x\,n}$, $D \in \mathbb{R}^{q\,x\,p}$.
Krylov methods aim is to compute projection matrices $V, W \in \mathbb{R}^{n\,x\,m}$ which, applied to the initial system, lead to a reduced stare space system given by

$$E_r\dot{x}_r = A_r x_r + B_r u, \tag{1.7}$$

$$y = Z_r x_r + Du, \tag{1.8}$$

where $x_r \in \mathbb{R}^m$, $u \in \mathbb{R}^p$, $y \in \mathbb{R}^q$, and $E_r, A_r \in \mathbb{R}^{m\,x\,m}$, $B_r \in \mathbb{R}^{m\,x\,p}$, $Z_r \in \mathbb{R}^{q\,x\,m}$.
These equations have a standardized format and thus can be insert into a various system simulation tools (like Matlab/Simulink). For example, in a study done by some Siemens engineers, this method had compressed a complex 3D simulation model with dimension of $n = 3.5x10^6$ to a reduced order model of dimension $m = 20$. This order reduction allows to evaluate the same input u with a faster than real-time responses.

1.3.3 Example of MOR applied to an EM's rotor (by Siemens)

Simulation needs to run in parallel with the real system, i.e. it requires to operate with real time capable models. Some commercial tools are able to generate reduced order models in the linear case, but in the electromagnetics system it is often necessary to face with Maxwell equations, made by ODE. Speaking about an EM, it is necessary to reduce rotor dynamics equations, but at the moment commercial solution doesn't exist.

According to a study done by Siemens [7], it is possible to obtain a simplified system using the Krylov subspace methods to generate the projection matrix. Starting from the space discretization of an EM rotor dynamics

$$M\ddot{u} + (D(\omega) + \omega G)\dot{u} + K(\omega)u = F(\omega, t) \tag{1.9}$$

Where

- *u* displacements
- *K* stiffness matrix
- *M* mass matrix
- *D* damping matrix
- *G* gyroscopic matrix
- *D* gyroscopic matrix
- *F(t)* outer force

The dimension of *u* generally is large and corresponds to the number of nodes. The reduction is given by the transformation

$$u = Rv \tag{1.10}$$

where *v* is of small dimension and *R* is the projection matrix to obtaining it. One possibility to generate the matrix *R* is to use Krylov subspace: the methods of projection in Krylov subspace consist in the projection of a problem of *n* dimension in a subspace with minor dimension. These methods, for each *r*, define an approximative solution $x^{(r)}$ of the linear system $Ax = b$ that belong to the K_r subspace. The Model Order Reduction methods are based on the Krylov subspace logic.

Once defined the projection matrix R, rotor equations (1.9) can be re-written onto the smaller subspace spanned by R, obtaining

$$R^T MR\ddot{v} + R^T(D(\omega) + \omega G)R\dot{v} + R^T K(\omega)Rv = R^T F(\omega, t) \tag{1.11}$$

The matrices depending on the angular velocity ω are split-off into a constant and a non-constant part, where the first one can be reduced in advance. Using some conversions, the 2nd ODE may be transformed into the standardized ω-dipendent state space model.

$$\begin{cases} \dot{x}(t) = A(\omega)x(t) + Bu \\ \quad y(t) = Cx(t) \end{cases} \tag{1.12}$$

However, many physical effects lead to nonlinear equations, where contact problems, large deformations and some material may be described only by nonlinear equation:

$$M\ddot{u} + f(\dot{u}, u) = F(t) \tag{1.13}$$

Applying the same reduction $u = Rv$ to the nonlinear case gives poor results and it is necessary improve more sophisticated methods.

2

Induction Motor and drives behaviours

Induction Motor (IM) is one of the most popular electric motor for industrial application due to its reliability and strong knowledge of controlling. The aim of this thesis is to evaluate the principal controlling behaviours due to the difficult to directly measure temperature and other electrical parameters by sensors and how a Digital Twin could benefit to the electric drive develop. How we will after show, usually it is not possible to insert any sensor everywhere we want and often the principal electrical quantities are estimated with low accuracy. Before we get to the heart of the thesis, it is better to present the principal characteristics of an Induction Motor and its principal behaviours to develop the electric drive.

2.1 Structure and principle of operation of an IM

Three-phase Induction Motor (IM), or asynchronous motor, constitute one of the most popular categories alternative-current motor for industrial application, with constant or variable speed. The electromechanics conversion that they use is based, according to the induction systems, on the direct application of the rotating magnetic field.

It is made by a stator (fixed part) and a rotor (rotating part), both with a cylindrical crown form of laminated ferromagnetic material and separated by an air gap. On the cylindrical surfaces of the stator facing with the air gap there are the quarries containing the stator winding. Instead, the rotor can be made in the same way as the stator (with three-phase winding wires), or using a cage made by alloy bars in short circuit with two rings. This second architecture is called "*squirrel cage rotor*" and it is the most popular solution thanks to its electro-mechanical advantages. With the same stator magnetic field applied to the rotor, this cage acts like it was made by a three-phase winding with the same stator quarries. To

better understand how an IM can produce torque to the rotor axle and which are the principal electromechanical behaviours, it is necessary to evaluate the dynamics that premises to obtain inducted fem by stator excitement.

A schematic representation of two poles (p=1) squirrel cage Induction Motor is showed in the Fig.2.1(a), where every stator phase is represented by a singular coil. The three phases are spatially arranged along the air gap with a reciprocal phase-shift of 120° to obtain a sinusoidal distribution of the excitement.

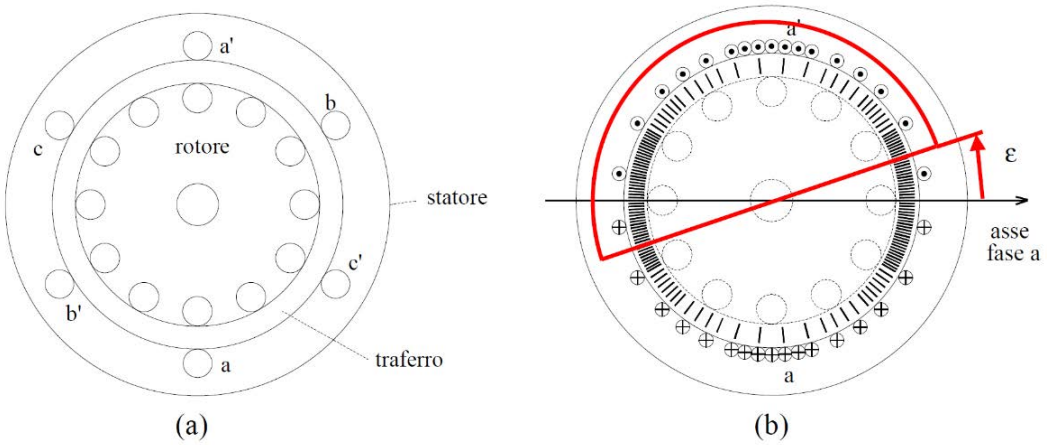

Figure 2.1: (a) two poles Induction motor schematic representation, (b) magnetic voltage distribution

For examples, powering the a-phase with a positive i_a current entering in a and exiting from a' without any other current in the motor, and assuming a sinusoidal distribution of the winding conductors for each phase (like showed in the Fig.2.1(b)), there is a sinusoidal distribution of magnetic voltage on the air gap. This magnetic voltage is:

$$A_a = H_a * g, \tag{2.1}$$

where H_a is the magnetic field (supposed to be radial) on the air gap, while g is the width of the ai gap. In the same figure, H_a magnetic field lines are represented in the considered instant by the black lines, where the thicker ones represent where the field is more intense.

To indicate the mechanical position and speed of the rotor respect its axle, θ_m radians [rad] and ω_m radians per second [rad/s] are used respectively, vice versa for the electromagnetic field on the air gap is used the electrical radians, then θ_{me} [rad el.] and ω_{me} [rad el./s]. The

cyclicality of the electromagnetic field depends by the number of polar couples (p), with an extension of 2π for each cycle. This allows to define the relation of the electro-mechanical quantities like

$$\theta_{me} = p * \theta_m, \tag{2.2}$$

$$\omega_{me} = p * \omega_m. \tag{2.3}$$

To evaluate the magnetic voltage A_a, it is necessary to calculate the amperespire, but before it is better to make some observations: in the first place, thanks to the circulation theorem, it is better to choose a semi-circumference with the diameter arranged by the position of ε (in the Fig.2.1 it corresponds to θ_m being p=1); in the second place, not considering the air gap crossings, the magnetic voltage drop can be considered negligible due to the hypothesis of an infinite magnetic permeance (μ=∞) in the iron.

The amperespire $n_c(\varepsilon)i_a(t)$ concatenated by the semi-circumference that moves with ε (where n_c is the total number of a-phase wires in the semi-circumference, counted + if crossed by positive current, or – if negative) are directly related by the magnetic voltage in the air gap by the expression

$$A_a(t,\varepsilon) = \frac{n_c(\varepsilon)i_a(t)}{2} \tag{2.4}$$

Thanks to the sinusoidal distribution of the winding wires, $n_c(\varepsilon)$ is maximum when ε=0 and equal to the total number N of a-phase coils (and it applies to the others phases), and it is null for ε=π/2. This permits to describe it like $n_c(\varepsilon) = Ncos(\varepsilon)$ and, looking to a three-phase system, the three currents $i_a(t)$, $i_b(t)$, $i_c(t)$ make it possible to obtain

$$\begin{cases} A_a(t,\varepsilon) = Ni_a cos(\varepsilon) \\ A_b(t,\varepsilon) = Ni_b cos(\varepsilon - \frac{2}{3}\pi) \\ A_c(t,\varepsilon) = Ni_c cos(\varepsilon - \frac{4}{3}\pi) \end{cases} \tag{2.5}$$

The magnetic voltage in the air gap, produced by the stator currents, is obtained by summing for every point and every moment the three contributions, getting the total equation

$$A_{abc}(t,\varepsilon) = N\left(i_a - \frac{1}{2}i_b - \frac{1}{2}i_c\right)\cos(\varepsilon) + N\left(\frac{\sqrt{3}}{2}i_b - \frac{\sqrt{3}}{2}i_c\right)\sin(\varepsilon) \qquad (2.6)$$

The equation (2.6) can be expressed using the space vectors (a different reference system for the three-phase ecosystem applying Clarks transformation), obtaining

$$A_{abc}(t,\varepsilon) = \frac{3}{2}Ni_\alpha\cos(\varepsilon) + \frac{3}{2}Ni_\beta\sin(\varepsilon) \qquad (2.7)$$

where $i_\alpha(t)$ and $i_\beta(t)$ are respectively the real and imaginary parts of the current space vector $\bar{\imath}_{\alpha\beta}(t)$ associated with the trio $i_a(t)$, $i_b(t)$, $i_c(t)$. Writing $\bar{\imath}_{\alpha\beta}(t)$ in its extended version

$$\bar{\imath}_{\alpha\beta}(t) = i_\alpha(t) + i_\beta(t) = \left|\bar{\imath}_{\alpha\beta}\right|e^{j\theta_i(t)} = \left|\bar{\imath}_{\alpha\beta}\right|[\cos\ \theta_i(t) + jsin\theta_i(t)] \qquad (2.8)$$

where $\theta_i(t)$ is the argument of the current space phasor referred to the real axle of the complex plan (which coincides with a-axel). Representing the magnetic voltage (2.7) with this extended current space vector (2.8), it becomes

$$A_{abc}(t,\varepsilon) = \frac{3}{2}N\left|\bar{\imath}_{\alpha\beta}\right|\cos(\varepsilon - \theta_i(t)) \qquad (2.9)$$

This equation (2.9) allows to attribute the physical meaning of the current: its argument shows the direction where, for each instant, is the maximum magnetic voltage in the air gap generated by stator windings, measured starting from a-axel, and its amplitude is proportional with this maximum value.

Due to the presence of a magnetic voltage in the air gap, it is possible to observe a magnetic field with intensity H=A/g and, therefore, a magnetic induction B=$\mu_0 H$=μ_0A/g. Being a squirrel cage IM described by a constant air gap width (g), the magnetic induction in the air gap can be easily obtained

$$B_{abc}(t,\varepsilon) = \frac{3}{2}k\left|\bar{\imath}_{\alpha\beta}\right|\cos(\varepsilon - \theta_i(t)) \qquad (2.10)$$

where *k*-constant describes air gap dimension and coil numbers of the stator windings.
Considering the magnetic induction, in the steady-state operation the motor is powered by three sinusoidal currents shifted of 2π/3 [rad el.] reciprocally and pulsing with ω_s=2πf (likes every stator parameters). The space vector associated to these currents have constant amplitude and rotate with a constant angular speed ω_i=dθ_i/dt, equal to phase-current pulsation. If in the starting condition the current space vector is placed in the a-axel (thus, $\theta_i(0) = 0$), the (2.10) becomes

$$B_{abc}(t,\varepsilon) = \frac{3}{2}k\left|\bar{\imath}_{\alpha\beta}\right|\cos(\omega_s t - \varepsilon) = B_M \cos\left(\omega_s t - \varepsilon\right) \tag{2.11}$$

When t=0, this equation represents a sinusoidal distribution of the magnetic induction in the air gap, with its maximum value at a-axel (ε=0); in the following cases, this maximum value revolves (and with it, all the space distribution of B_{abc}) describing the rotating magnetic field. The position of this maximum is given by $\varepsilon=\omega_s t$ [rad el.] and, consequently, the rotation speed of the rotating magnetic field is

$$\frac{d\varepsilon}{dt} = \omega_s\ [rad\ el./s] \tag{2.12}$$

where, in [rad/s] it becomes

$$\omega_0 = \frac{\omega_s}{p}\ [rad/s] \tag{2.13}$$

where *p* is the numbers of pole couple.
In practice, the field rotating speed is expressed in rotations per minute by

$$n_0 = \frac{60\omega_0}{2\pi} = \frac{60 f_s}{p}\ [rpm] \tag{2.14}$$

where f_s is the stator frequency.

2.2 Induction Motor behaviour in sinusoidal regime

As we have seen, feeding the stator with a three-phase equilibrate system of currents pulsing with ω_s, in the air gap it is possible to obtain a rotating magnetic field with ω_0. Each stator phase concatenates an alternative magnetic flux $\lambda(t)$ pulsing with ω_s. The voltage at the clamps have to balance the ohmic voltage drop (pulsing with ω_s) and the cons-f.e.m. $d\lambda/dt$ (always with ω_s) induced by the concatenated flux variation.

If the rotor rotates with a speed of $0<\omega_m<\omega_0$ in the same direction of the rotating magnetic field (B_{abc}), this last one is rotating, respect to the rotor, at ω_0-ω_m. It is therefore useful to define the slip (s) as

$$s = \frac{\omega_0 - \omega_m}{\omega_0} = \frac{n_0 - n}{n_0} = \frac{\omega_s - \omega_{me}}{\omega_s} \tag{2.15}$$

In the rotor side, cage bars response as if they were made by coils powered by three-phase induced voltages pulsing with ω_r, called slipping pulsation, and it is equal to

$$\omega_r = s\omega_s \tag{2.16}$$

defining the slipping frequency $f_r = sf_s$ (being $\omega=2\pi f$).

These induced voltages cause the circulation of three alternating and equilibrate currents with ω_r and their amplitude depends on the amplitude of the induced voltages and from the impedance of rotor cage at the slipping frequency. This leads to the circulation of another rotating magnetic field produced by the rotor with a rotating speed, respect to the rotor, with ω_s and, respect to the stator, with $s\omega_0 + \omega_m = (\omega_0 + \omega_m) + \omega_m = \omega_0$. This means that the rotating magnetic field produced by stator and rotor currents are synchronous with each other, so they are fixed among themselves. This permit to obtain the resulting rotating magnetic field in the air gap by their individual sum.

These conditions are true only with a sinusoidal regime and constant rotor rotating speed. In the dynamic conditions, where currents have variable amplitude and frequency, these are variable with rotor speed too.

To evaluate the effective torque developed by the IM in the sinusoidal regime, it is necessary to observe the force produced in the rotor: taking a generic conductor of length *l*, crossed by a current (i) and immersed in an induction magnetic field (B), the orthogonal force applied to the wire is $f=Bli$. For the squirrel cage rotor, the Fig.2.2 (a) shows a generic instant of the air gap induction $B_{abc}(\varepsilon)$ produced by stator currents that runs with a speed of $v=r\omega_0$, where r is the air gap ray.

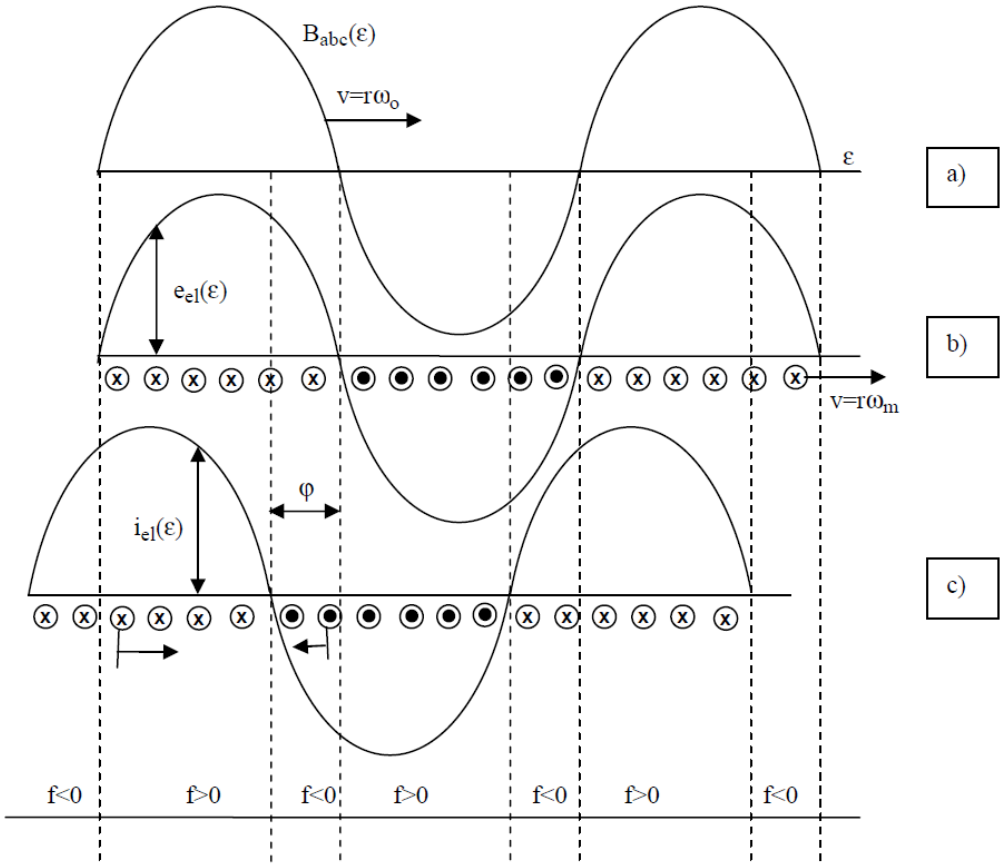

Figure 2.2: f.e.m. and currents distribution in the squirrel cage rotor, (a) $B_{abc}(\varepsilon)$ distribution produced by stator currents in a generic instant, (b) inducted f.e.m. distribution, (c) rotor currents distribution

In a generic bar of the rotor cage, rotating with an absolute speed of $v=r\omega_m$ and a relative speed respect to the $B_{abc}(\varepsilon)$ of $v=sr\omega_0$, the elemental inducted f.e.m. (e_{el}) is equal to

$$e_{el} = Blv = B(\varepsilon)lsr\omega_0 \qquad (2.17)$$

The distribution of amplitude of this f.e.m. follows value and sign of the $B_{abc}(\varepsilon)$, likes showed in the Fig.2.2 (b). It will be to its maximum value at the same point of the maximum of $B_{abc}(\varepsilon)$, following the same sign of the rotating magnetic field.
These inducted voltages (e_{el}) cause the circulation of the currents (i_{el}) in the singular bars. These, not being the cage purely resistive but ohm-inductive, do not allow the same distribution as e_{el} along the air gap, but present a sinusoidal form with a delay respect to them of φ degrees, equal to

$$\varphi = \arctan\left(\frac{X_{el,s}}{R_{el}}\right) \tag{2.18}$$

where $X_{el,s}$ is the elemental reactance of each bar at the slipping frequency (f_r), while R_{el} is its resistance. The distribution of this current is illustrated in Fig.2.2 (c).
Now it is possible to evaluate the resulting torque produced by the interaction of the rotor currents and the induction magnetic field $B_{abc}(\varepsilon)$: for each bar of the rotor cage it is possible to find an elemental force

$$f_{el} = Bli = B(\varepsilon)li_{el} \tag{2.19}$$

obtaining the elemental torque

$$m_{el} = f_{el}r \tag{2.20}$$

The resulting generated torque M, positive if directed in the same direction of the induction magnetic field (otherwise it is negative), is equal to the sum of all the elemental torque produced by each bar. This means, if N_b is the total bar number, it can be obtained by multiplying N_b with the mean value of the torque distribution in the air gap, i.e.

$$M = \frac{N_b lr}{2\pi}\int_0^{2\pi} B(\varepsilon)\, i_{el}(\varepsilon)\, d\varepsilon = \frac{N_b lr\hat{B}\hat{I}_{el}}{2}cos\varphi \tag{2.21}$$

This expression can be rewritten remembering that

$$\begin{cases} \hat{E}_{el} = \hat{B} l s r \omega_0 \\ \hat{E}_{el} = \hat{I}_{el} Z_{el,s} \end{cases} \tag{2.22}$$

where $Z_{el,s}$ is the elemental impedance at the slipping frequency (f_r); resolving the system (2.22) for $\hat{B}$, it is

$$\hat{B} = \frac{\hat{I}_{el} Z_{el,s}}{l s r \omega_0} \tag{2.23}$$

whereby it is possible to obtain the torque

$$M = \frac{N_b (\hat{I}_{el})^2 Z_{el,s}}{2 s \omega_0} cos\varphi = \frac{{I_{el}}^2 R_{el} N_b}{s \omega_0} \tag{2.24}$$

where I_{el} is the rms value of the current for each bar, which is in the sinusoidal regime worth $I_{el}=\hat{I}_{el}/\sqrt{2}$. The fraction numerator corresponds to the total dissipated power due to the Joule effect in the rotor cage, i.e.

$$P_{jr} = {I_{el}}^2 R_{el} N_b = 3 {I_r}^2 R_r \tag{2.25}$$

where R_r and I_r are, respectively, rotor resistance and rms current value for each phase.
In this way, it is possible to express the torque as

$$M = \frac{3 {I_r}^2 R_r}{s \omega_0} \tag{2.26}$$

The corresponding generated mechanical power, remembering ω_m= (1- s) ω_0, is

$$P = M \omega_m = \frac{3 {I_r}^2 R_r}{s} (1 - s) \tag{2.27}$$

The total power transmitted from stator to rotor is called transmitted power (P_{tr}) and it is equal by summing mechanical power (P_m) and the dissipated power (P_{jr}), i.e.

$$P_{tr} = P_m + P_{jr} = \frac{3{I_r}^2 R_r}{s} \tag{2.28}$$

Looking to these equations, it is useful to make some considerations: the torque (2.26) depends from the rotor current amplitude and the shift between these and the respective f.e.m. (i.e. the angle φ); the slipping frequency (f_r) for $s \sim 0$, that is the proximity to the nominal operating conditions, is small ($\varphi \sim 0$) and rotor circuit is almost resistive ($X_r=\omega_r L_r=2\pi f_r L_r$, it is small due to the lower frequency). Consequently, it is possible to assume a linear dependence of the currents respect to the f.e.m.. So, for small slip value, torque grows with the slip itself if the maximum amplitude of the induction magnetic field in the air gap produced by stator currents is constant.

As the slip increases (and the rotor frequency, too), rotor impedance cannot longer be considered purely resistive due to the growing inductive effect; in this case, rotor current is no longer linear with *s* variation and it is shifted later than the inducted rotor voltage (e_{el}) of the angle φ. This means that the torque grows with s to a certain its maximum value.

Another important observation is about rotor resistance R_r: the produced torque is commensurate to the dissipated rotor power and, with a hypothetical $R_r=0$ rotor, it is not possible generate it for each $s \neq 0$. It is not possible to realize rotors with resistance to bigger to not have excessive dissipated power, so it is necessary individuate to correct compromise of R_r. Last but not least, torque has the same sign of *s*: for each $s>0$, we have the same conditions just seen and the IM works like a motor; instead, for $s<0$ the relative motion between rotating field and rotor is reversed, like the verses of current (i_{el}) and voltage (e_{el}). In this case, the torque is negative and IM is working as generator.

2.3 Induction Motor dynamic behaviour

How we have seen, electromechanically speaking, rotor cage works as if it were made by three-phase windings, close to the stator side (same number of conductors and poles). This allows to evaluate dynamics behaviours without worrying about which is the real motor structure.

In the first place, to describe IM function it is necessary to start from the general equations of the voltages of its stator and rotor phases *a, b, c*, with the convention of users.

For the stator they are

$$\begin{cases} U_{sa}(t) = R_s i_{sa}(t) + \dfrac{d\lambda_{sa}(t)}{dt} \\ U_{sb}(t) = R_s i_{sb}(t) + \dfrac{d\lambda_{sb}(t)}{dt} \\ U_{sc}(t) = R_s i_{sc}(t) + \dfrac{d\lambda_{sc}(t)}{dt} \end{cases} \tag{2.29}$$

While for the rotor

$$\begin{cases} U_{ra}(t) = R_r i_{ra}(t) + \dfrac{d\lambda_{ra}(t)}{dt} = 0 \\ U_{rb}(t) = R_r i_{rb}(t) + \dfrac{d\lambda_{rb}(t)}{dt} = 0 \\ U_{rc}(t) = R_r i_{rc}(t) + \dfrac{d\lambda_{rc}(t)}{dt} = 0 \end{cases} \tag{2.30}$$

Every concatenated flux in (2.29) and (2.30) equations are made by the combined effects of all currents present in the motor. Assuming that the magnetic circuit is free of eddy currents and also does not manifest saturation and magnetic hysteresis, each concatenated flux, like $\lambda_{sa}(t)$, can be expressed as

$$\lambda_{sa}(t) = \lambda_{ssa}(t) + \lambda_{sra}(t) \tag{2.31}$$

where the two contributes are

$$\begin{cases} \lambda_{ssa}(t) = L_{ss} i_{sa}(t) + L_M i_{sb}(t) + L_M i_{sc}(t) \\ \lambda_{sra}(t) = l_{Msr}(\vartheta_{me}) i_{ra} + l_{Msr}\left(\vartheta_{me} + \frac{2}{3}\pi\right) i_{rb} + l_{Msr}\left(\vartheta_{me} + \frac{4}{3}\pi\right) i_{rc} \end{cases} \tag{2.32}$$

Thanks to the cylindrical symmetry of the structure, the auto-induction coefficient L_{ss} and the mutual-induction L_M have been considered constant and independent from rotor position (ϑ_{me}), while all the mutual-induction of stator-rotor $l_{Msr}(\vartheta_{me})$ can be expressed with a cosenosuidal function $l_{Msr}(\vartheta_{me}) = L_{Msr}\, cos(\vartheta_{me})$, obtaining

$$\begin{aligned} \lambda_{sra}(t) = L_{Msr}\, cos(\vartheta_{me}) i_{ra} + L_{Msr}\, cos\left(\vartheta_{me} + \frac{2}{3}\pi\right) i_{rb} \\ + L_{Msr}\, cos\left(\vartheta_{me} + \frac{4}{3}\pi\right) i_{rc} \end{aligned} \tag{2.33}$$

Doing these considerations for the others five phases and applying fluxes expressions to the stator and rotor voltage equations, it is possible to get the differential system that describes electrical motor dynamics that must be evaluated. It is really complex due to the dependence of any parameters by rotor position (ϑ_{me}).

If we consider an IM without stator neutral wire and, thanks to the structural symmetry, if we assume to have the three cons-f.e.m. that arise on each winding without any homopolar component (the way where the unbalanced current part run), we can simplify motor description by using the three-phases space vectors representation. Anyway, even though this homopolar component was present, it would not lead to any torque modification obtained by the IM.

2.3.1 Stator and rotor equations in rotating reference system dq

Being lot of parameters depending from rotor position, an easy way to evaluate their conditions is adopting an orthogonal rotating reference system (dq) with an angular speed $\omega_{dq}(t)$ respect to the stationary reference system α-β.

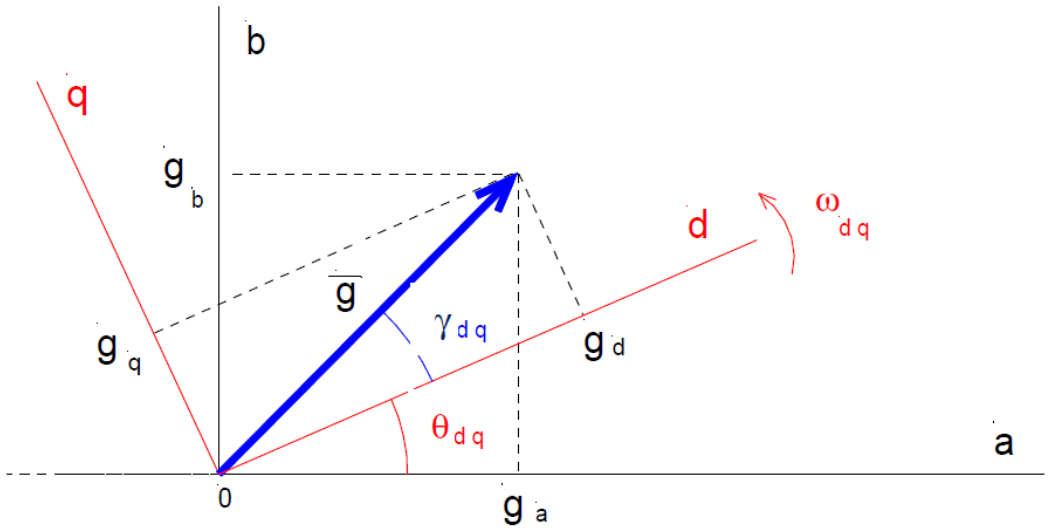

Figure 2.3: α-β and d-q referent system relationship

Looking to the Fig.2.3, these reference systems are given by the relations

$$\begin{cases} \bar{g}_{\alpha\beta} = g_\alpha + jg_\beta = |\bar{g}|e^{j\gamma_{\alpha\beta}} \\ \bar{g}_{dq} = g_d + jg_q = |\bar{g}|e^{j\gamma_{dq}} \end{cases} \tag{2.34}$$

where $|\bar{g}| = |\bar{g}_{\alpha\beta}| = |\bar{g}_{dq}|$ and $\gamma_{\alpha\beta} = \gamma_{dq} + \vartheta_{dq}$, with ϑ_{dq} corresponding to the instantaneous position of the d-q reference system respecting to the α-β one. It is so possible to write

$$\bar{g}_{dq} = \bar{g}_{\alpha\beta}e^{-j\vartheta_{dq}} \tag{2.35}$$

which can be expressed in its matrix form

$$\begin{pmatrix} g_d \\ g_q \end{pmatrix} = \begin{bmatrix} \cos(\vartheta_{dq}) & \sin(\vartheta_{dq}) \\ -\sin(\vartheta_{dq}) & \cos(\vartheta_{dq}) \end{bmatrix} \begin{pmatrix} g_\alpha \\ g_\beta \end{pmatrix} \tag{2.36}$$

The matrix permit to switch into the different reference system; looking to the (2.36), to do that it is necessary to know the position of the system (i.e. the angular position ϑ) with which we want to synchronize the rotating reference system.

Applying this reference system into the IM relations, it is possible to obtain different equations according to which reference we want to follow. It is necessary to define respect to what it is referred to thanks to the corresponding apex, as stator (s), rotor (r) or as a generic one (x).

Adopting a rotating reference system synchronized with the stator ($d^s q^s$), the voltage relation becomes

$$\bar{U}_s^s = R_s \bar{\imath}_s^s + \frac{d\bar{\lambda}_s^s}{dt} \tag{2.37}$$

where λ_s^s is the stator flux space vector, equal to

$$\bar{\lambda}_s^s = L_s \bar{\imath}_s^s = \bar{\lambda}_{ss}^s + \bar{\lambda}_{sr}^s = L_s \bar{\imath}_s^s + L_m \bar{\imath}_r^s \tag{2.38}$$

In this flux equation it is possible to identify some important parameter:

- $L_s = L_{ss} + |L_{Mss}|$ is called synchronous stator induction (or easily, stator induction),
- $L_m = \frac{3}{2} L_{mrs}$ is the synchronous mutual induction,
- $\bar{\imath}_r^s = \frac{2}{3}(i_{ra} + i_{rb}\, e^{j\frac{2}{3}\pi} + i_{rc}\, e^{j\frac{4}{3}\pi}) e^{j\vartheta_{me}}$ is rotor current space vector referred to the stator ($d^s q^s$), where ϑ_{me} is the position of the fixed rotor reference system ($d^r q^r$) respect to stator one.

In a generic reference system ($d^x q^x$), (2.37) and (2.38) equations become

$$\begin{cases} \bar{U}_s^x = R_s \bar{\imath}_s^x + \dfrac{d\bar{\lambda}_s^x}{dt} + j\omega_x \bar{\lambda}_s^x & (2.39) \\ \bar{\lambda}_s^x = L_s \bar{\imath}_s^x + L_m \bar{\imath}_r^x & (2.40) \end{cases}$$

For the rotor side the approach is similar, but is useful observe how voltage value is equal to zero being rotor cage on short circuit; for a reference system made by two orthogonal axes fixed with the rotor ($d^r q^r$), voltage equation becomes

$$0 = R_r \bar{\imath}_r^r + \frac{d\bar{\lambda}_r^r}{dt} \tag{2.41}$$

where $\bar{\lambda}_r^r$ is the rotor flux space vector

$$\bar{\lambda}_r^r = \bar{\lambda}_{rr}^r + \bar{\lambda}_{rs}^r = L_r \bar{\imath}_r^r + L_m \bar{\imath}_s^r \tag{2.42}$$

In this flux equation it is possible to identify some important parameter:

- $L_r = L_{rr} + |L_{Mrr}|$ is called *synchronous rotor induction* (or easily, rotor induction),
- $L_m = \frac{3}{2} L_{mrs}$ is the *synchronous mutual induction*.

In a generic reference system ($d^x q^x$), (2.41) and (2.42) rotor equations become

$$\begin{cases} 0 = R_r \bar{\imath}_r^x + \frac{d\bar{\lambda}_r^x}{dt} + j(\omega_x - \omega_{me})\bar{\lambda}_r^x & (2.43) \\ \bar{\lambda}_r^x = L_r \bar{\imath}_r^x + L_m \bar{\imath}_s^x & (2.44) \end{cases}$$

To study and develop any IM behaviour, it is necessary to define the same reference system for every single part to permit the correct correlation from each other. Looking to these last equations, it is possible observe some interesting facts:

- These equations do not depend on rotor angular position (ϑ_{me}), but from its rotational speed (ω_{me});
- The two Rotor voltage equations components (d and q) depend form each other due to the current or flux components of the other axel every time rotor speed is different from zero. Due to this mutual relationship, even stator voltage equations are described with a similar d-q influence.

Thanks to these stator and rotor equations, it is now possible to obtain the torque equations whereby develop the control scheme of an IM. Depending on how the different equations are developed, torque expression can be characterized by the interaction of λ_r, λ_s, i_r and i_s.

Each different form allows to create its own block diagram. In the Matlab-Simulink simulation scheme that we will see later, the IM has been developed following the torque equation obtained from rotor flux (λ_r) and stator current (i_s).

2.3.2 Simulink torque equation

In order to better understand the final equation of the torque, it is advisable to cover all the steps. In the first place, (2.39) stator voltage equations are expressed in the reference system fixed with the rotor ($d^r q^r$):

$$\begin{cases} u_{sd} = R_s i_{sd} + \dfrac{d\lambda_{sd}}{dt} - (\omega_{me} + \omega_{slip})\lambda_{sq} \\ u_{sq} = R_s i_{sq} + \dfrac{d\lambda_{sq}}{dt} + (\omega_{me} + \omega_{slip})\lambda_{sd} \end{cases} \tag{2.45}$$

where ω_{slip} is the difference of mechanical motor speed and rotor flux speed.
IM can be interpreted as an induction transformer with a transformation ratio $n = \frac{L_M}{L_R}$; in this way, it is possible to transport rotor electrical parameters to the stator side (identified with the subscript x_{rs})

$$\bar{\imath}_{rs} = \frac{\bar{\imath}_r}{n} \tag{2.46}$$

$$\bar{\lambda}_{rs} = n\,\bar{\lambda}_r \tag{2.47}$$

Replacing (2.46) and (2.47) expressions on the stator flux equation (2.38)

$$\lambda_s = L_s i_s + L_M \frac{\lambda_{rs}}{n L_r} - \frac{L_M^2 i_s}{L_r} \tag{2.48}$$

and rewriting n with its own form (2.48) becomes

$$\lambda_s = \left(L_s - \frac{L_M^2}{L_r}\right) i_s + \lambda_{rs} \tag{2.49}$$

It is possible to identify the transient inductance (L_t) as

$$L_t = L_s - \frac{L_M^2}{L_r} \tag{2.50}$$

Rotor voltage equations (2.43) can be expressed by the stator side too by adopting the *n* value, obtaining

$$\begin{cases} 0 = R_{rs}\bar{\imath}_{rsd} + \dfrac{d\bar{\lambda}_{rsd}}{dt} - \omega_{slip}\bar{\lambda}_{rsq} \\ 0 = R_{rs}\bar{\imath}_{rsq} + \dfrac{d\bar{\lambda}_{rsq}}{dt} + \omega_{slip}\bar{\lambda}_{rsd} \end{cases} \tag{2.51}$$

where $\bar{\imath}_{rs}$ is extracted from (2.44) equation

$$\frac{\bar{\lambda}_{rs}}{n} = L_M\bar{\imath}_s + L_r\bar{\imath}_{rs}n \tag{2.52}$$

So

$$\bar{\imath}_{rs} = \frac{\bar{\lambda}_{rs}}{\frac{L_M^2}{L_r}} - \bar{\imath}_s \tag{2.53}$$

The ratio of the two inductances can be expressed like a singular-one L_φ, and that is equal to

$$L_\varphi = \frac{L_M^2}{L_r} = L_s - L_t \tag{2.54}$$

To obtain the mechanical torque expression of the IM, it is necessary to multiply voltage equations with the respective currents (U_s- $i_s dt$ and U_r- $i_r dt$) so as to realize the power balance

$$\begin{aligned}\left(U_{sd}^{s} i_{sd}^{s} + U_{sq}^{s} i_{sq}^{s}\right)dt = &\left[R_s (i_{sd}^{s})^2 + R_s \left(i_{sq}^{s}\right)^2 + R_r (i_{rd}^{s})^2 + R_r \left(i_{rq}^{s}\right)^2\right] dt + \\ &+\left[i_{sd}^{s} d\lambda_{sd}^{s} + i_{sq}^{s} d\lambda_{sq}^{s} + i_{rd}^{s} d\lambda_{rd}^{s} + i_{rq}^{s} d\lambda_{rq}^{s}\right] dt + \\ &+\omega_{me}\left[\lambda_{rq}^{s} i_{rd}^{s} - \lambda_{rd}^{s} i_{rq}^{s}\right] dt\end{aligned} \tag{2.55}$$

The first part represents the electrical energy spent in the time *dt*, and it is characterized only by stator parameters; the second part is composed of three different elements identified by the square bracket: the first one represents the energy transformed in to heat by windings resistance, the second stay for the magnetic energy stored by stator and rotor magnetic circuit, and the last one quantifies the mechanical energy developed in the time *dt*.

Remembering that mechanical power is $P = \omega_m * m$ and $\omega_{me} = p * \omega_m$, the torque expression can be expressed as

$$m = \frac{3}{2} p \left(\lambda_{rq}^{s} i_{rd}^{s} - \lambda_{rd}^{s} i_{rq}^{s}\right) \tag{2.56}$$

where $\frac{3}{2}$ is necessary to power conservation moving on to the stationary reference system. This torque equation depends on rotor currents and fluxes, but replacing appropriately the parameters from (2.40) and (2.44), it is possible to obtain other equations with different combinations of depending quantities. Every different torque equation allows to identify an own block diagram.

In the Simulink scheme adopted for the different simulations, torque equation is expressed in function of rotor flux (λ_r) and stator current (i_s), and that is

$$m = \frac{3}{2} p \frac{L_M}{L_r} \left(\lambda_{rd} i_{sq} - \lambda_{rq} i_{sd}\right) \tag{2.57}$$

This last equation (2.57) can be easily re-written by its polar coordinates

$$m = \frac{3}{2} p \frac{L_M}{L_r} \left|\bar{\lambda}_r\right| \left|\bar{\imath}_s\right| \sin\left(\vartheta_{i_s} - \vartheta_{\lambda_r}\right) \tag{2.58}$$

where it is possible to define the load angle $\psi = \vartheta_{i_s} - \vartheta_{\lambda_r}$.

Respecting to the PMSM (Permanent Magnet Synchronous Motor), in the IM rotor flux is not generated by a permanent magnet (and then a constant), but from the stator and rotor currents, where, the latter, are generated by the inducted f.e.m. produced by stator magnetic field. Thanks to the last torque equation (2.58), we can observe the delicate concept that stator currents produce torque in two ways: one by a direct relation (by $|\bar{\imath}_s|$), the other by rotor flux generation (by $|\bar{\lambda}_r|$).

For this reason, it is necessary to implement an IM electric drive where we can handle the two different parameters, obtaining a direct separated control of rotor flux ($\bar{\lambda}_r$) by real stator current component (i_{sd}), and torque (m) by the imaginary one (i_{sq}). Sometimes, these currents take the name of their effects, thus i_{sd} is called flux current (i_λ) and i_{sq} is called torque current (i_τ). This is only possible by adopting a particular reference system according to the Field Oriented Control (FOC) method that we will see in the next pages.

2.4 Max Torque Per Ampere (MTPA)

Looking to a PMSM, the easier way to simplify expressions complexity is by adopting a reference system synchronous with the rotor (so, with a rotation speed equal to ω_{me}), with the real d-axis coinciding with the polar rotor axis. In this way, rotor permanent magnet vector λ_{pm} is only described by its real component getting an additional simplification of the equations. Its torque equation is so described by constant parameters and the only controllable element to manage it are the stator currents (i_{sd} and i_{sq}).

For every different type of PMSM motor (isotropic, anisotropic and reluctance) it is possible to identify a particular condition which allows to obtain the Max Torque Per Ampere (MTPA). This means, with a certain load torque demand, to generate the requesting torque by using less current is possible.

For the Induction Motor this condition usually is not convenient. How we have seen before, torque equation is described by different combinations of flux and current references. By placing the d-axis of the rotational reference system in correspondence of the rotor flux vector, it is possible to obtain some very important equation simplification, improving the electric drive control logic. Unfortunately, rotor flux vector is not constant as in the PMSM condition due to the changing condition of the parameters and, for this reason, it is necessary

to develop a control system that can follow its trend for every working status. How we will see later, this is the most important aspect to evaluate at the expense of maximum efficiency, like the MTPA condition.

2.5 Field Oriented Control (FOC)

How we have seen previously, stator and rotor equations can be expressed by a certain reference system. The aim of a well implemented torque control is to find the easier and most reliable way to follow IM and load behaviours. To do this, it is therefore necessary to individuate the most convenient reference system to develop an effective control.
Starting from rotor flux equation (2.44) in a generic reference system ($d^x q^x$), it is possible to obtain rotor current

$$\bar{\imath}_r^x = \frac{\lambda_r^x}{L_r} - \frac{L_M}{L_r}\bar{\imath}_s^x \tag{2.59}$$

and substituted on rotor voltage equation (2.43), we have

$$0 = \frac{R_r}{L_r}\bar{\lambda}_r^x - \frac{R_r L_M}{L_r}\bar{\imath}_s^x + \frac{d\bar{\lambda}_r^x}{dt} + j\omega_x^r\bar{\lambda}_r^x \tag{2.60}$$

where ω_x^r is the speed of a generic reference system respect to the rotor, and that is $\omega_x^r = \omega_x - \omega_{me}$. This last equation (2.60) can be decomposed in its real (d) and imaginary (q) parts

$$\begin{cases} 0 = \frac{R_r}{L_r}\lambda_{rd}^x - \frac{R_r L_M}{L_r} i_{sd}^x + \frac{d\lambda_{rd}^x}{dt} - \omega_x^r\lambda_{rq}^x \\ 0 = \frac{R_r}{L_r}\lambda_{rq}^x - \frac{R_r L_M}{L_r} i_{sq}^x + \frac{d\lambda_{rq}^x}{dt} + \omega_x^r\lambda_{rd}^x \end{cases} \tag{2.61}$$

Being $(\lambda_{rd}^x)^2 + (\lambda_{rq}^x)^2 = \left|\bar{\lambda}_r\right|^2$, multiplying the first part of the equation by λ_{rd}^x and the second by λ_{rq}^x and making the term sum, it is possible to obtain

$$\frac{1}{2}\frac{d\bar{\lambda}_r^2}{dt} + \frac{R_r}{L_r}\bar{\lambda}_r^2 = \frac{R_r L_M}{L_r}\left(i_{sd}^x \lambda_{rd}^x - i_{sq}^x \lambda_{rq}^x\right) \tag{2.62}$$

Analysing this last equation (2.62) and the torque one (2.57), it is possible to make some important observations: the aim of the control is to realize a separated torque and flux control and it is achievable by adopting a reference system synchronous with rotor flux ($d^\lambda q^\lambda$), where its d-axel is superimposed with rotor flux vector. This solution can be represented by the next Fig.2.4.

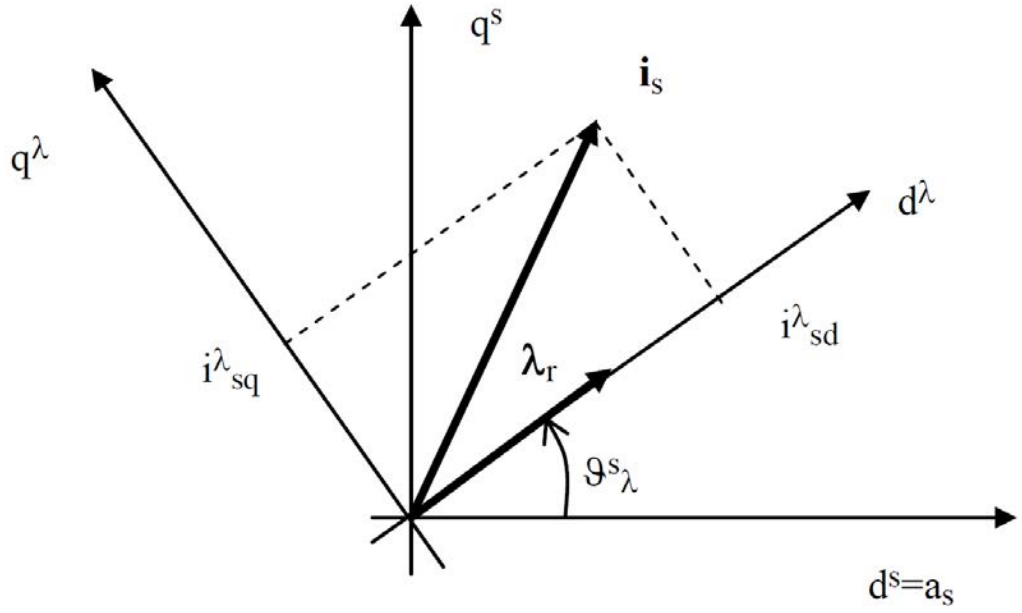

Figure 2.4: Field Oriented Control (FOC) representation

In this case $\bar{\lambda}_r = |\bar{\lambda}_r| = \lambda_{rd}^\lambda$, so

$$\begin{cases} \lambda_{rd} = |\bar{\lambda}_r| \\ \lambda_{rq} = 0 \end{cases} \tag{2.63}$$

whereby the flux (2.62) and torque (2.57) equations become

$$\begin{cases} \dfrac{d\bar{\lambda}_r}{dt} + \dfrac{R_r}{L_r}\bar{\lambda}_r = \dfrac{R_r L_M}{L_r} i_{sd}^{\lambda} & (2.64) \\ m = \dfrac{3}{2} p \dfrac{L_M}{L_r} \bar{\lambda}_r i_{sq}^{\lambda} & (2.65) \end{cases}$$

In this way, it is possible to obtain an easier scheme by controlling separately rotor flux with the current i_{sd}, while with i_{sq} the torque. It means decouple the mutual influence of the two behaviours, finding the easier and reliable way to control the motor.
To realize it, it is necessary to know the correct position of rotor flux vector, but in practice it is not measurable. The position ϑ_{λ}^{s} of this vector, i.e. of the reference system ($d^{\lambda}q^{\lambda}$), have to be estimated or rebuild starting from direct measurements of the accessibly parameters of the IM, like voltages, currents or speed. To do this, different solutions are available and they can be classified by two different approach:

- *Direct FOC*: these controlling techniques are based on algorithms able to rebuild rotor flux vector λ_r^s starting from direct electromechanical measures available from the motor; by extrapolating its argument (ϑ_{λ}^{s}), it is possible to know the position of the d-axel of the reference system, while vector module can be managed to control the amplitude of rotor flux.

- *Indirect FOC*: instead of rebuild rotor flux vector, these techniques dictate exact feeding conditions to the IM to place forcibly the d-axel of the reference system on the rotor flux vector.

2.5.1 Simulation's FOC

The controlling scheme developed for the Simulink model is based on direct FOC approach starting from the direct measures of stator currents (i_s) and rotor rotating speed (ω_{me}); recalling rotor voltage equations (2.51) and the current i_{rs} (2.53)

$$\begin{cases} 0 = R_{rs} i_{rsd} + \dfrac{d\lambda_{rsd}}{dt} - \omega_{slip}\lambda_{rsq} \\ 0 = R_{rs} i_{rsq} + \dfrac{d\lambda_{rsq}}{dt} + \omega_{slip}\lambda_{rsd} \\ \bar{\imath}_{rs} = \dfrac{\bar{\lambda}_{rs}}{L_\varphi} - \bar{\imath}_s \end{cases}$$

Looking to the steady-state condition, it is necessary to define the slipping speed (ω_{slip}) thanks by the q-axel flux component is null, so

$$\begin{cases} \dfrac{d\lambda_{rd}}{dt} + \dfrac{R_r}{L_r}\lambda_{rd} = \dfrac{R_r L_M}{L_r} i_{sd} + \omega_{slip}\lambda_{rsq} \\ \dfrac{d\lambda_{rq}}{dt} + \dfrac{R_r}{L_r}\lambda_{rq} = \dfrac{R_r L_M}{L_r} i_{sq} - \omega_{slip}\lambda_{rsd} \end{cases} \tag{2.66}$$

but in FOC condition $\lambda_{rd} = \left|\bar{\lambda}_r\right|$ and $\lambda_{rq} = 0$, and we have

$$\begin{cases} \dfrac{d\lambda_{rd}}{dt} + \dfrac{R_r}{L_r}\lambda_{rd} = \dfrac{R_r L_M}{L_r} i_{sd} & (2.67) \\ 0 = \dfrac{R_r L_M}{L_r} i_{sq} - \omega_{slip}\lambda_{rsd} & (2.68) \end{cases}$$

The first equation (2.67), rewritten on Laplace domain, becomes

$$\Lambda_r(s) = \frac{L_M}{1 + s\tau_r} I_{sd}(s) \tag{2.69}$$

where $\tau_r = \frac{L_r}{R_r} = \frac{L_\varphi}{R_{rs}}$ is the electrical time constant of the rotor.

The second-one (2.68), rewritten by ω_{slip} becomes

$$\omega_{slip} = \frac{\frac{R_r L_M}{L_r} i_{sq}}{\lambda_r} \tag{2.70}$$

and this ω_{slip} is the slipping speed which allows to have the q-component of rotor flux null.

2.6 MTPA vs FOC

Starting from rotor voltage equation with its d-q components (2.66), in the steady-state condition they become

$$\begin{cases} \frac{R_r}{L_r}\Lambda_{rd} - \Omega_{slip}\Lambda_{rsq} = \frac{R_r L_M}{L_r} I_{sd} \\ \frac{R_r}{L_r}\Lambda_{rq} + \Omega_{slip}\Lambda_{rsd} = \frac{R_r L_M}{L_r} I_{sq} \end{cases} \tag{2.71}$$

Resolving by Λ_{rd} and Λ_{rq}, it is possible to realize the Fig.2.5, which allows to observe the different trend of the rotor flux (Λ_r) in the different rotation speed condition (Ω_x^r) in steady-state regime.

In the different working circumstance, it is possible to observe what happens if we adopt a different control strategy: the diameter of the circumference is directly proportional to the stator current I_s and the different working condition is placed along the circumference. How we have seen before, the FOC condition is given when we adopt a reference system synchronous with the rotor flux and its d-axis superposed to it.

Always looking to the figure, the available motor torque is described by the blue area enclosed by the triangle made from the circumference diagonal and the rotor flux vector. To find the MTPA condition, i.e. the maximum torque available for a certain stator current I_s, it is necessary to identify the maximum of the blue area. This is given by a particular condition when the angle ϑ (between the two vectors) is equal to 45°.

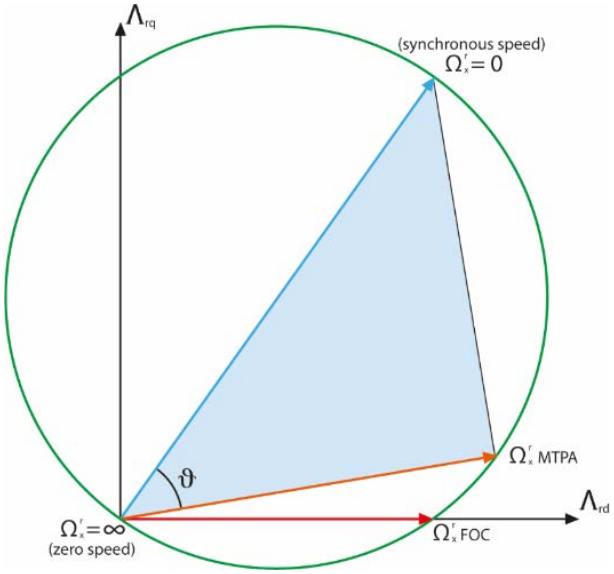

Figure 2.5: Rotor flux trend in the different speed conditions

This means that the MTPA working condition is not the same of the FOC one, as showed in the Fig.2.6. Indeed, FOC aim is to permit a decoupled control of rotor flux by i_{sd} and motor torque by i_{sq}, and this could not be the best efficiency condition.

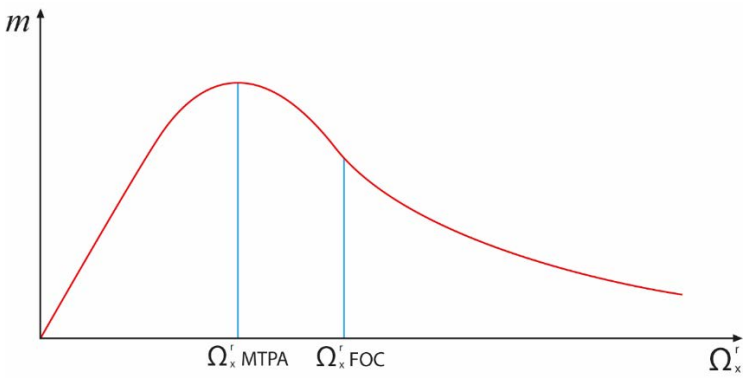

Figure 2.6: Torque in the different speed conditions

3

Simulation scheme and its behaviour

How we have seen in the previous chapter, electrical parameters are extremely important not only to observe the electromechanical energy conversion, but for the logic scheme too. During its normal work, an EM can handle long sessions with a constant load without any break. Especially under these conditions, the engine can easily overheat and its electrical parameters could change significantly, leading to a worsening of the control performance.
Normally, EM datasheets are described with constant value (and their controlling scheme too) and it is not possible to know their variations during the different working condition. In fact, usually the cooling system could be made to work preventively on the sole assumption of the possible EM temperature, wasting energy and performance of the entire system.
Speaking of an IM, electric drive system is developed following a Field Oriented Control logic, which it is described by engine electrical parameters. If the FOC is not calibrated instant by instant according to the real electrical values, it is possible to lose its FOC condition, spending more energy to obtain the same final demanding load torque. Or worst, with engines realized by permanent magnets it is extremally important to maintain the correct temperature to not demagnetize them, and this could be an irreversible damage that could permanently cause the loss of EM performance.

3.1 Thermal and hysteresis behaviours

Electrical resistance value of a system depends on its geometry and the type of material from which it is made from, and that is

$$R = \rho \frac{l}{S} \tag{3.1}$$

where ρ is the average electrical resistivity of the specific material, l is its length and S is the surface of the analysed system. While the geometric parts stay generically constant during the time, the electrical resistivity depends on the temperature according to a certain specific coefficient for each different material. This is true for linear trend material. This coefficient is called temperature coefficient (α) and allows to identify the electrical resistivity in a certain temperature (T, usually expressed in Kelvin) by the law

$$\rho_T = \rho_o(1 + \alpha(T - T_o)) \tag{3.2}$$

where ρ_o is the electrical resistivity at *20°C* (*293.15 K*).
An increasing electrical resistance can lead to a rise of the heat losses due to Joule effect, where it is

$$P_j = Ri^2 \tag{3.3}$$

Inductances suffer of the same problem but, being characterized by very small electrical resistance value, temperature variation has very little impact to the heat losses behaviour. However, they are characterized by other problems that cannot always be overlooked.
Working on alternate feeding system, inductors are continuously charged and discharged allowing a certain energy flow through the circuit. The trend of this energy flow depends on the type of material and it can be linear or not linear. In a first step, usually, to simplify electromechanical studies this trend is considered linear.
An inductor is characterized of certain value called inductance (L) defined as

$$L = \frac{\varphi_c(t)}{i(t)} \tag{3.4}$$

where $\varphi_c(t)$ is the concatenated flux from the inductor and $i(t)$ the current crossing it.

Every material is characterized by a certain magnetic permeability (μ) (or even magnetic constant) and that could be not linear; especially ferromagnetic materials, it could be particularly consistent with a high dependence in function of induction magnetic field (B) and magnetic field (H). Inductors with ferromagnetic cores experience additional energy losses due to hysteresis and eddy currents in the core, which increase with frequency. At high currents, magnetic core inductors also show sudden departure from ideal behaviour due to nonlinearity caused by magnetic saturation of the core. In these conditions, the inductance value could be no more a constant and it is necessary to evaluate its trend looking to these different cases.

3.1.1 Look Up Table (LUT)

How we have seen before, EMs manufactures do not provide accurate enough datasheets, usually representing the values on nominal working conditions. This is due to the fact that EMs have an extremely non-linear behaviour, so the parameters that characterize them vary significantly depending on load conditions, such as voltage and current, and on external conditions, such as the temperature. A considerable testing effort is required to obtain these informations, with the associated cost in terms of energy, instrumentation and highly skilled personnel.

In second way, to obtain the parameters trend it is necessary to evaluate every single aspect by a FEM application, requesting lot time to calculate every part. For a real-time control response, this is not acceptable. To develop a real-time capable control, a possible intelligent approach is to extract in real-time all the desired parameters relative to the EM, akin to having a massive Look Up Table (LUT).

A Look Up Table (LUT) is an array that replaces runtime computation with a simpler array indexing operation. These tables may be pre-calculated and stored in static program storage, calculated as part of a program initialization phase, or even stored in hardware in application-specific platforms. In this case, it is used to validate input values by matching against a list of valid (or not valid) items in an array. The LUT is obtained by a FEM simulation and it can be realized with different levels of quality depending on the type of application. For example, for a real-time implementation is not required a high-resolution knowledge of the

parameters, indeed it is preferred to have a performing and sufficiently accurate control rather than a high-fidelity parameters estimation.

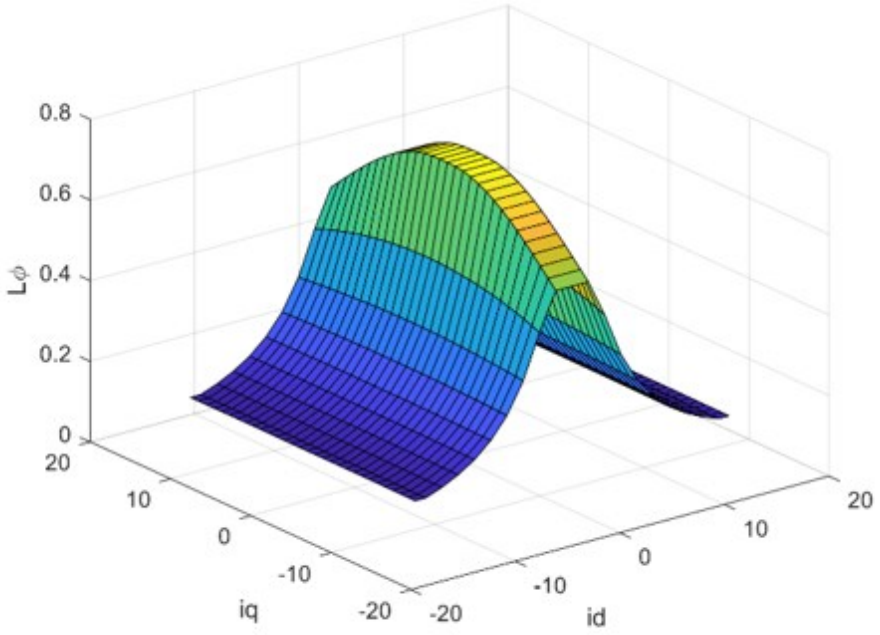

Figure 3.1: Look Up Table of L_{φ}

As showed in the Fig.3.2 of the Simulink model, EM electrical parameters are evaluated starting from stator currents i_d e i_q as input. These could be considered as coordinates to find the respective values that were already pre-calculated for all possible EM working conditions.

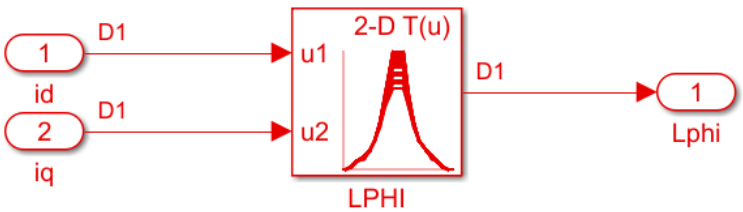

Figure 3.2: Simulink Look Up Table working condition

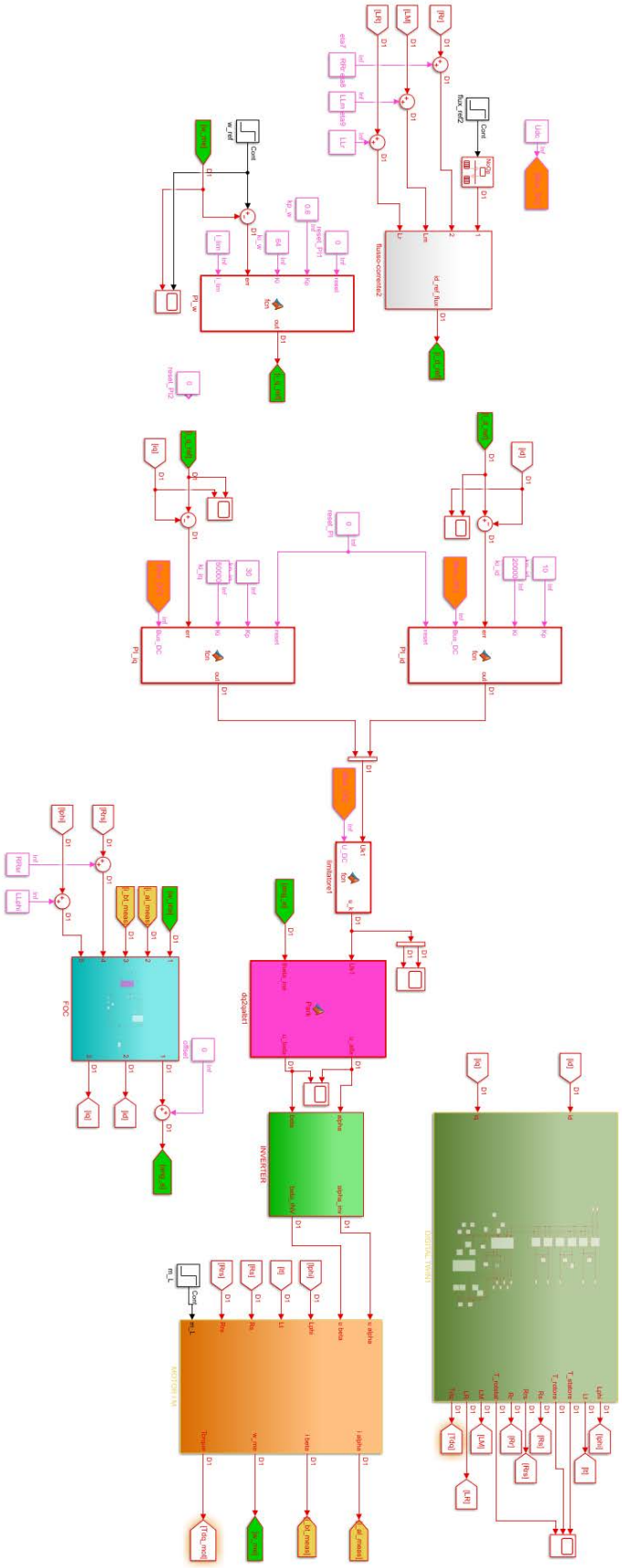

Figure 3.3: Overview of the Simulink scheme

3.2 Simulink scheme description

An overview of the Simulink scheme is showed in the Fig.3.3. For a first evaluation of the EM behaviour, it is necessary to observe the logic behind every single scheme part of the scheme that makes up the control system. Still talking about an Induction Motor (IM), the complete simulation scheme is composed by:

- *Speed regulator* (R_ω): Fig.3.4, by comparing reference speed (ω_m^*) with the real (or estimated) speed (ω_{me}), a PI regulator provide to evaluate the q-reference of stator current (i_q^*).

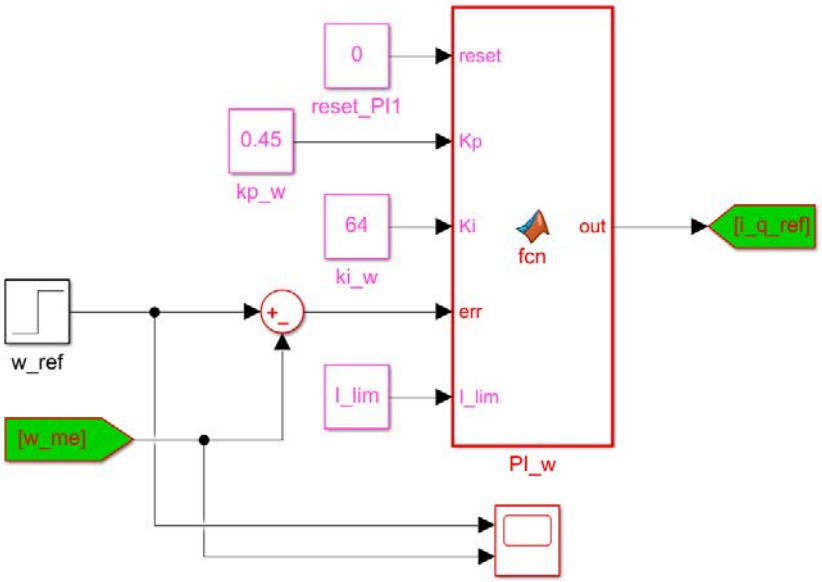

Figure 3.4: Simulink speed regulator block

- *Flux regulator* (R_λ): Fig.3.5, a flux reference (λ_r^*) is required to evaluate the d-reference stator current (i_d^*), which have always to be adequate to the real IM parameters trend. Being it characterized from motor parameters, it is useful to evaluate its trend with constant (pink blocks) or variable values (red blocks) defined by the Digital Twin. In these simulations, it will be always considered as constant on its nominal value.

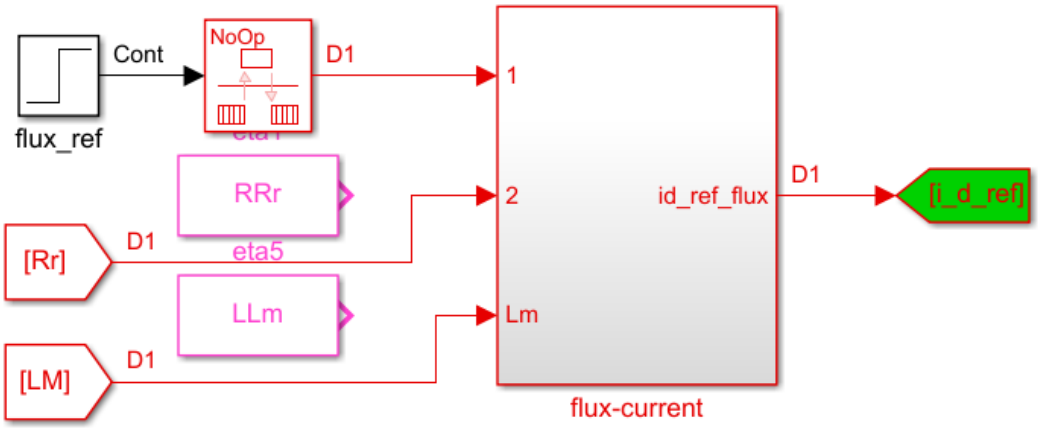

Figure 3.5: Simulink flux regulator block

- *Current regulator (R_i)*: as showed in the Fig.3.6, the two reference currents evaluated in the previous blocks are compared with their respective measured currents, and the possible error will be the input of a PI regulator that will evaluate the d-q reference voltage values (u_d and u_q). These last two signal values will be transformed in the stationary reference system α-β thanks to the angle ϑ_{me} (i.e. rotor position) estimated by the FOC block. by an inverter to real physics voltage to use to powering the IM. The PI constants have been evaluated adopting the Ziegler-Nichols method, that will be explained in the next chapter.

- *IM block*: it represents the real IM behaviour by a block scheme where, to replace the electrical parameters with the dynamic values estimated by the Digital Twin block, it is realized with more inputs than usual as showed in the Fig.3.7. Normally these inputs are only the two inverter voltages by assuming constant every electrical component inside the motor. To applicate the evaluated parameters by the Digital Twin, motor block is realized with other inputs, like L_φ, L_t, R_s and R_{rs}. Looking to the Fig.3.8, the IM scheme is modified to allow to set the different electrical parameters, represented with red line.

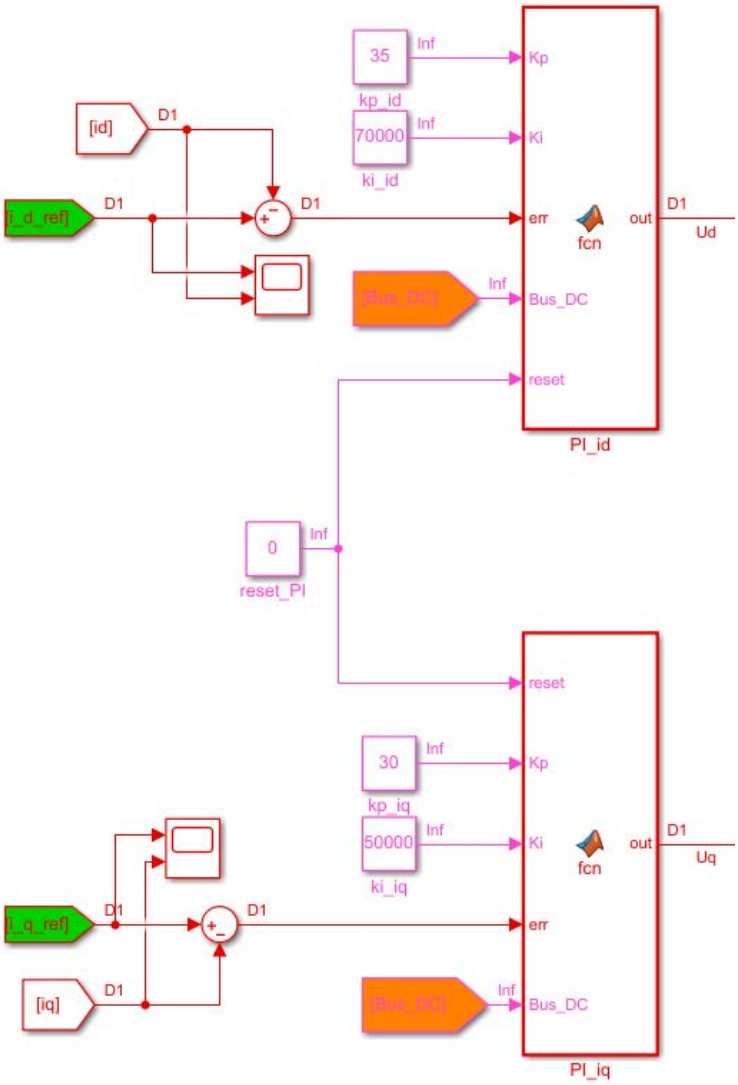

Figure 3.6: Simulink current regulator blocks

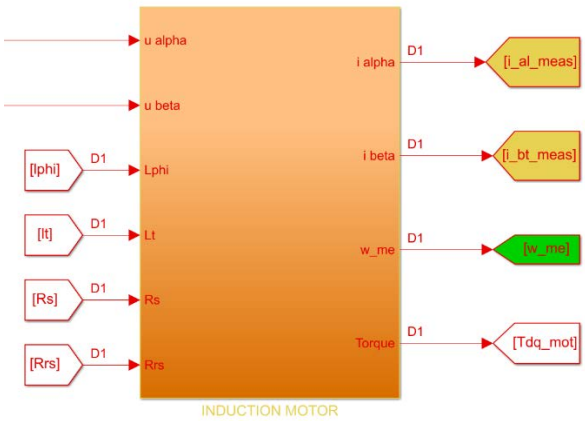

Figure 3.7: Simulink Induction Motor block with more inputs than usual

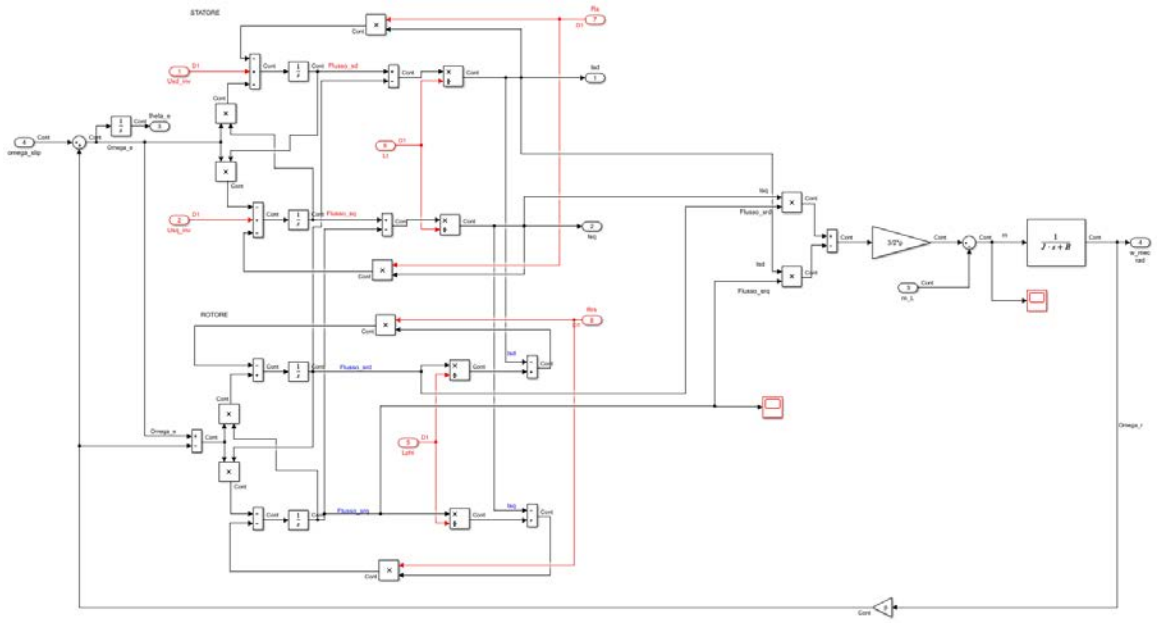

Figure 3.8: Inside the Simulink Induction Motor block, modified to allow to set the electrical parameters as input

- *FOC block*: Fig.3.9, how we have seen previously, for a smarter and reliable control it is necessary to adopt a reference system synchronous with rotor flux ($d^{\lambda}q^{\lambda}$), where this way to control the IM is called Field Oriented Control (FOC). Starting from stator currents (i_{sd} and i_{sq}) and rotor rotation speed (ω_{me}), this block rebuilds rotor flux vector with which it is possible to calculate the slipping speed and, by summing ω_{me}, it is obtained flux rotation speed ω_{λ}. Given its rotation speed, it is easy to get the position ϑ_{λ}. The input R_{rs} and L_{φ} values can be easily switched from constant to variable trend to evaluate FOC reliability during the different parameter conditions.

- *Digital Twin block*: with the two currents measured in the motor block as input, the real electrical parameters are identified thanks to the Look Up Table (LUT) which had already been previously realized. DT block is able to evaluate many other aspects and, considering the importance of this block, it will be presented in detail later.

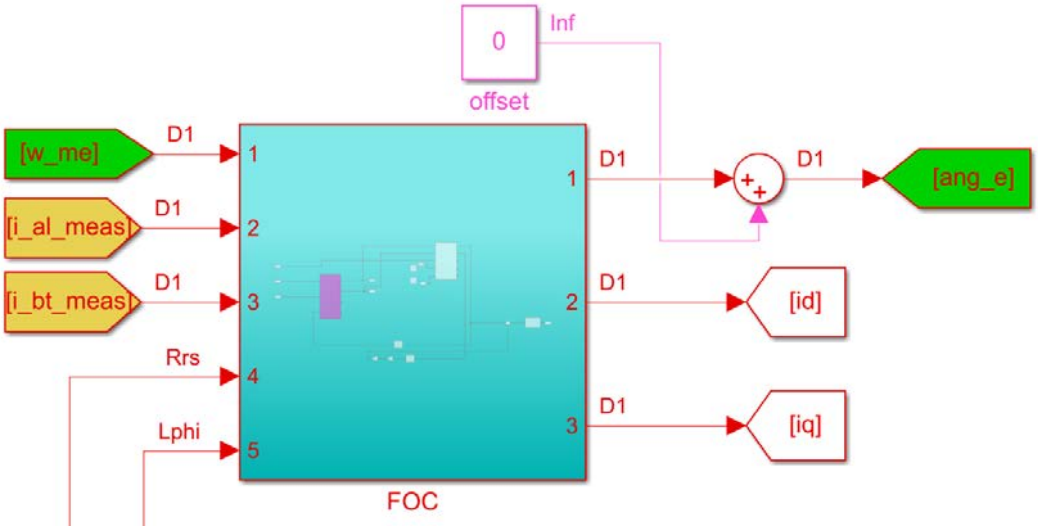

Figure 3.9: Simulink FOC block with electrical parameters as input to permit to evaluate their effect on the controlling behaviour.

3.2.1 PID regulation adopting Ziegler-Nichols method

A PID regulator is a controller where, evaluating the error between a reference value and its measured one, applies a correction based on its Proportional (P), Integral (I) and Derivative (D) terms, hence the name. It can be represented by the equation

$$u(t) = K_P\, e(t) + K_I \int_0^t e(\tau)d\tau + K_D \frac{de(t)}{dt} \tag{3.5}$$

and, applying the Laplace transform in (s) it becomes

$$U(s) = E(s)\left[K_P + \frac{K_I}{s} + K_D s\right] \tag{3.6}$$

Every part has a specific role:

- (P) Proportional term, it is directly proportional to the input error by a gain factor K_P. Using proportional control alone will result in an error between the reference and the

actual process value, because it requires an error to generate the proportional response. If there is no error, there is no corrective response.

- (I) Integral term, it accounts for past error values and integrate them over time to produce the integral term, which aim is to eliminate the residual error by adding a control effect due to the historic cumulative value of the error. When the error is eliminated, the integral term will stop growing. It is characterized by a gain factor K_I.

- (D) Derivative term, it estimates the future trend of the error evaluating its rate of change. More rapid is the change and greater will be the controlling response. It is characterized by a gain factor K_D.

Every PID must be calibrated according to the system where it is integrated by choosing the proper gain values K_P, K_I and K_D. There are lots of different theorist or practical methods the evaluate these values, and we have used the Ziegler-Nichols one. It is one of the most empirical adopted method and it consist in a few easy steps:

1) Starting from a closed loop scheme, integrative (I) and derivative (D) gain values must be set to zero ($K_I = K_D = 0$).

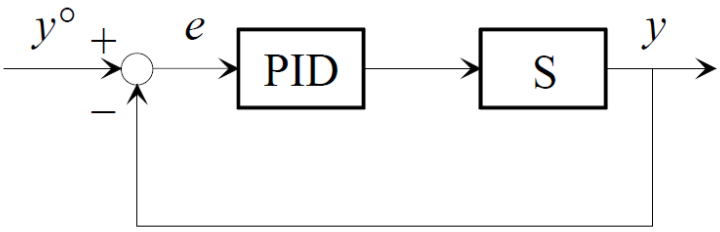

Figure 3.10: closed loop of the control scheme

2) With very small value of K_P, a step signal is applied as reference value.

3) Progressively, the previous point must be repeated for each K_P value, which have to be increase step by step. It is necessary to do this operation until a permanent oscillation is established inside the closed loop, like in the Fig.3.11.

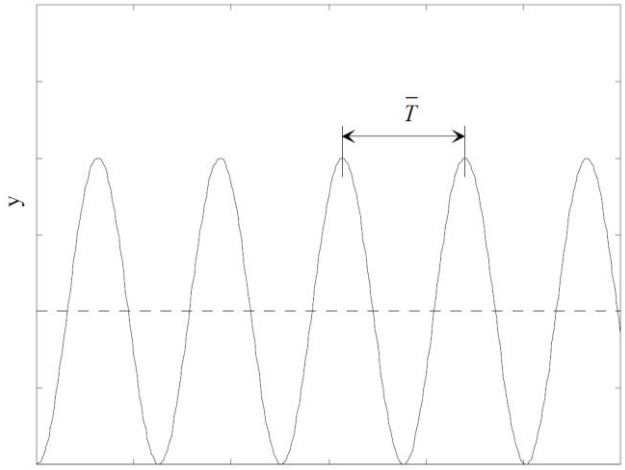

Figure 3.11: Period of the permanent oscillation for the correct K_P value

4) Defined $\overline{K_P}$ as gain value of this permanent oscillation and $\bar{T}$ its oscillation period, the PID values will be calibrated following the Tab.3.1

	K_P	T_I	T_D
P	$0.5\overline{K_P}$	/	/
PI	$0.45\overline{K_P}$	$\frac{\bar{T}}{1.2}$	/
PID	$0.6\overline{K_P}$	$\frac{\bar{T}}{2}$	$\frac{\bar{T}}{8}$

Table 3.1: P, PI and PID different value combination

where $T_I = \frac{K_P}{K_I}$ and $T_D = \frac{K_D}{K_P}$.

This method could not always be applicable, especially for instable system where could be dangerous working on its stability limit or, also for big K_P gain value, it is not sure reach its permanent oscillation.

3.2.2 Digital Twin block

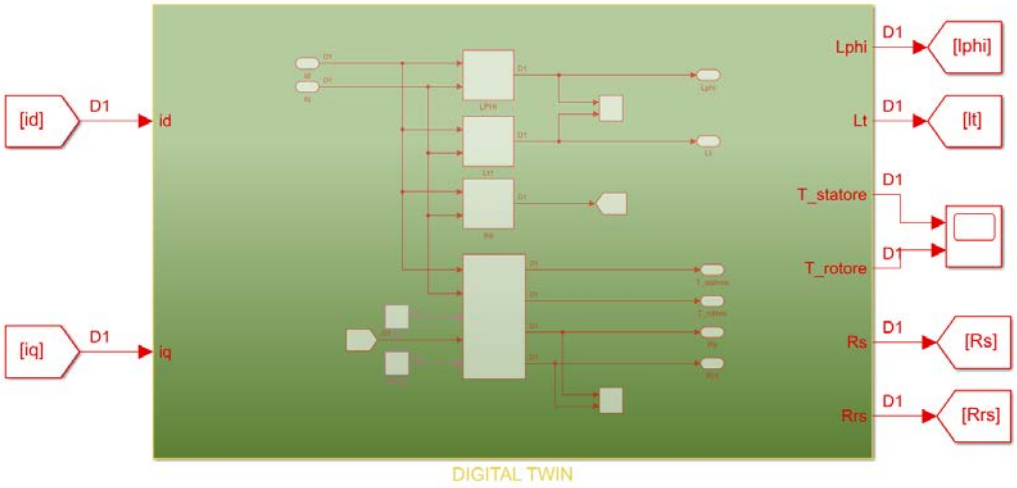

Figure 3.12: Digital Twin block

Digital twin block could be developed for lot of different aims depending on the role that it will have in the system. In this case, it is designed to identify the real instantaneous electrical parameters to evaluate the different behaviours of the electric drive control, so as to study how its application could introduce better performance. Starting from stator d-q currents, it is able to rebuild the principal electrical quantities. To do that, Digital Twin block is made by more different parts:

- *Electromagnetic parameters estimation*, where the inductance values, i_{rq} rotor current and a torque estimation are defined by the Look Up Table (LUT) pre-realized. It is particularly efficient thanks to the high quality of the LUT and its simple operating mechanism, where the respective working values is given by a quick search for the corresponding match point of i_d and i_q currents.

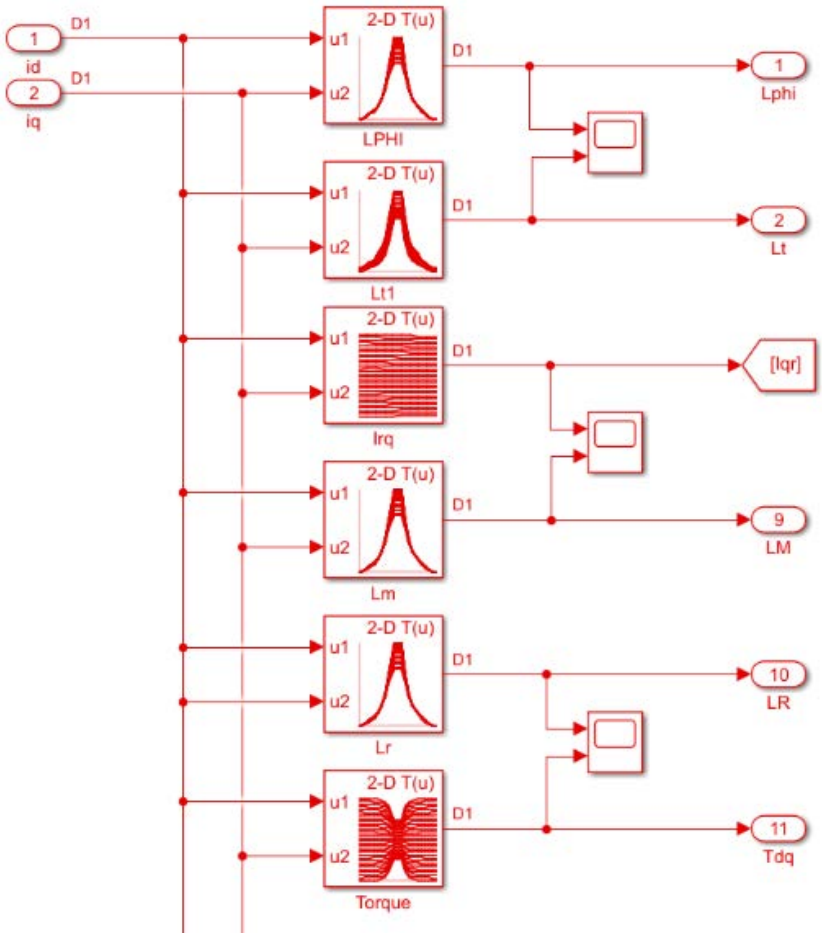

Figure 3.13: Parameters estimation thanks to the different Look Up Table

- *Thermal trend estimation*, where it is possible to evaluate every moment the temperature where we want by using a virtual sensor. In this way resistance value can be estimated with a good approximation in real-time (Fig.3.14 red). Temperature is an important value to consider also for the cooling system due to the impossibility to measure it directly by a physical sensor positioned inside motor's rotor. The "Predictive Twin" block (Fig.3.14 green), is one of the other possible DT advantages where, if the EM has to work for many hours without changing its working condition, it is possible to predict the temperature that will be reached after a certain time.

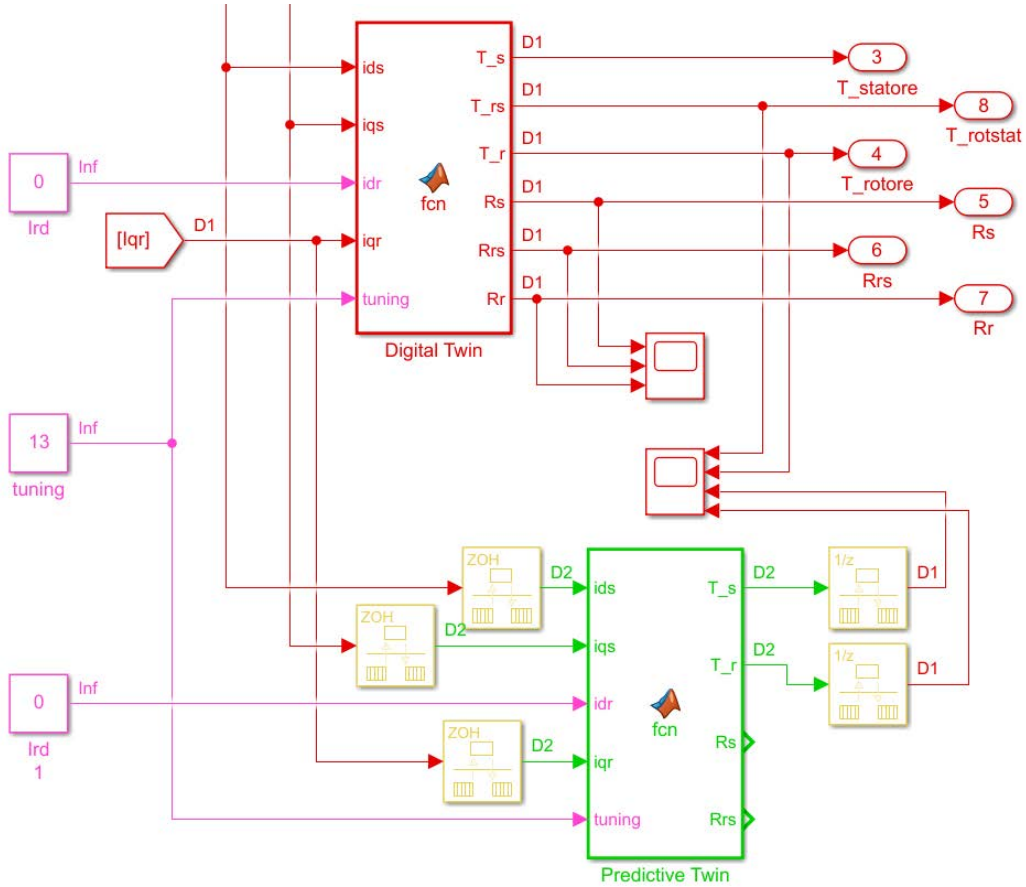

Figure 3.14: Digital Twin (red) for temperature and resistances estimation, Predictive Twin (green) to estimate the temperature during stationary condition

The function block (*fcn*) is the heart of the digital twin block for thermal application where, thanks to a reduced order model of the motor, it is possible to insert a virtual sensor everywhere we want. By resolving a very small numbers of ordinary differential equations, temperature trend is evaluated starting from the currents every 1e-6 second.

Its operation is based on the paper [8] "*Computationally efficient 3D finite-element based dynamic thermal models of electric machines*": the idea is to decompose the full order system into two parts by using the orthogonality property of the thermal eigenmodes and, taking only the significantly exited eigenmodes one, are used to build the dynamic model, while the others are treated as static modes. It is therefore necessary to realize an automatic process based on a proposed "extent of excitation" calculation to select the eigenmodes that should be included in the reduced-order dynamic model (ROM).

Starting from FEM model of the motor, the thermal behaviour is represented by ordinary differential equation (ODE) like

$$D\vec{t} + K\vec{t} = \vec{q} \tag{3.7}$$

where $\vec{t}$ is the nodal temperature vector of the FE mesh, K is the FE matrix that corresponds to thermal conductivity, and D is the FE matrix that corresponds to specific heat. Both K and D are $n\ x\ n$ symmetric matrices generated by the FEM assembly process, where n is the number of nodes in the 3D FE mesh. The vector $\vec{q}$ corresponds to the inputs of the thermal model and it can be categorized as

$$\vec{q} = \sum_k P_k \overrightarrow{f_k} + \sum_l H_l \overrightarrow{g_l} \tag{3.8}$$

The vectors $P_k\overrightarrow{f_k}$ correspond to different loss mechanisms of the machine, including conduction losses, core losses, friction and windage losses. The scalar P_k is the total amount of loss, while the vectors $\overrightarrow{f_k}$ correspond to the normalized loss distribution in the machine. The vectors $H_l\overrightarrow{g_l}$ correspond to convective heat transfer on the different boundaries of the machine. The scalar H_l is the heat flux density, while the vectors $\overrightarrow{g_l}$ correspond to the normalized heat flux distribution on the machine boundaries.

An eigenmode is defined as an eigenvector $\overrightarrow{v_i}$ associated with an eigenvalue λ_i that satisfies the generalized eigenvector equation applied to the (3.7)

$$(K - \lambda_i D)\overrightarrow{v_i} = 0 \tag{3.9}$$

Both K and D are symmetric and they can be diagonalized in *d* and *k* matrices as

$$\begin{cases} V^T D V = d \\ V^T K V = k \end{cases} \tag{3.10}$$

and successively separate the eigenvectors into *m* "dynamic (*d*)" and (*n* – *m*) "static (*s*)" vectors, so

$$\begin{cases} V_d^T D V_d = D_d \\ V_s^T D V_s = D_s \end{cases} \tag{3.11}$$

$$\begin{cases} V_d^T K V_d = K_d \\ V_s^T K V_s = K_s \end{cases} \tag{3.12}$$

It is possible to re-write the (3.7) using a change of basis $\vec{t} = V\vec{x}$, and it becomes

$$d\vec{x} + k\vec{x} = V^T\vec{q} \tag{3.13}$$

To reduce the order of the dynamic system, the "static" eigenmodes are assumed to converge to their steady-state values instantaneously and $\vec{t}$ becomes

$$\vec{t} = V_d\overrightarrow{x_d} + (K^{-1} - V_d k_d^{-1} V_d^T)\vec{q} \tag{3.14}$$

Substituting (3.14) in the (3.8), the temperatures can be calculated as

$$\vec{t} = V_d\overrightarrow{x_d} + \sum_k P_k\overrightarrow{u_k} + \sum_l H_l\overrightarrow{s_l} \tag{3.15}$$

where $\overrightarrow{u_k}$ and $\overrightarrow{s_l}$ can be precalculated by performing matrix-vector solves

$$\begin{cases} \overrightarrow{u_k} = (K^{-1} - V_d k_d^{-1} V_d^T)\overrightarrow{f_k} & (3.16) \\ \overrightarrow{s_l} = (K^{-1} - V_d k_d^{-1} V_d^T)\overrightarrow{g_l} & (3.17) \end{cases}$$

The (3.7) is finally expressed by its dynamic reduced order model by

$$d_d\overrightarrow{x_d} + k_d\overrightarrow{x_d} = \sum_k P_k\overrightarrow{f_{v,k}} + \sum_l H_l\overrightarrow{g_{v,l}} \tag{3.18}$$

where vectors $\overrightarrow{f_{v,k}} = V_d^T\overrightarrow{f_k}$ and $\overrightarrow{g_{v,l}} = V_d^T\overrightarrow{g_l}$ can also be pre-calculated. Since both d_d and k_d are diagonal matrices, all the "dynamic" eigenmodes are decoupled and can be simulated separately.

To decompose the system, the most significantly excited eigenmodes are considered as dynamic modes. To select the eigenmodes, the extent of excitation of the *i*-th eigenmode for each type of excitation is calculated

$$E_i = \begin{cases} \vec{v}_i^T \vec{f}_k \\ \vec{v}_i^T \vec{g}_l \end{cases} \tag{3.19}$$

To select the eigenmodes that need to be modelled as dynamic states, a threshold is set and the eigenmodes that have at least one extent of excitation that exceed the threshold value are selected as the dynamic modes.

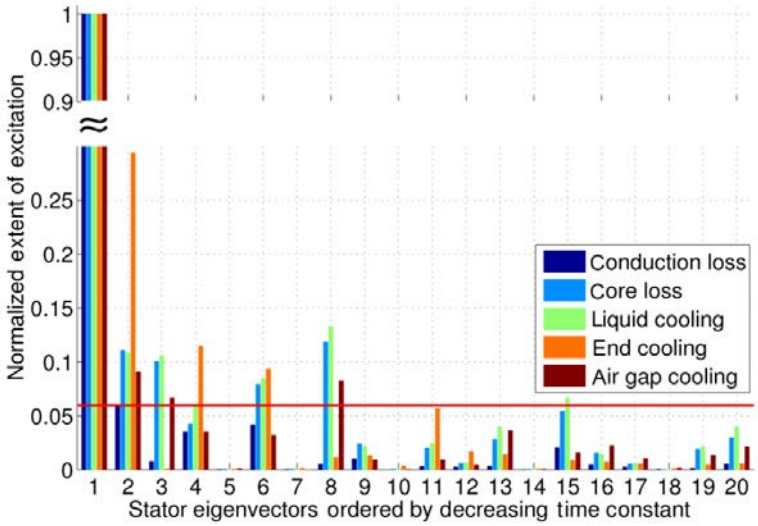

Figure 3.15: Eigenmodes selection by a threshold value

Looking to the Fig.3.15, the threshold value is represented by the red line and equal to 0.06. This value permit to choose the 1st, 2nd, 3rd, 4th, 6th, 8th and 15th eigenmodes as dynamic modes and result in a 7th-order model for the stator. Thus, adjusting the threshold value, the number of dynamic states included in the reduced-order model can be automatically adjusted. Once obtained a faithful following trend, the reduced-order model is generated.

4

Simulations

The aim of these simulations is to observe which advantages is possible to obtain by applying the Digital Twin parameter estimations in the different scheme blocks of the electric drive system, while the motor is always described with evolving parameters. Being an IM, we will focus on the FOC working condition given the importance of having separate control of motor excitation (i.e. rotor flux λ_r by i_{sd}) and applied torque (by i_{sq}). This datasheet corresponds to a system for an irrigation usage that could work for many hours without stopping. Such condition corresponds to lots of the classic industrial application of the electric motors, where it is necessary to guarantee reliability and stability during all the working condition.

4.1 Simulation data

In this simulation we will observe a particularly extreme case where the IM is not equipped with a cooling system, and the temperature could increase without any limit. It is characterized by a simulation time of 700 [s], 30 [rad/s] of reference speed and 15 [Nm] of load torque.

Looking to the Fig.3.14, the "*Tuning*" block is used to speed up the IM electric parameters evolving trend, with the aim to reduce time simulation without changing its behaviour. It multiplies currents trend inside the DT block to cause a faster evolution of the temperature (i.e. of the parameters), without affecting the original system. For the first simulation we will set tuning value at 13.

Upcoming simulations have been done with the aim of evaluating the importance (and thus the influence) of the singular parameters on the best fitting FOC condition, by adopting the constant or the estimation one parameter made by the DT block. Usually, how we have seen,

motor parameters are given with any indication of their different temperature or working condition trend and the electric drive cannot follow the real situation.

Being the purpose of these simulations to study the Field Oriented Control behaviours on different conditions, IM block is described with the Digital Twin estimated parameters to represent a real thermal trend (Fig.4.3), while all the other blocks that compose the electric drive system are defined with constant or variable parameters, where they will be enabled manually for the different simulation conditions. Looking to the Fig.4.1 and Fig.4.2, it is possible to identify the Digital Twin estimated parameters looking to the red square-arrow blocks, while the constant values are described by the pink square block.

Analysing every single part of the electric drive, there are only two principal blocks that are described by motor's parameters: the FOC block (Fig.4.1) rebuilt rotor d-flux vector starting from stator currents i_s and rotor speed ω_{me} and, with R_{rs} and L_{φ}, evaluate the slipping speed to obtain the rotor flux rotational speed, and so its position; the flux regulator block (Fig.4.2) evaluate the i_d reference current needed to obtain a certain demanding flux (in this simulation it is equal to 1.7 Vs and always constant), where it needs R_r, L_M and L_r to calculate the correct necessary current.

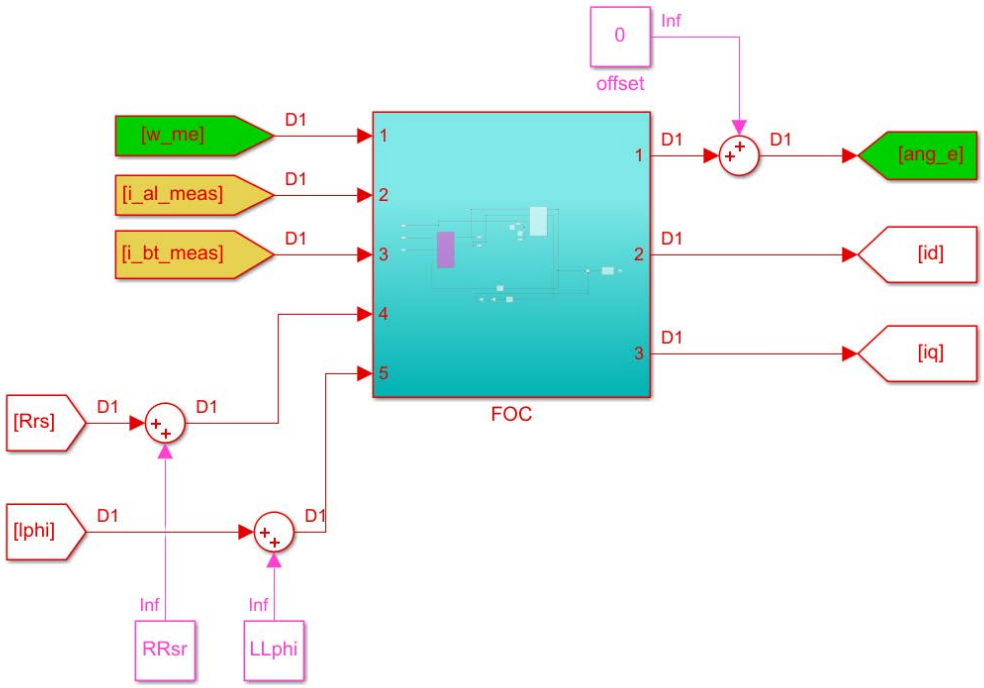

Figure 4.1: FOC block with different input

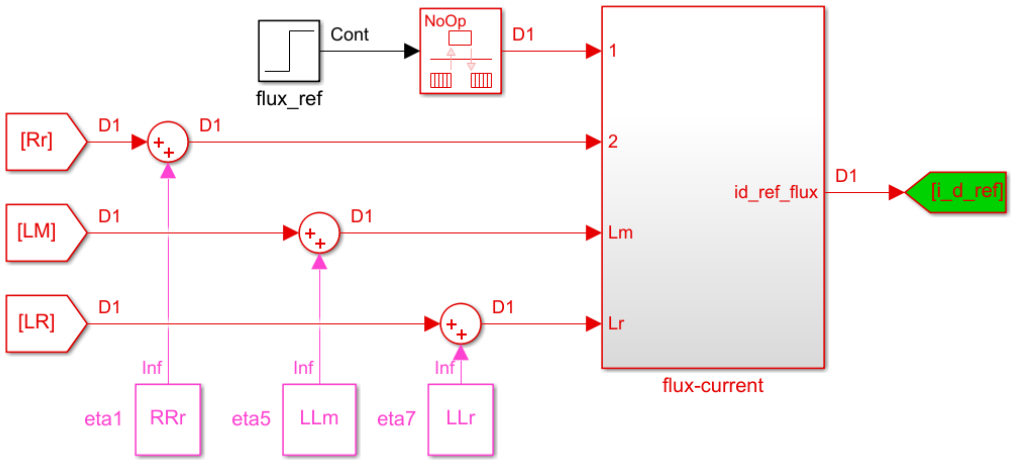

Figure 4.2: Flux regulator block with different input

While IM block is continuously updated with Digital Twin estimated parameters, the other blocks are described by constant or adequate values for evaluate the different drive behaviours. In the first part it will be studied the behaviour of the electric drive with constant values (as it is in the major of the real application), and, successively with their dynamic trend. In a second moment, to evaluate which is the most influential parameter that have to be defined with major precision, the electric drive will be simulated adopting every parameter as constant, except the one that we want to study the influence.

Looking to the typology of the parameters, we expect to see how inductance values will be depending from current trends (being them the source of the concatenated flux), how it is possible to observe looking to the Look Up Table in the previous chapter. As far as resistance is concerned, the values will be directly connected with temperature trend, which is estimated by the Digital Twin block and used to evaluate the instantaneous values starting from the resistivity of the material that compose the conductors (copper).

In the next page there are the principal data of the elements that compose the simulated system

```
%========================== Inverter DATA ==============================


Udc = 300;                  % BUS DC voltage [V]
f_s = 10e3;                 % Inverter switching frequency [Hz]
t_s = 1/f_s;                % Inverter switching time [s]
Tc = t_s;                   % Sampling time [s]
Ts = Tc;                    % Sampling time [s]
T_tot = 700;                % Simulation time [s]


%======================== Induction Motor DATA ==========================


p = 1;                      % Polar pairs
RRs = 2.982;                % Stator resistance [Ω]
RRr = 2.978;                % Rotor resistance [Ω]
LLm = 0.41;                 % Mutual inductance [H]
LLM = LLm;                  % Mutual inductance [H]
LLt = 0.0148;               % Transitional stator inductance [H]
LLr = 0.42;                 % Synchronous rotor inductance [H]

LLphi = LLM^2/LLr;          % Lphi inductance [H]
LLs = LLphi+LLt;            % Synchronous stator inductance [H]
RRsr = (LLm^2/LLr^2)*RRr; % Rotor resistance as seen from stator side [Ω]
tau_r = LLphi/RRsr;         % Rotor time constant [s]

U_lim = Udc/sqrt(3);        % Phase voltage magnitude limit [V]
I_lim = 12;                 % Magnitude current limit [A]


%============================ Load DATA ================================


B = 1e-5;                   % Estimated friction [Nms]
J = 0.02;                   % Estimated inertia [Kgm²]
m_L = 28;                   % Breaking torque [Nm]


%========================== Drive DATA ==============================


Omega_ref = 30;             % Speed reference [rad/s]
Flux_ref = 1.7;             % Flux reference [Vs]
kp_id = 10;                 % Kp of id PI regulator
ki_id = 20000;              % Ki of id PI regulator
kp_iq = 30;                 % Kp of iq PI regulator
ki_iq = 50000;              % Ki of iq PI regulator
kp_w = 0.06;                % Kp of speed PI regulator
ki_w = 64;                  % Ki of speed PI regulator
```

4.2 Simulations

Before presenting results of the simulations, it is very important to remember how the simulation scheme is organized and which is the aim of this work: the IM block is always characterized by adaptive parameters elaborated by the Digital Twin block, simulating a real behaviour trend (as illustrated in the Fig.4.3). Instead, the other blocks that compose its electric drive, the one which are described by motor's parameters, are adequate with constant or variable values to evaluate the influence of them in the controlling behaviour.

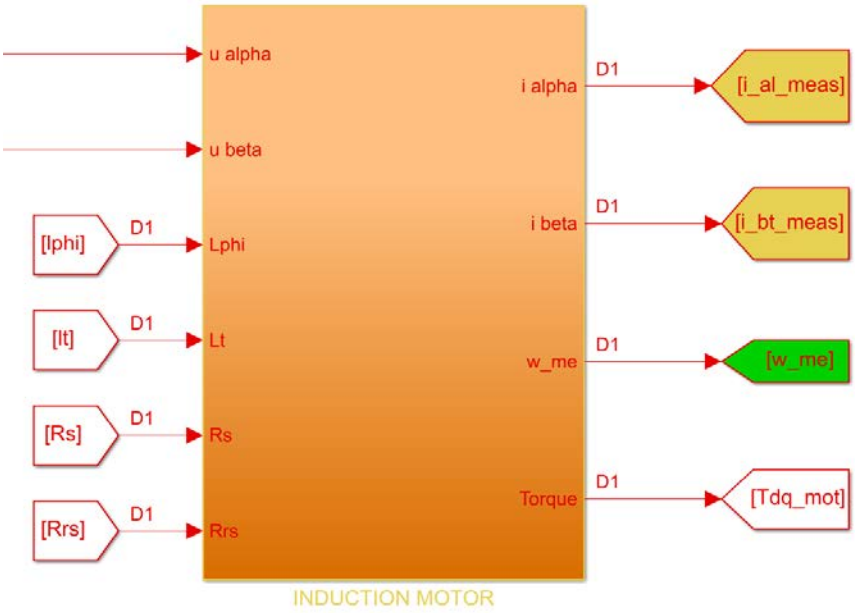

Figure 4.3: Induction Motor block is always described with the adapting parameters evaluated by the Digital Twin block

By enabling constant or estimated valued manually, will be presented the results of the four simulations with different input values in the two blocks (showed in the Fig.4.1 and Fig.4.2), in order:

1- All constant values (pink)
2- All variable values (red)
3- *L* variable from Digital Twin (red) and *R* constant (pink)
4- *R* variable from Digital Twin (red) and *L* constant (pink)

4.2.1 Constant values as input

In these conditions only the IM block is working with adapting parameters provided by the Digital Twin block. Conversely, all the other blocks are described by constant values (R_{rs}, R_r, L_φ, L_M and L_r) to evaluate what happened if the reference system elaborated by the FOC block is not synchronized with the real one presented in the motor.

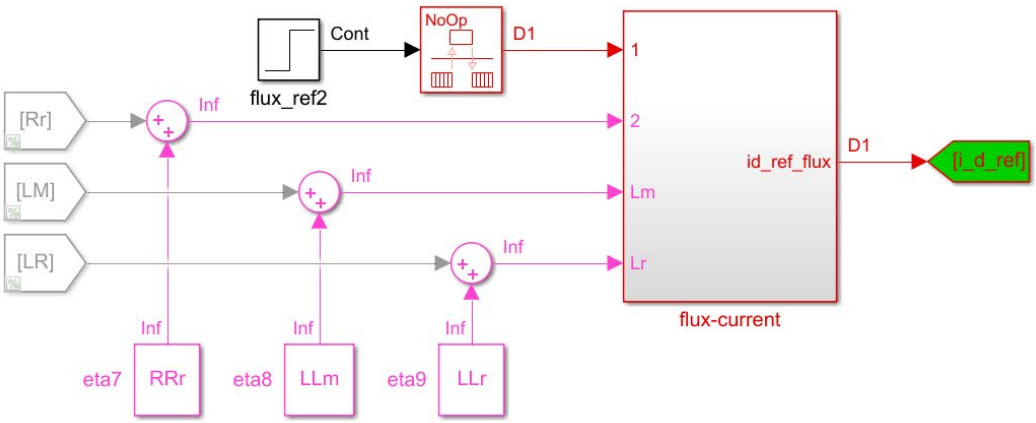

Figure 4.4: Flux block with constant parameters as input

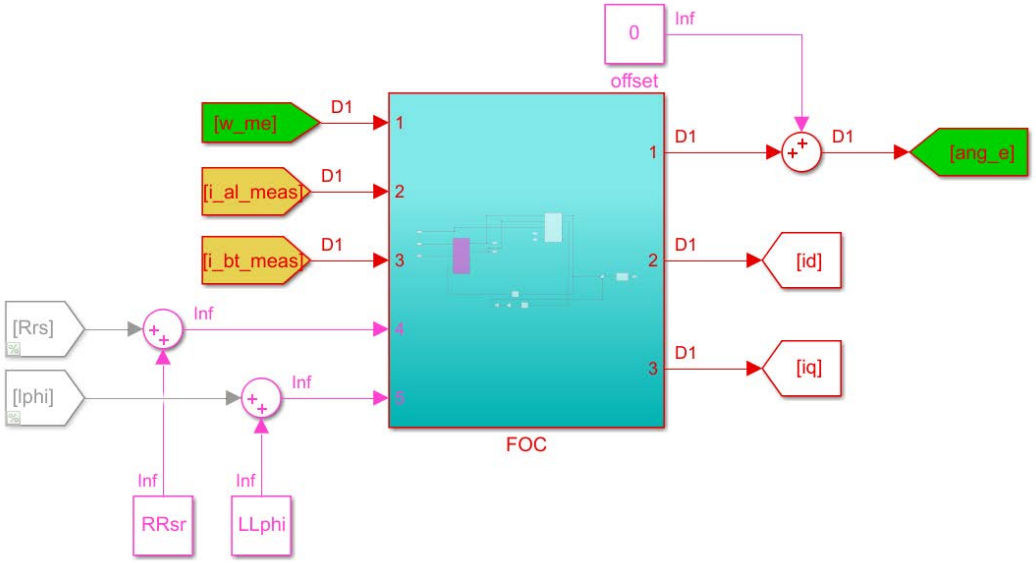

Figure 4.5: FOC block with constant parameters as input

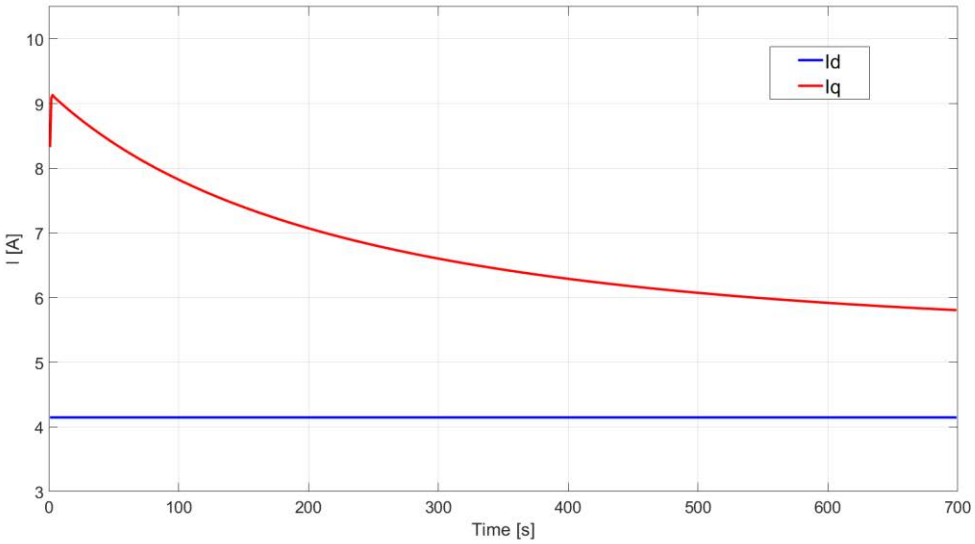

Figure 4.6: i_d (blue) and i_q (red) currents with constant values

The Fig.4.6 shows the i_d and i_q currents trend during the simulation. Being the working condition constant (always same load torque, speed and flux reference), they should be approximately linear and equal to a fixed value. In fact, the i_d current, that is directly elaborated by constant values, is always constant. But this is not true for the i_q current due to the effective λ_{srd} flux present in the IM block. How we can see in the Fig.4.7, the initial d-flux is particularly minor respect to the requested one (about 1 *Vs* respect to 1.7 *Vs*). This is due to the wrong parameters in the electric drive respect to the evolving values of the IM block, which are always constant and equal to their nominal working condition.

During the simulation, the load torque request is always satisfied thanks to i_q and λ_{srd} trends where, being one decreasing and the other increasing respectively, they compensate each other obtaining a constant torque (as showed in the equation 4.1). Resolving the torque equation (which is the 2.65) with the magnetic flux constant to 1.7 *Vs*, the respective i_q current is equal to 5.88 *A*, reached approximately at 650-700 seconds of the simulation. These values were calculated assuming to work in FOC condition.

$$m = \frac{3}{2}\, p\, \frac{L_M}{L_r}\, \bar{\lambda}_r(\uparrow)\, i_{sq}^{\lambda}(\downarrow) \tag{4.1}$$

Looking to the Fig.4.8, the classic temperature in nominal condition, about 200°*C* (473 *K*), is reached approximately at 650-700 seconds, likes for the current (5.88 *A*) and for the magnetic flux (1.7 *Vs*). This is possible thanks to the achievement of the nominal conditions of the IM, i.e. where the constant value of the parameters has been set.

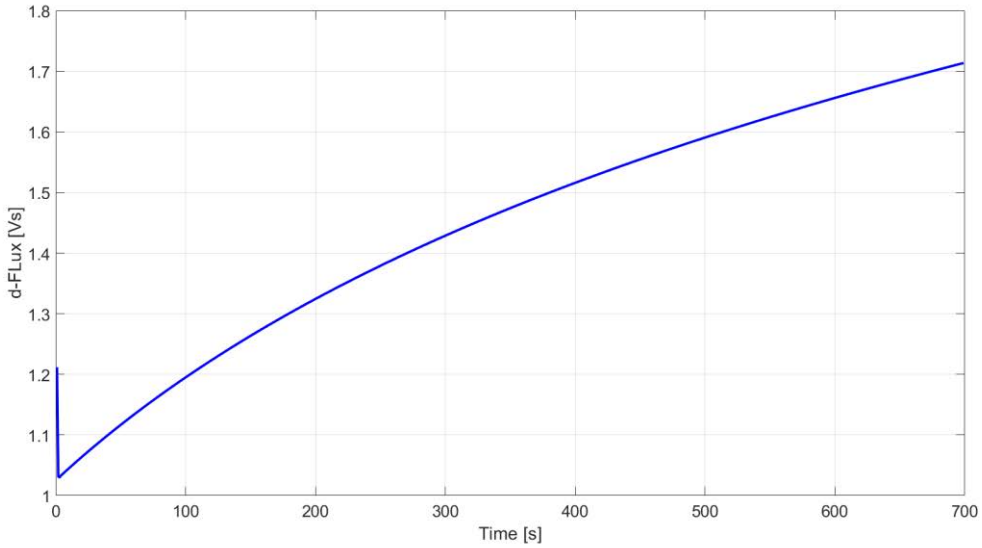

Figure 4.7: λ_{srd} flux (d-axis) elaborated by the IM

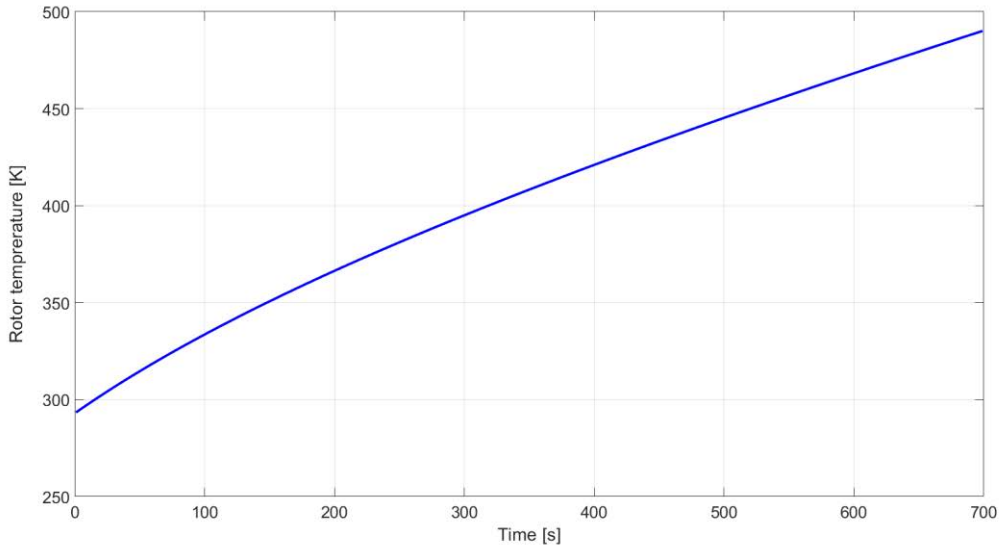

Figure 4.8: Rotor temperature trend estimated by the Digital Twin block

This means to feed the motor with values that are not correct to generate the effect that we want to obtain, i.e. the electric drive is not correctly calibrated and the IM works in different condition. This allows us to highlight how the FOC condition is reached at 650-700 second of the simulation, i.e. when the IM block is described by parameters close to the constant values present in the electric drive blocks.

An important fact that absolutely have to be presented is the peak of the i_q current in the first part of the simulation: being the maximum limit current acceptable equal to 12 *A* and the initial magnetic flux about 1 *Vs*, to satisfy the load torque demand the current could easily reach the maximum limit. For this reason, in this simulation the load torque is set with a lower value respect to its nominal condition, i.e. 15 *Nm* rather than 28 *Nm*. It is necessary to remember how this working condition is particularly rare, given how are usually present the tables of the most important parameters that describes approximatively their trend during the different working condition.

4.2.2 Variable values as input

Respecting the previous simulation, in this test all the parameters that describe the electric drive are variable and they follow exactly the one present in the IM block. In this way, the controlling scheme will be always updated with the real motor trend.

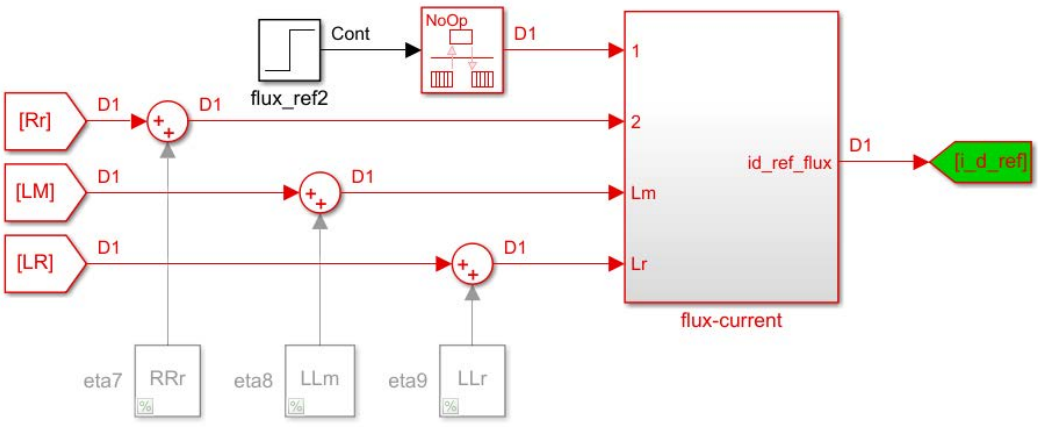

Figure 4.9: Flux block with variable parameters as input

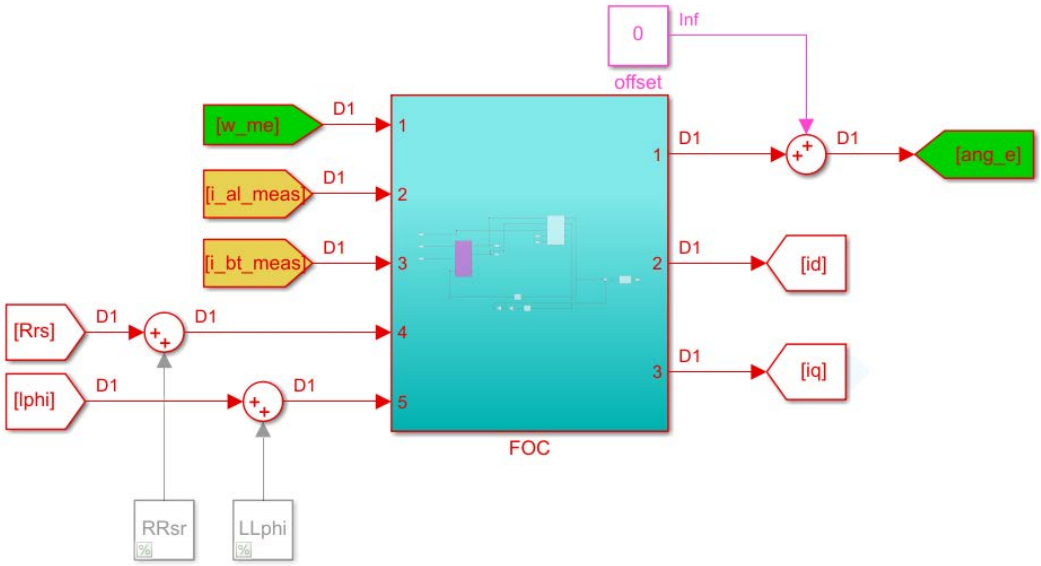

Figure 4.10: FOC block with variable parameters as input

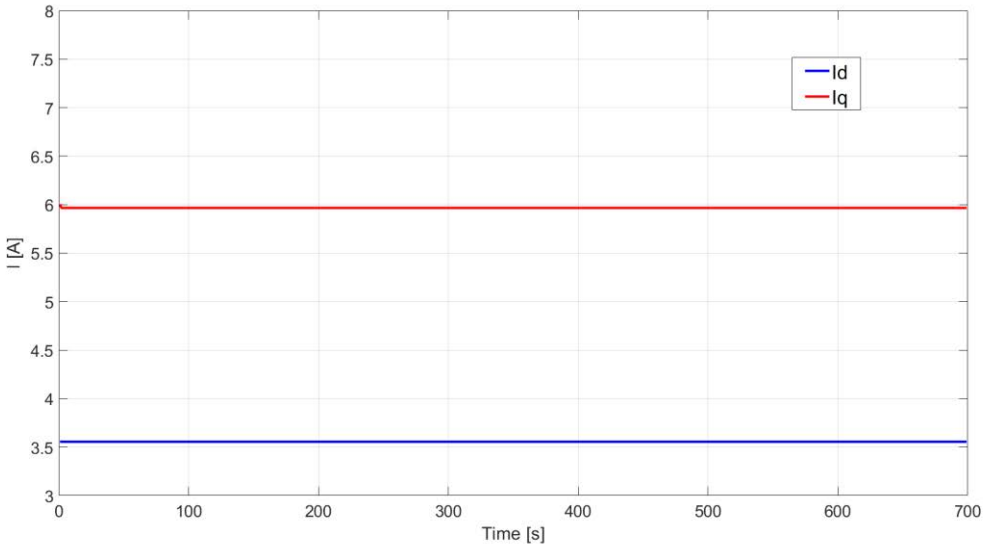

Figure 4.11: i_d (blue) and i_q (red) currents with variable values

Looking the Fig.4.11, adopting an electric drive that can continuously suit with the real motor trend, currents behaviour is not only constant during all the simulation time, but their values are lower than the previous case. Thanks to it, there is a benefit for the temperature trend too. In fact, how is showed in the Fig.4.12, in the same simulation time rotor temperature reach about 440 K (167°C), with a difference of about 45 K respect to previous simulation.

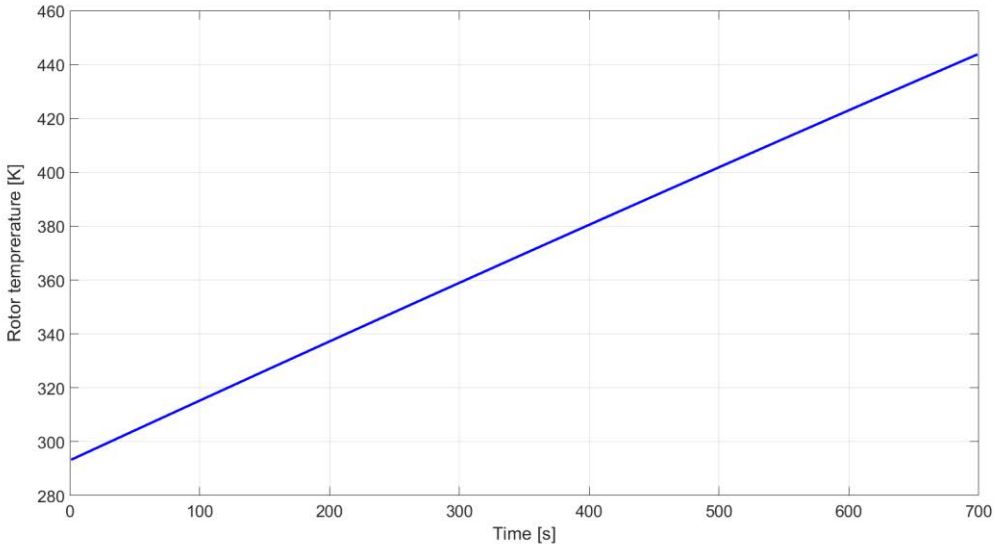

Figure 4.12: Rotor temperature trend estimated by the Digital Twin block

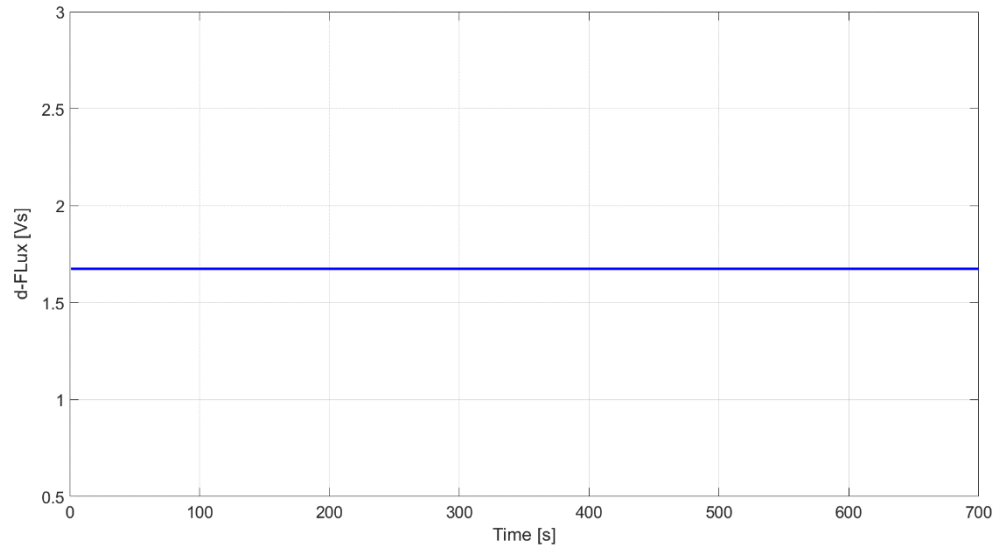

Figure 4.13: λ_{srd} flux (d-axis) elaborated by the IM

Having a controlling scheme always synchronous with motor's trend allows to correctly follow rotor flux vector, guaranteeing the efficiency of the FOC method for every different working condition. In fact, rotor flux amplitude is always equal to the request one, with a reduction due to the factor $n = \frac{L_M}{L_r}$ (≈ 0.976).

4.2.3 *L* variable and *R* constant

The next step is to evaluate which is the most important parameter that must be continuously followed to realize a reliable and faithful control of the IM. In this case all the inductance values are continuously adapted with the real IM parameters (red), while all the resistances are maintained constant as in the first simulations (pink).

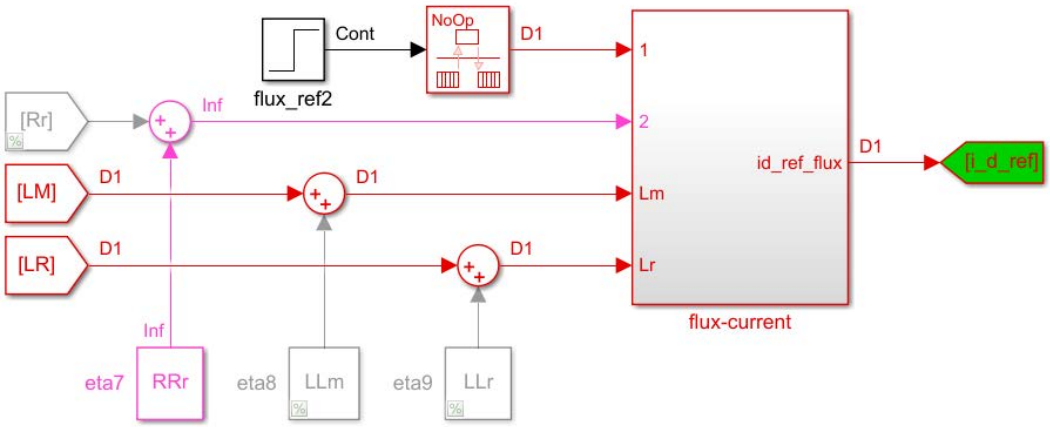

Figure 4.14: Flux block with *L* variable and *R* constant values as input

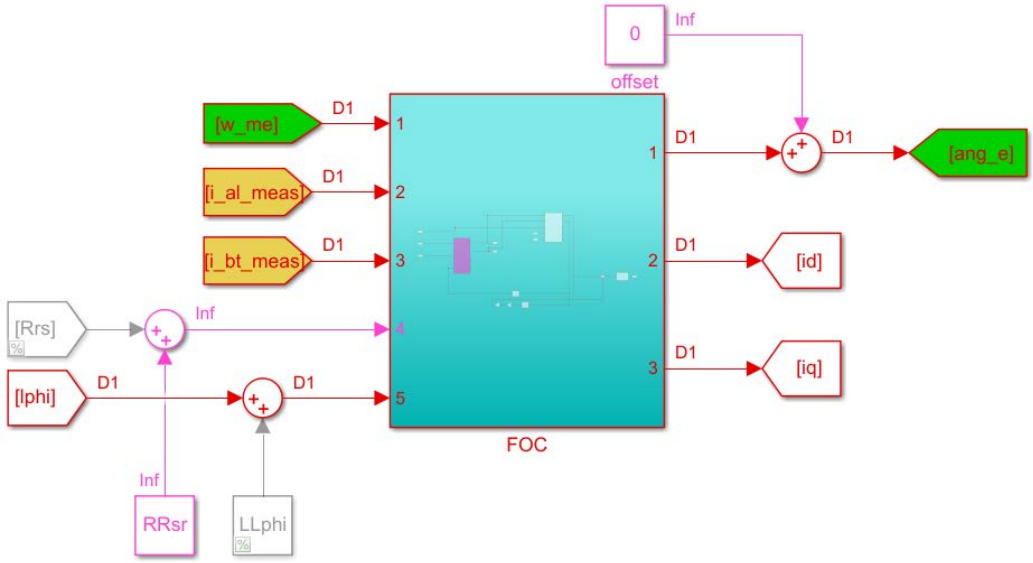

Figure 4.15: FOC block with *L* variable and *R* constant values as input

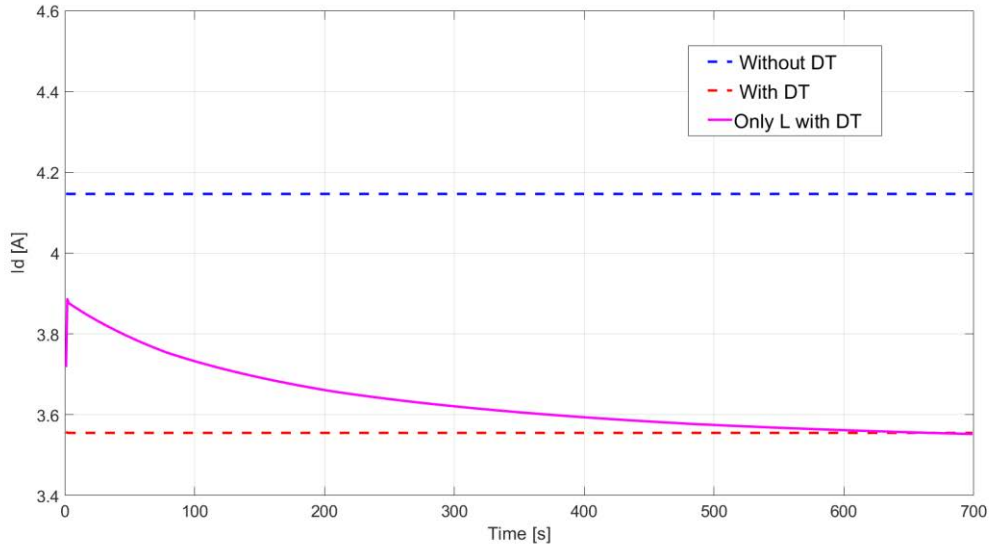

Figure 4.16: i_d trend with *L* variable and *R* constant values as input

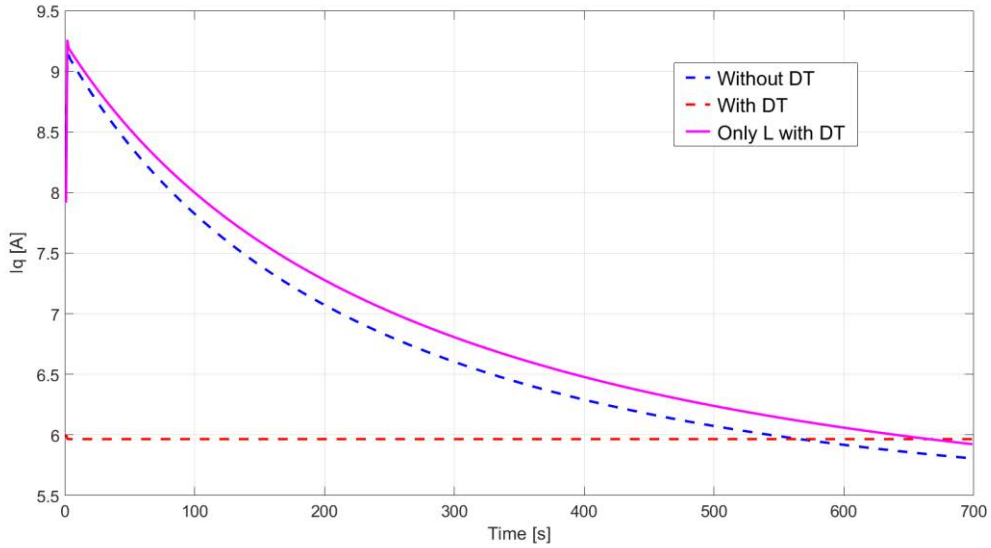

Figure 4.17: i_q trend with *L* variable and *R* constant values as input

Looking to the Fig.4.16 and Fig.4.17, currents trend is particularly useful to better understand the influence of the parameters. The i_d current is directly connected to the d-flux trend due to the flux-current block and, looking to the Fig.4.18, it is possible to observe how the correct knowledge of the L values trend is not enough to reach the FOC condition for every working status. Respect to the first situation, with all constant parameters (blue dotted line), it starts from a lower value (about 3.9 *A*) and decreases until the nominal value is

reached. This is due thanks to the possibility of the flux-current block to better follow the IM trend but, not being in FOC working condition until the end of the simulation, is not constant as in the second simulations (where all the parameters have variable values).
The i_q current follows the same trend of the constant parameters simulation (blue dotted line) due to the effective rotor flux, which is not constant as the requested one and it reach its nominal value only when the control is in FOC condition, i.e. temperature is close to 200°C.

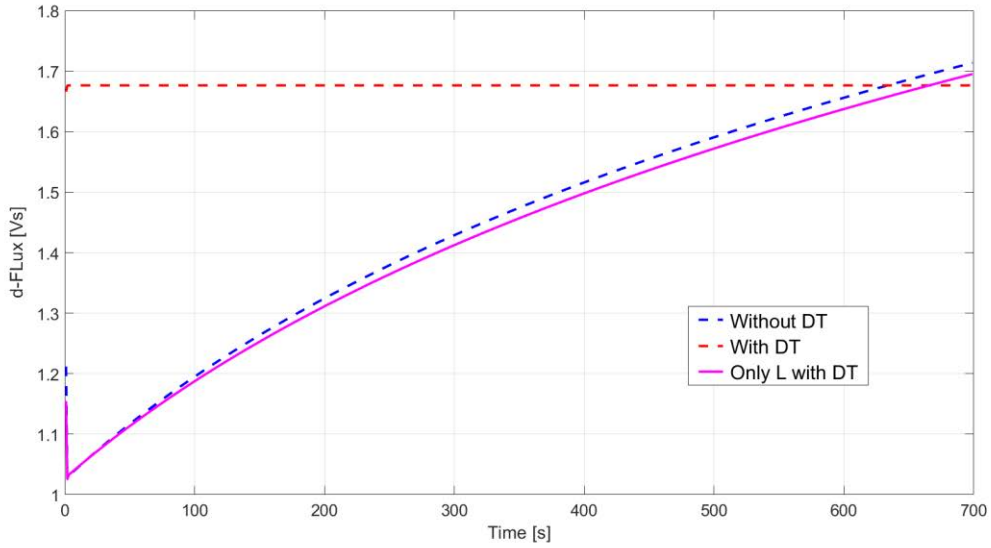

Figure 4.18: λ_{srd} flux (d-axis) trend elaborated by the IM block with *L* variable and *R* constant values as input

Adopting this kind of solution is useful only to better adequate the i_d current necessary to obtain the magnetic flux, reducing its mean value during the upcoming condition until the nominal conditions are reached. As for the conditions of FOC, this is not enough useful and it is not possible to observe any particular advantages to adopting this kind of solution.

4.2.4 *R* variable and *L* constant

As in the previous simulation, the aim is to evaluate which is the most important parameter that must be continuously followed to realize a reliable and faithful control of the IM. In this case all the resistance values are continuously adapted with the real IM parameters (red),

while all the inductances are maintained constant as in the first simulations (pink). Being resistance values particularly depending on temperature trend, one would expect to see a better behaviour of the FOC situation of the control.

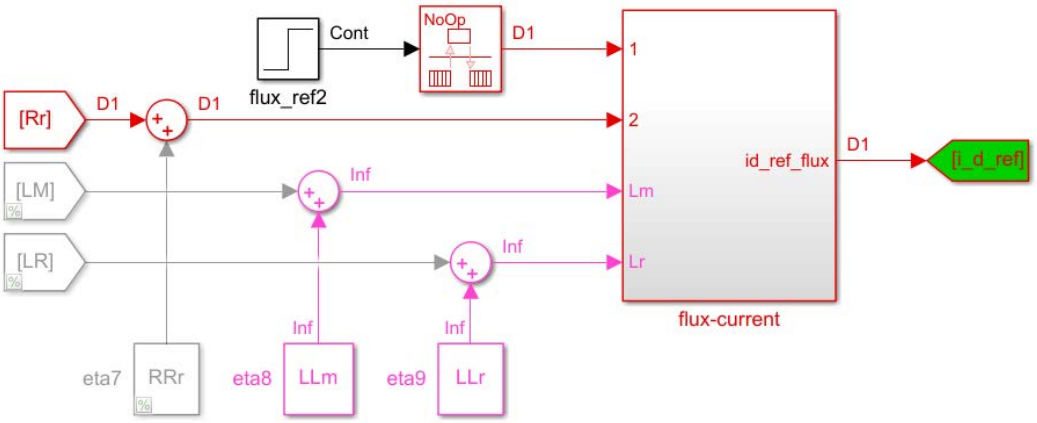

Figure 4.19: Flux block with *R* variable and *L* constant values as input

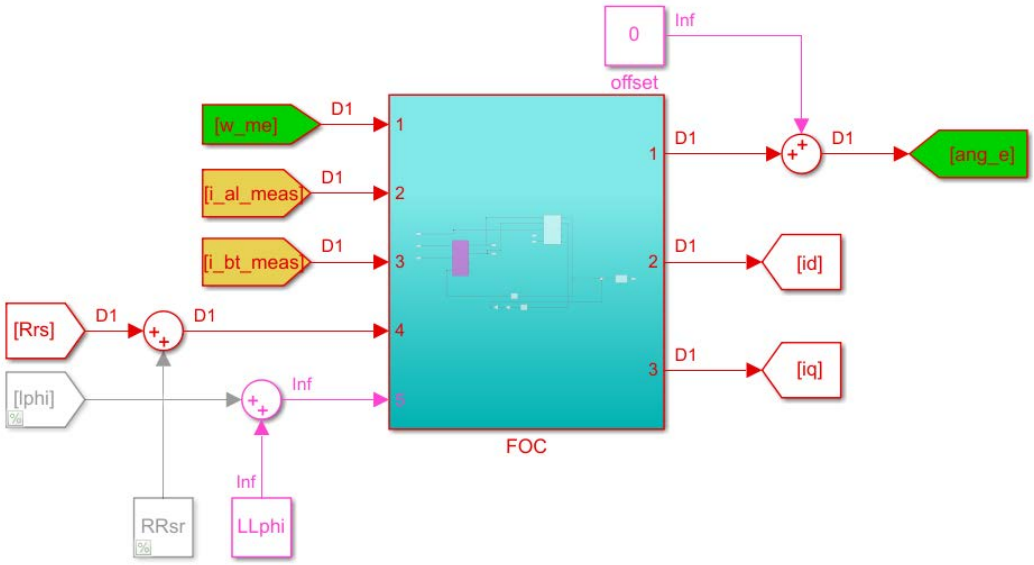

Figure 4.20: FOC block with *R* variable and *L* constant values as input

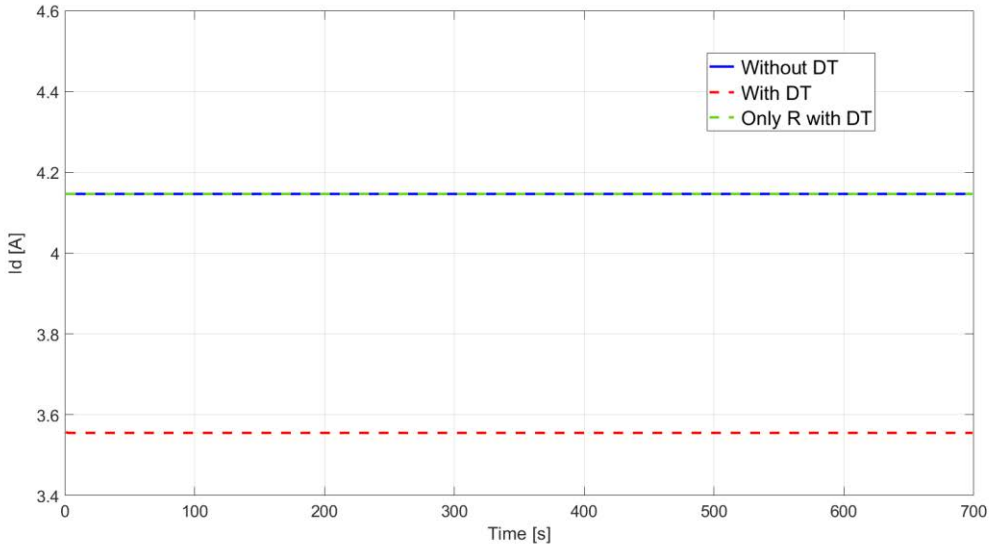

Figure 4.21: i_d trend with *R* variable and *L* constant values as input

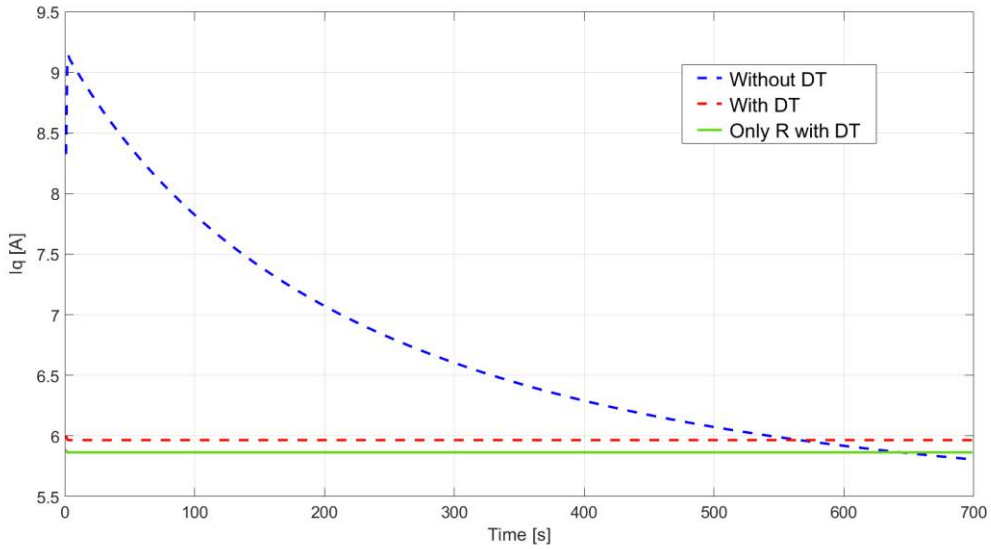

Figure 4.22: i_q trend with *R* variable and *L* constant values as input

How it is possible to observe in the Fig.4.21, the exact knowledge of the resistance values for the flux-current block is not useful due to its high depending of the inductance trend. For this reason, looking only to the flux-current block behaviour, one can assume that the important parameter that must be followed are the inductance, while the knowledge of the resistance value is not particularly necessary.

On the contrary, as far as the current i_q, this simulation demonstrates how it is very important to follow resistance values to fit the best FOC condition is possible. In fact, looking to Fig.4.22 and Fig.4.23, flux and current are always constant and close to their nominal values.

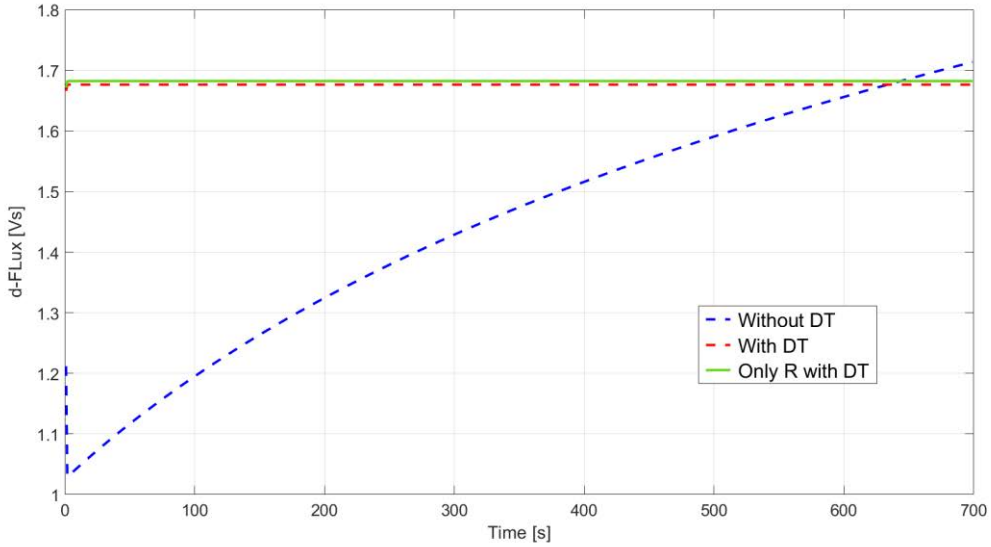

Figure 4.23: λ_{srd} flux (d-axis) trend elaborated by the IM block with *L* variable and *R*

This allow to make the first important comments: looking to best FOC condition, it is necessary to know as much as possible the variation of the rotor resistance rather than the inductance trend. This can be explained remembering how, during the first period, temperature value starts from ambient condition (assumed 20°*C* – 293.15 *K*) until reaching the classic IM working condition (usually, 200°*C* – 473.15 *K*). Resistance value is directly depending on the resistivity of the material, which changes during the temperature range.

4.3 Simulation results

Thanks to these simulations, it is possible to make some important observations about the advantages of using Digital Twin in parallel with the classic electric system. In the first place, an electric drive which is not adapted with the real motor's behaviour leads to working in not efficiency condition and, until temperature trend is far respect the classic nominal situation, could not be possible to deliver the demanded load torque. As we can see in the

previous chapter 4.2.1, the d-flux module not corresponding to the required one (1 *Vs* respect to 1.7 *Vs*), which is gradually reached only when temperature is close to that where the constant parameters have been evaluated. This means starting with a higher i_q current to satisfy the torque request, with the possibility of leading to the critical condition of easily reaching the current limit (12 *A*). In fact, in these four simulations load torque was set to 15 *Nm* and not to 28 *Nm*, for which the engine was designed.

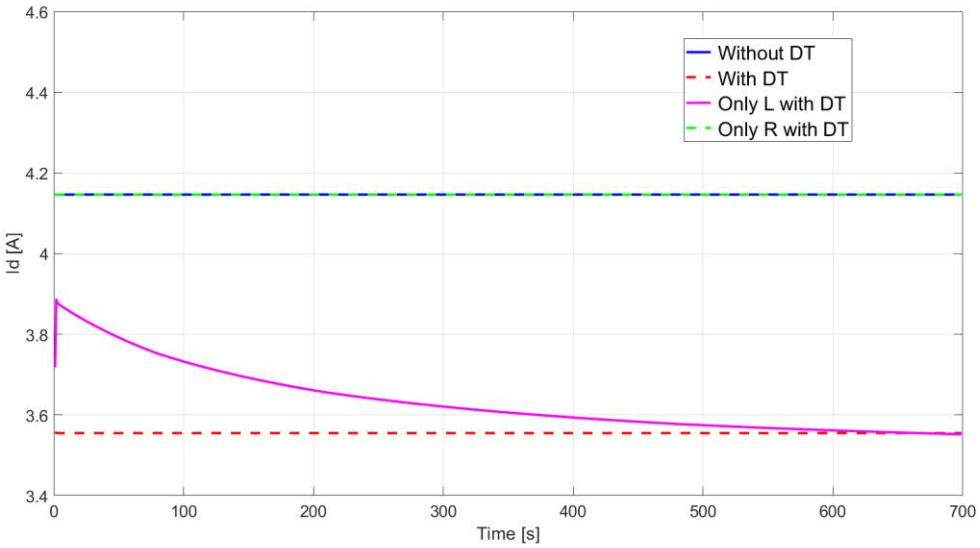

Figure 4.24: i_d current trend in the different simulations

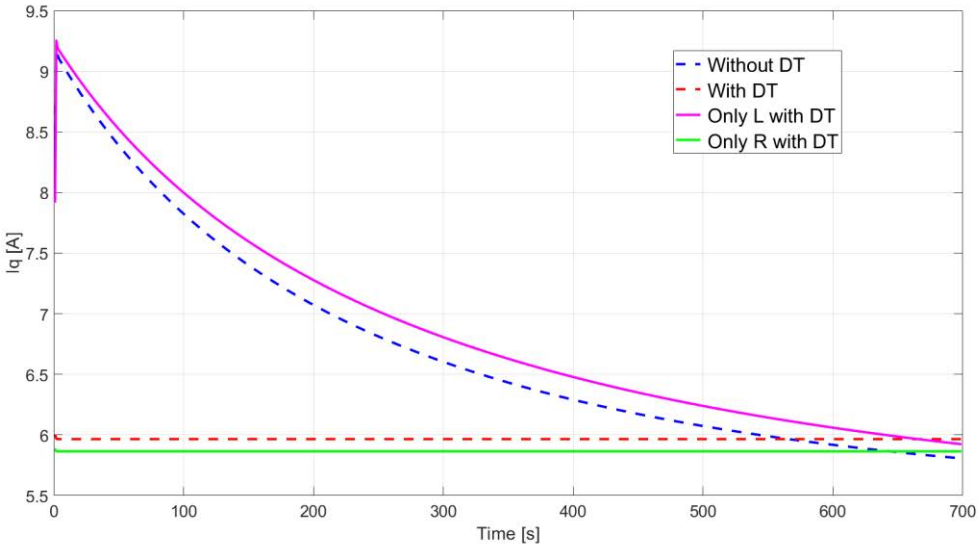

Figure 4.25: i_q current trend in the different simulations

In this context, it is useful to remember how this particular working condition are rare to find in the real application, where a kind of table of the principal parameters is present to fit approximately motor behaviour. In fact, looking to the simulation 4.2.2 (i.e. with al variable parameters) all the requested references are satisfied in any working condition, also resulting in a decrease in current consumption. In this way, at the same time the increase in temperature is lower than the previous simulation.

Simulations 4.2.3 and 4.2.4 are useful to better understand which is the importance of the trend estimation of the singular parameters. The two blocks where we changed motor's values respond in different way: The FOC block is particularly sensitive to the temperature trend, so to the resistance changing value. This is because inductance trend is depending particularly from current variation, but always maintaining a deviation from its nominal value not very large (for example, in the first simulation L_{φ} constant value is 0.40 H, while the DT trend estimation reach its maximum at 0.417 H). Instead, from 20°C to 200°C resistance is subject to a variation range particularly important, starting from 1.65 Ω and reaching 2.92 Ω. How it is possible to observe in the chapter 4.2.4, following resistance trend allow to the electric drive to follow almost the real flux position, i.e. FOC working condition.

As far as flow-current blocking is concerned, the situation is the opposite. Being magnetic flux highly dependent from inductance values trend, with variable resistance in the flux-current block the reference d-current is evaluated likes in the first simulation (4.15 A).

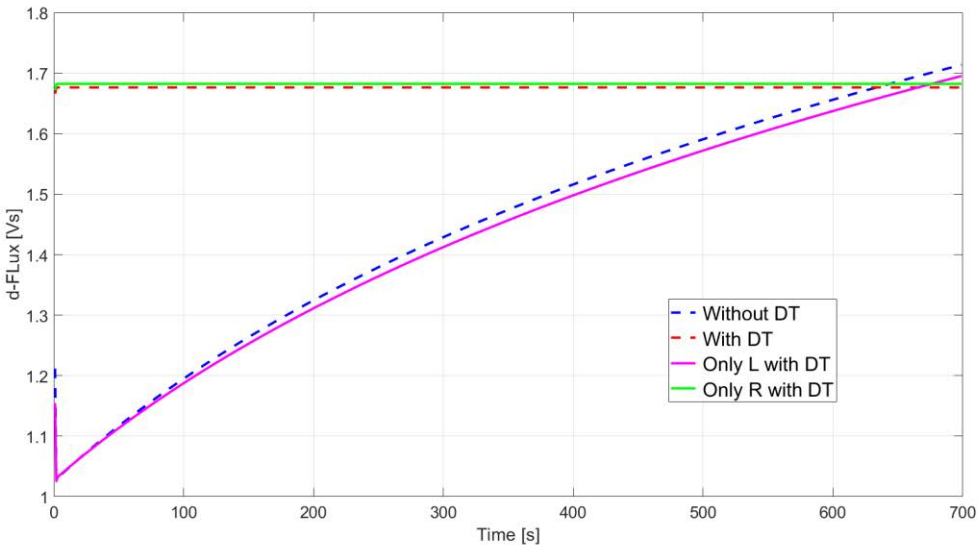

Figure 4.26: λ_{srd} flux (d-axis) trend elaborated by the IM block in the different simulations

This allow us to make the first conclusions: the FOC block needs to follow with higher accuracy resistance value (R_{rs}) to better fit with the real IM magnetic flux vector position and guarantee the FOC working condition in the different situations. In fact, setting the real load torque request (28 Nm), there is no problem to maintain everything under control. Instead, flux-current block is described by the opposite dependence, i.e. it is particularly sensitive by inductance variation than the resistance. Looking to the different simulations, it is possible to assume that d-flux trend depends on FOC circumstance, so by an accurate knowledge of the resistance value (R_{rs}). Inductance values must be particularly accurate in the flux-current block, where the i_d reference current is evaluated with a smart value, i.e. the minimum necessary to obtain that required flux. In this way, the motor is excited with the effective required current and it is not over- or under- powered than necessary.

Another useful observation is given looking to voltage trends: as it is possible to see in the Fig.4.27, U_d suffers from a non-linear growth (blue line) with constant values due to the influence of the d-q parameters, not being in FOC condition. Instead, with variable elements its trend is linear (red line) and it changes only to compensate the growing effect of the resistive voltage drop, caused by the resistance variation trend due to the increasing temperature. These observations can be done for U_q too.

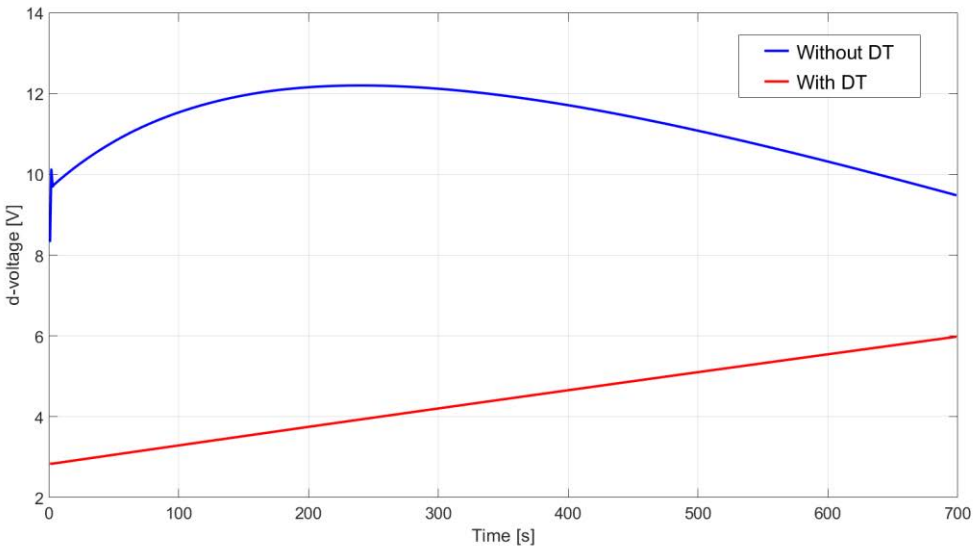

Figure 4.27: U_d voltage trend with constant and variable values

4.4 Simulation with variable load torque

To better observe the advantages of using the Digital Twin of an IM on the drive behaviours, the next simulations are realized as in the chapter 4.2.1 (all constant values) and 4.2.2 (all variable values), but with a different load torque request. Simulation scheme are the same of Fig.4.4 and Fig.4.5 for constant values, while Fig.4.9 and Fig.4.10 for the variable one. Flux reference is always set to its nominal value (1.7 *Vs*) and the reference speed is 20 *rad/s*. Simulation time is of 1800 seconds, being it the duration of the load torque evolution.

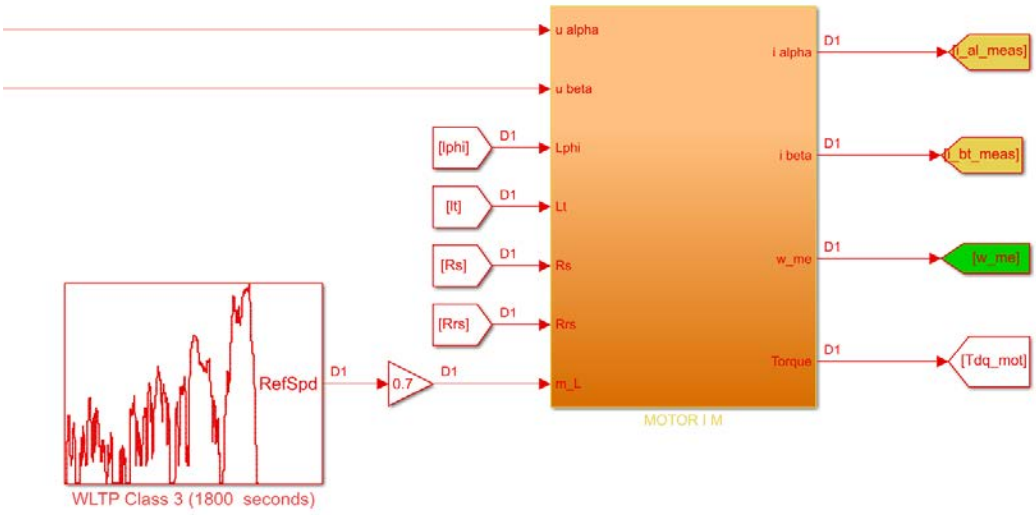

Figure 4.28: IM with variable load torque

As is showed in the Fig.4.28, the only difference is given by load torque trend, which represented by a WLTP speed reference engaged only by its numerical trend and not with the real output meaning. It is also reduced by a factor of 0.7 to better match the engine characteristics.

Looking to the Fig.4.29, if constant values are set as input of the flux-current block, the i_d reference current that being evaluated is always constant (blue line). Instead, adopting the variable parameters that have been evaluated by the Digital Twin, current value (red line) is always adapted to better follow the real motor behaviour, guaranteeing everywhere and in every condition the requested flux, as is showed in the Fig.4.32. How it is possible to observe, i_d mean value is particularly lower than the constant one.

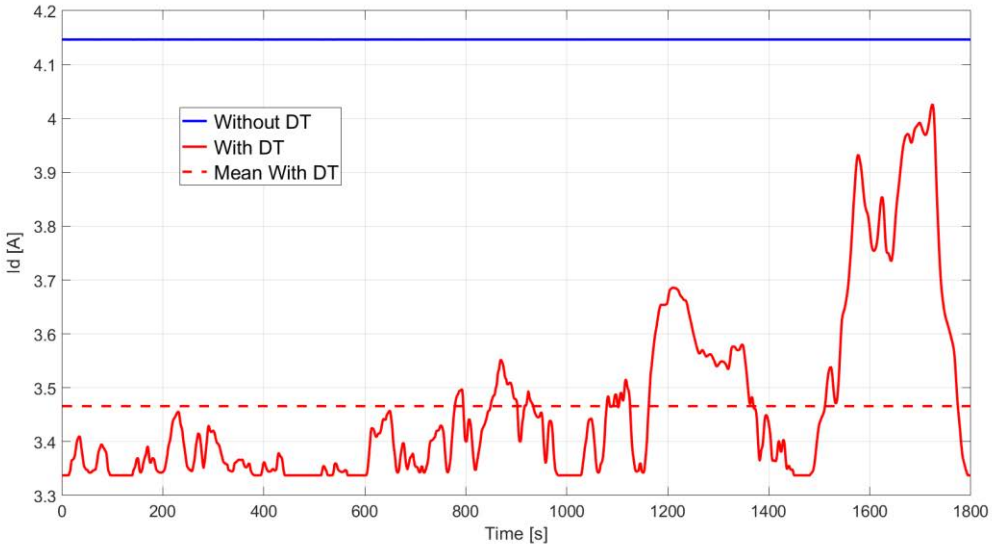

Figure 4.29: i_d current with and without Digital Twin

This last aspect is not true for the i_q current too. In fact, as is showed in Fig.4.30, the mean value of the current obtained with variable parameters (red line) is higher respect to the constant case. This fact is due to the variable load torque trend respect to the constant flux delivery and, to guarantee the balance of the system, i_q current must change continuously. And this can be lower or, as in this case, higher respect to the constant situation.

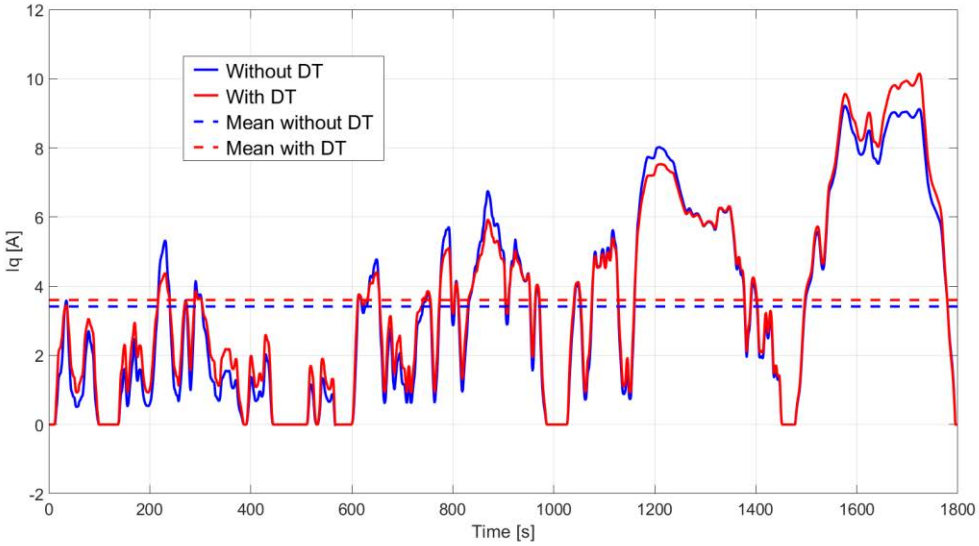

Figure 4.30: i_q current with and without Digital Twin

Looking to the temperature trend in the Fig.4.31, being the mean value of the i_d particularly lower respect to the constant case, the total absorbed current is minor (5 *A* respect to 5.37 *A*). Being less current, this leads to a lower temperature growth and, as a result, less power is dissipated due to the Joule effect.

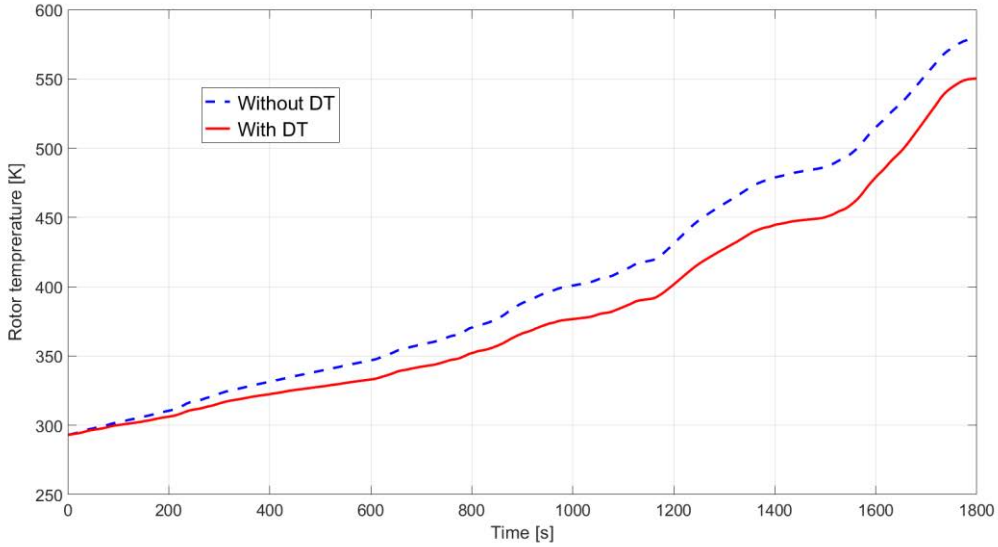

Figure 4.31: Rotor temperature increasing trend with and without Digital Twin

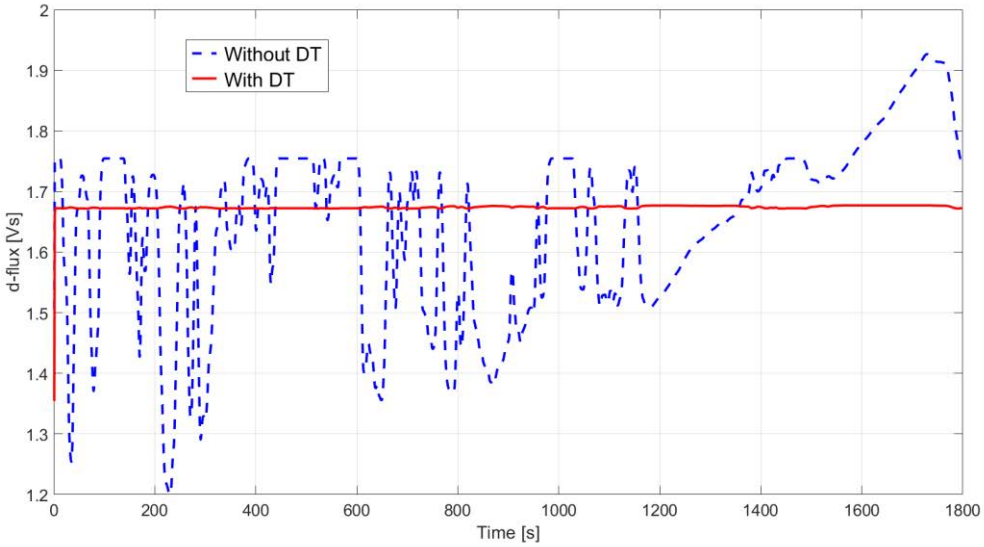

Figure 4.32: λ_{srd} flux (d-axis) trend elaborated by the IM block, with and without Digital Twin

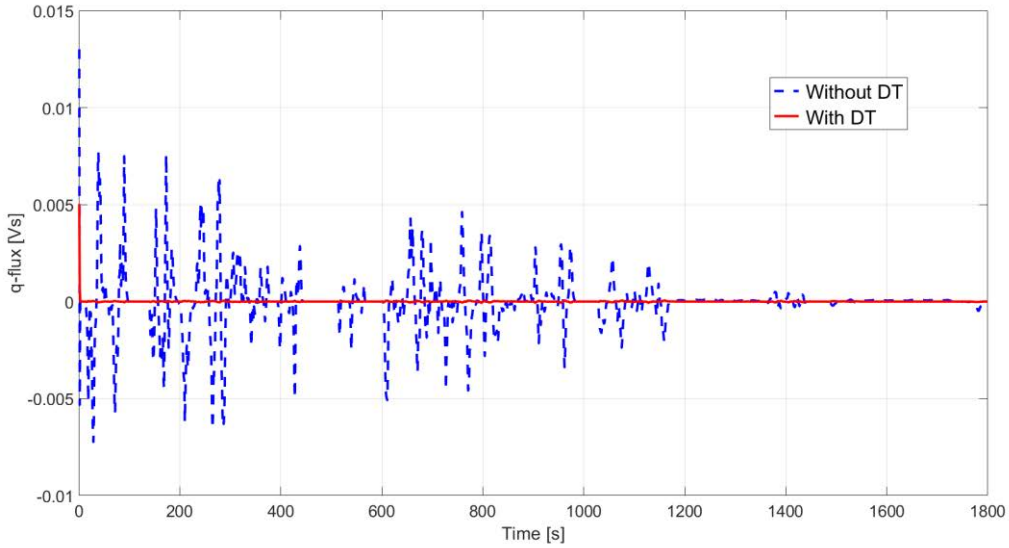

Figure 4.33: λ_{srq} flux (q-axis) trend elaborated by the IM block, with and without Digital Twin

Looking to Fig.4.32, adopting a Digital Twin in the electric drive behaviour allows to maintain the demanding flux always constant. This fact is true thanks to the FOC trend, which is always guaranteed. As it is possible to observe in the Fig.4.33, the λ_{srq} flux (q-axis) trend is close to zero in every condition. With constant parameters, its value is not particularly big, but its trend is significantly disturbed, causing the loss of the FOC condition. This last simulation is an additional confirmation of the advantages of using a Digital Twin of the motor in the electric drive behaviour, obtaining a more reliable and secure control being able to follow the real motor dynamics. In this way, it is also possible to guarantee the necessary working condition to properly follow the demanding circumstance.

4.5 Predictive Twin

Digital Twin is a high capability technology that can be developed for different application according to a precise aim. In the previous simulations, it was developed to follow electromagnetic and thermal behaviour of an IM during its different working condition, instant by instant.

In many industrial applications, EMs can work for many hours without never stopping or changing its working condition. In this context, a Digital Twin can show other advantages: taking the thermal model inside the Digital Twin block (Fig.4.34 red square), it is possible to adapt its calculation trend so as to get a prediction of the future IM parameters conditions after a desired time. This modified block is so called Predictive Twin and it is represented by a green square. This is possible thanks to an easy shortening where, instead of calculating the variation for every step, the temperature trend is extended until a desired time.

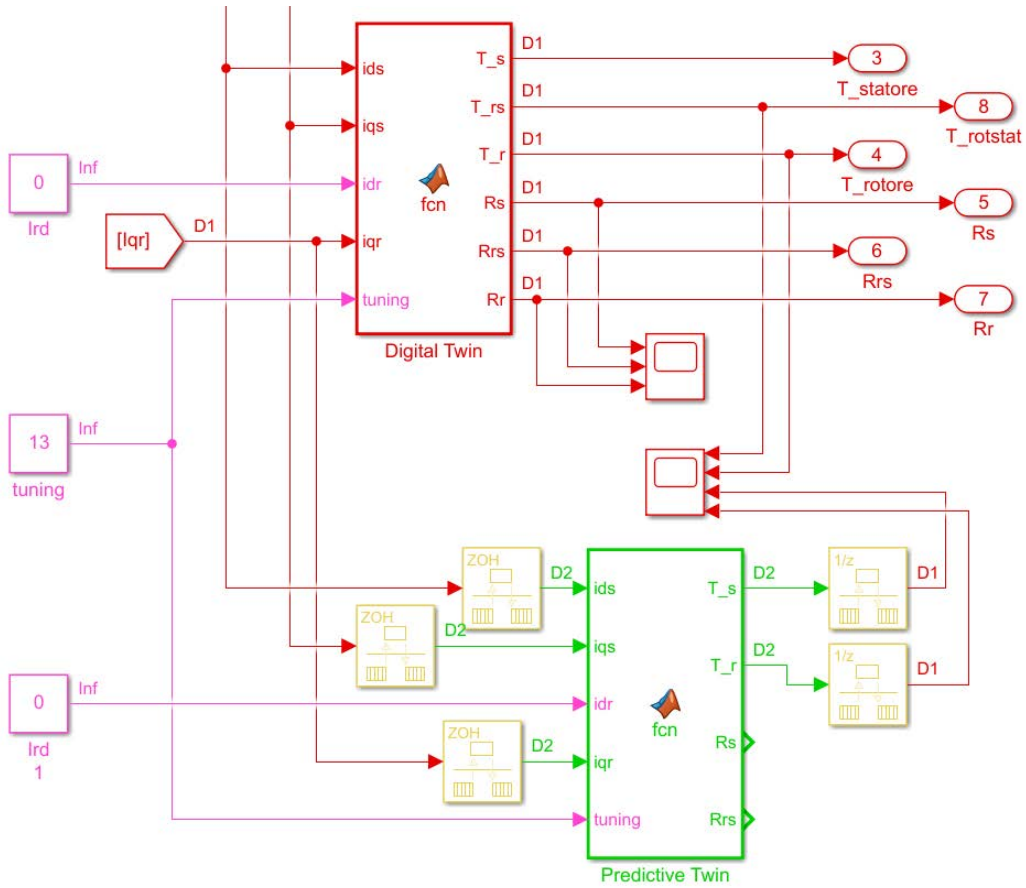

Figure 4.34: Thermal and predictive twin models inside the Digital Twin block

For example, in this application the Predictive Twin aim is to estimate which will be temperature and resistance values at 700 seconds, with constant load torque (15 *Nm*) and rotation speed (30 *rad/s*) requirements. To have a more accurate estimation, the electric drive has been modified with all the parameters variable evaluated by the principal Digital Twin block. In this way the simulation results will be the same of the chapter 4.2.2.

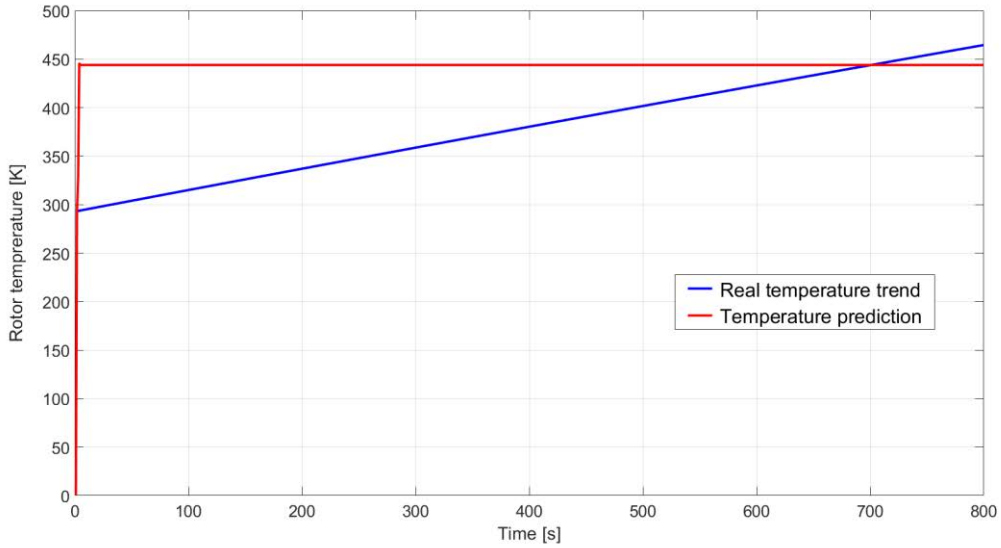

Figure 4.35: Rotor real temperature trend (blue) and its prediction (red) at 700 seconds.

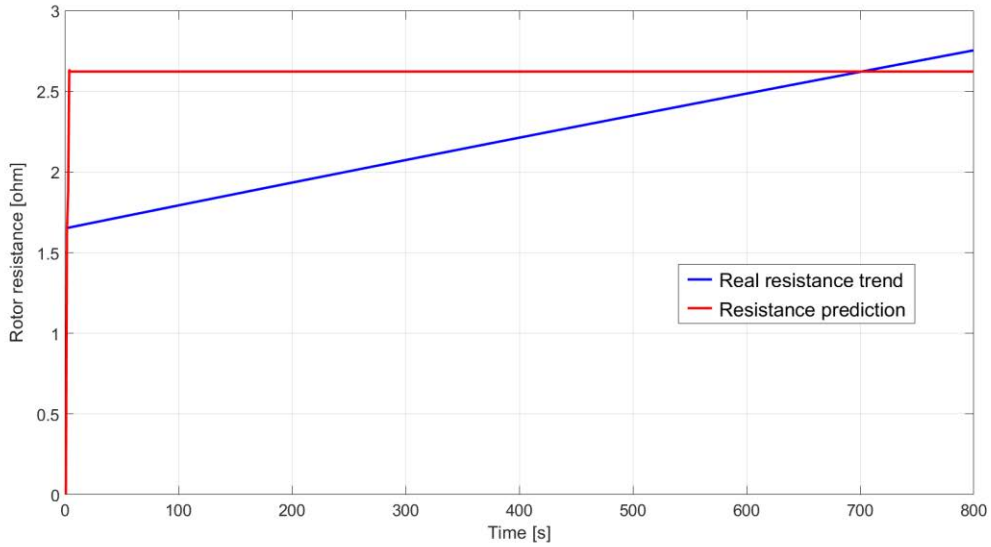

Figure 4.36: Rotor real resistance trend (blue) and its prediction (red) at 700 seconds.

As it is possible to observe in the Fig.4.35 and Fig.4.36, temperature and resistance prediction are particularly accurate e reliable, intercepting the real value at the desired time. Another important aspect is the speed with which it can predict the value: as showed in Fig. 4.37, in only 3 seconds the Predictive Twin is able to evaluate with precision which will be the temperature, and consequently the resistance, at 700 seconds. But, if the system needs to know about the final value in less time is possible, in just 2 seconds there is already a good

estimation. The blue line seems constant because of the little window of time represented, but its real trend is the one showed in the Fig.4.35.

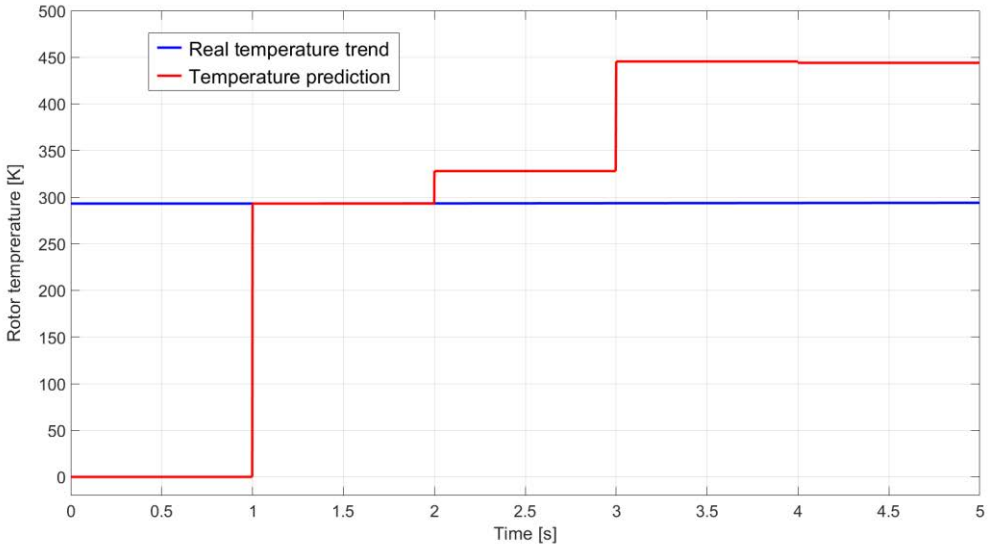

Figure 4.37: Required time to evaluate rotor temperature at 700 seconds (red)

But what are the advantages of using this type of Predictive Twin? As has been said previously, if the working condition are constant and stable for long time it is possible to estimate which will be the future temperature and, so, the parameters trend. Thanks to it, the cooling system can be preventively adequate and/or activated only when really necessary.
Another possible application is the torque estimation where, only by reading i_d and i_q currents, it is possible to evaluate which should be the load torque. This is possible thanks to the Look Up Table (LUT), where the mesh elaborated by the FEM software are reduced by a MOR, obtaining a reliable and capable system.

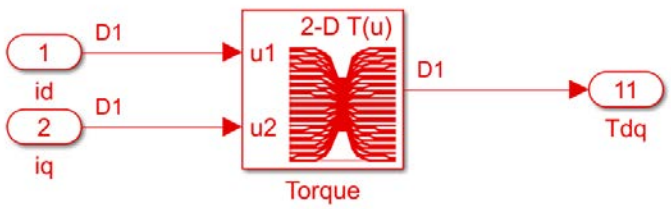

Figure 4.38: Look Up Table of the torque estimation

This is possible since the torque equation is directly described by the i_q current and the rotor flux λ_{srd}, which can be managed by the i_d current. In this way it is possible to realize a LUT that can represent the IM torque trend with different i_d and i_q trends.

Being these currents directly measured by the IM block, it is necessary to make some important observations compared to what we have seen in previous simulations: i_q current is directly dependent to the FOC accuracy and, consequently, the i_d current must be adequate to guarantee the requested flux value. This means, to get a reliable torque estimation, it is necessary to operate in perfect FOC condition for every working behaviours, so as to power the motor with the correct currents. As it is possible to observe in the Fig.4.39, if the FOC condition is not guaranteed, the torque estimation cannot be considered sufficiently reliable.

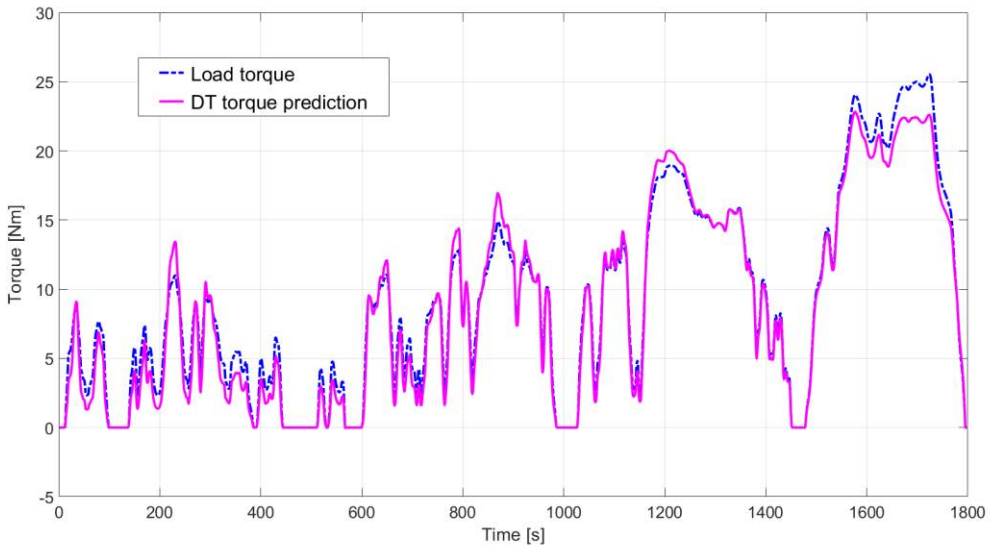

Figure 4.39: Torque prediction with constant values

Instead, if the FOC condition is always guaranteed the torque prediction is sufficiently accurate, as showed in the Fig.4.40. Numerically, it is useful evaluate the higher error of the two circumstance: with constant values (Fig.4.39), the higher deviation from the requested torque is 2.93 *Nm* at 1722 seconds, while with variable values (Fig.4.40) it is equal to 0.74 *Nm* at 1734 seconds. This second error is not small enough to consider the torque prediction absolutely reliable, but it is certainly a very good clue to evaluate its trend. To reduce the error, it may simply be necessary to make a more precise LUT.

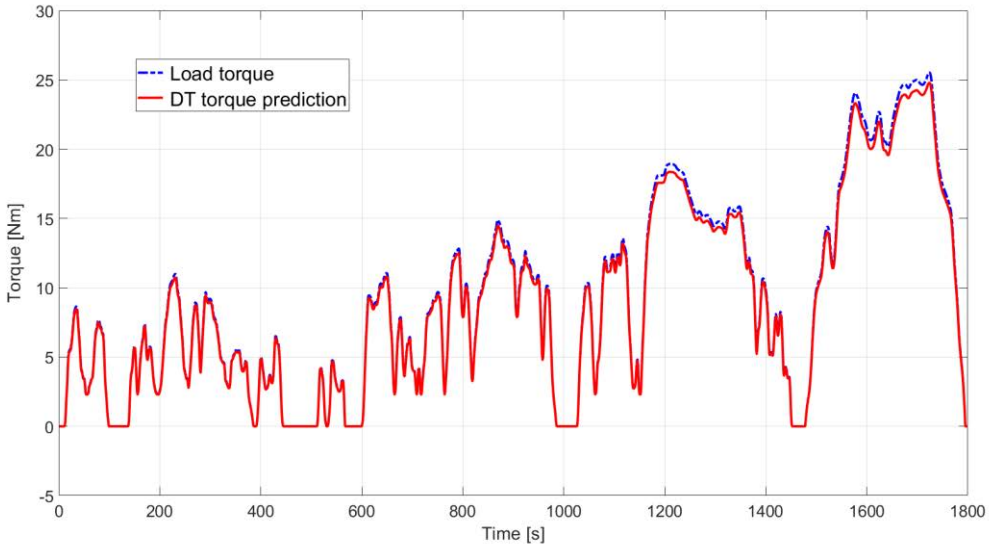

Figure 4.40: Torque prediction with variable values

Torque prediction is not useful to improve electric drive behaviour not being a retroactive torque control to adjust a possible error, but it is particularly important for safety and fault detection system. Recalling what was said in the first chapter, one of the important advantages of the Digital Twin technology is the possibility to interact with the system remotely, with continuous updates to be always performing and reliable.

Assuming to have a high-quality level of torque prediction, in the first case, by setting a maximum acceptable tolerance value of the torque error, it is possible to develop a safety-protocol to follow if this error exceeds the set limit.

Another important possible application is the fault detection system where, if the predicted torque is often different from the required one, it is possible to develop a graphic interface where to show the different warning message, according on the type of the detected anomaly. This second application is particularly advantageous thanks to its independence from physical sensor, adopting only the measured currents.

5

Practical results

To better observe the reliability of the Digital Twin technology, it is useful evaluate its behaviour in a real application. In these next pages will be shown the results obtained by Hexadrive Engineering experiment of their Digital Twin applied to an IM.

5.1 Test stand

The test stand scheme is showed in the Fig.5.1 and it composed by:

- *Induction Motor* (Fig.5.3): is the motor that have been studied.
- *PMSM* (Fig.5.3): is the motor that must simulate the load circumstance, featuring with a torquemeter and a speed sensor.
- *Inverter* (Fig.5.4): Same inverters of the two motors, one is by-passed to allow the control by the dSpace (IM), while the other is in its commercial form (PMSM).
- *Variac* (Fig.5.6): autotransformer to regulate BUS DC voltage level.
- *LEM probe* (Fig.5.6): Hall effect sensor to read current's value.
- *dSpace board control* (Fig.5.5): is the way whereby the computer can interface with the physical asset to read and control the IM behaviour.
- *Computer*: thanks to Matlab/Simulink and the dSpace software it is possible to read and control all the system behaviour.

The aim is to observe the real Digital Twin behaviour in a physical asset. In the first part, has been evaluated the comparison from the electromagnetic torque given from FEM simulation, direct measurement and its DT estimation. Successively, a comparison of the temperature evaluated by the FEM simulation and the DT has been made, by placing a virtual sensor where desired.

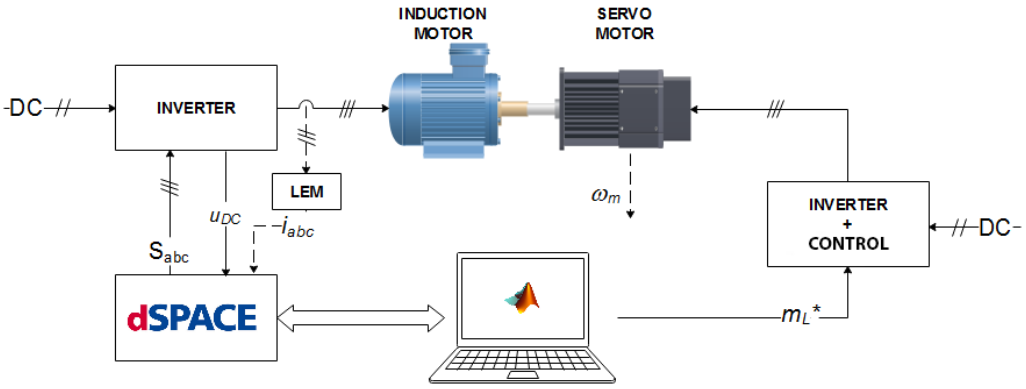

Figure 5.1: Scheme of the test stand

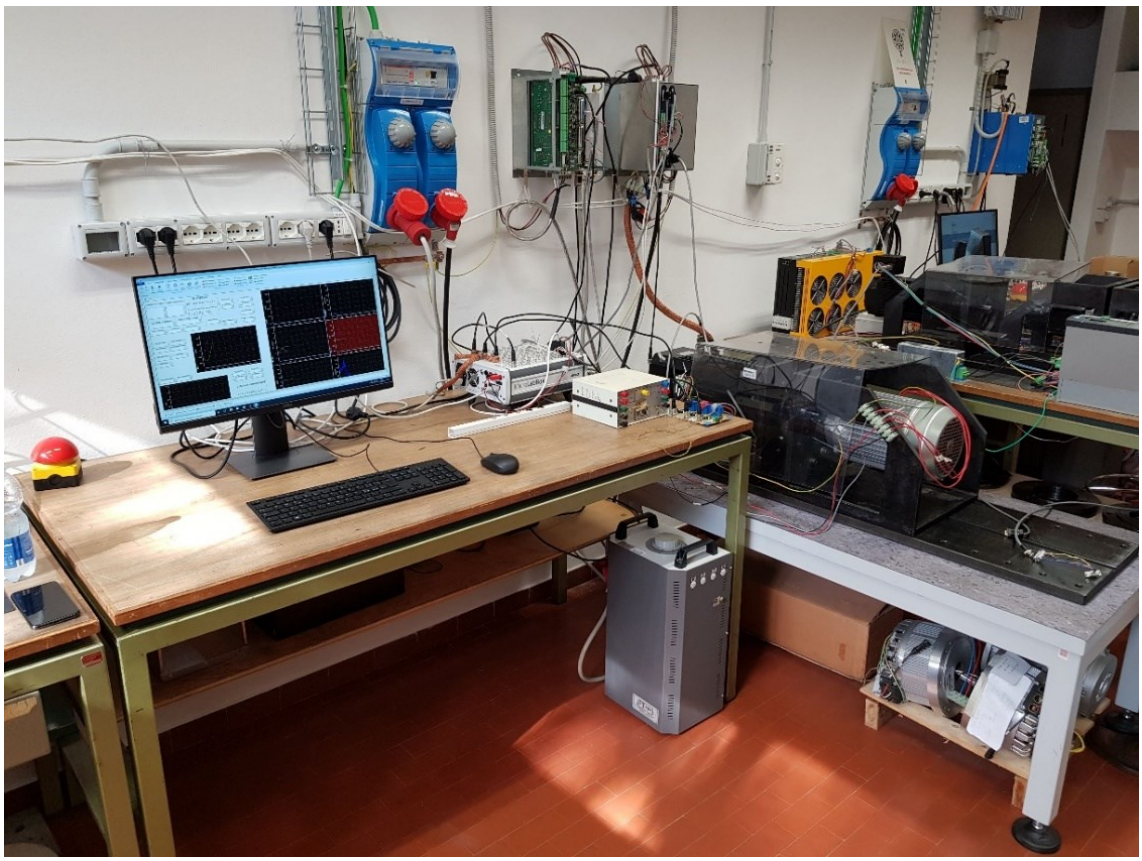

Figure 5.2: Overview of the test stand

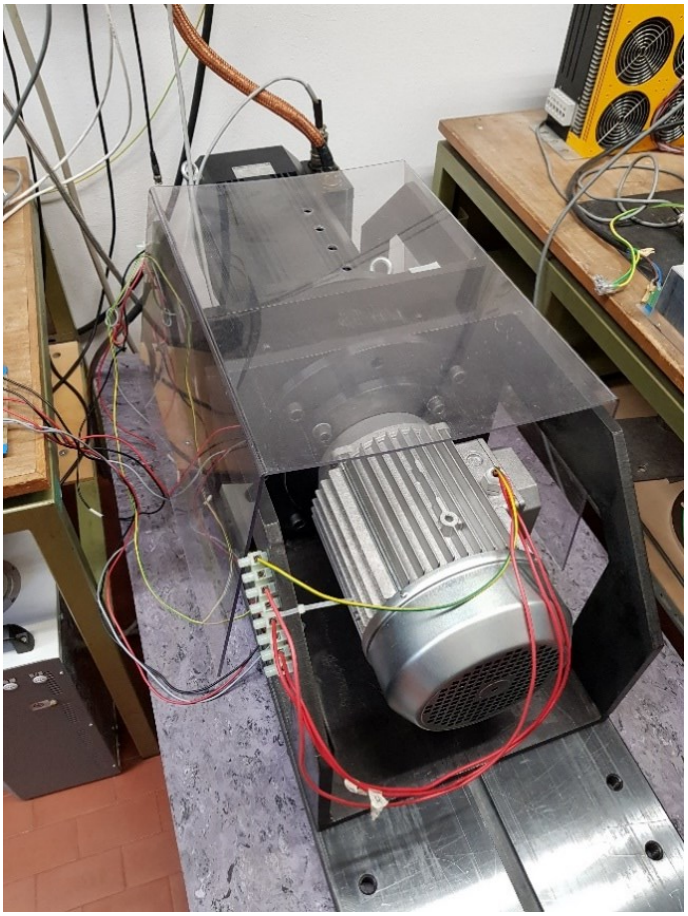

Figure 5.3: Induction Motor and PMSM

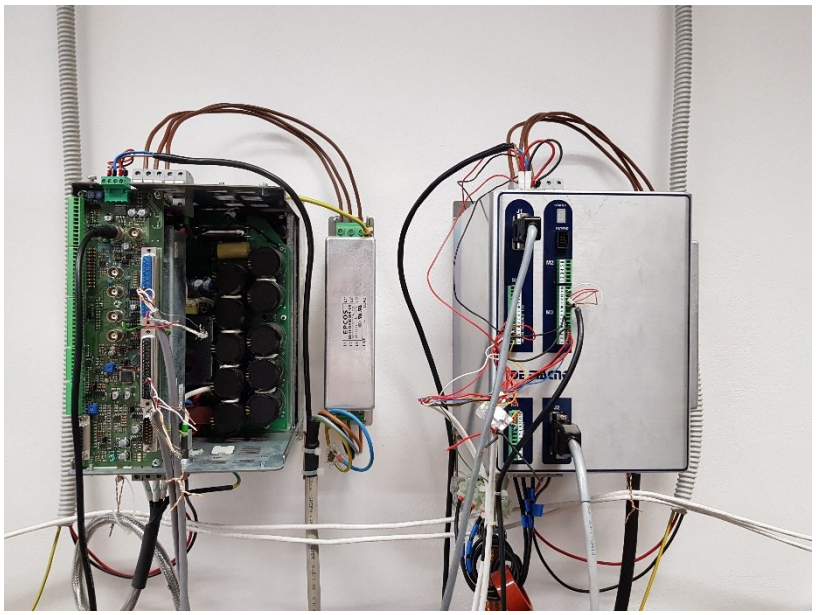

Figure 5.4: Same inverters of the two motors, on the left is by-passed to allow the control by the dSpace (IM), while in the right is its commercial form (PMSM)

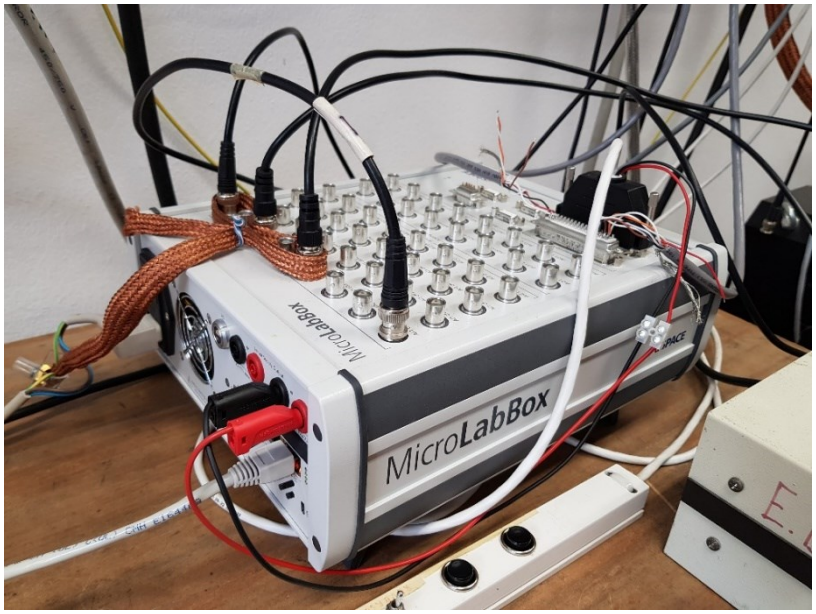

Figure 5.5: dSpace board control

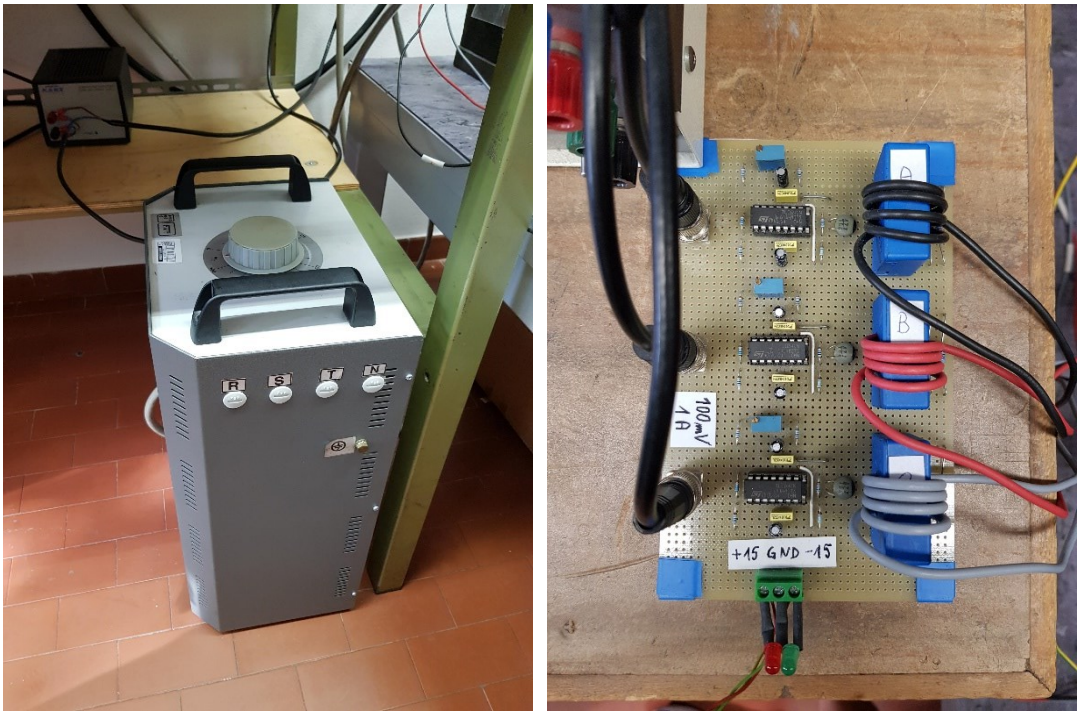

Figure 5.6: a) Variac, which regulates the BUS DC voltage level of the two inverters

b) LEM current probe (Hall effect sensor)

5.2 Test results

In their last publication [9], Hexadrive Engineering shows the results of their digital twin, which is capable to replicate the electromagnetic and thermal behaviours of an Induction Motor (IM). Starting from a FEM model, it is post-processed with the aim to making it suitable for Model Order Reduction process. Studying the right compromise in order to obtain a real-time performance, it is necessary to evaluate its accuracy comparing it with FEM model. By applying virtual sensors where necessary, with only measuring the three-phase stator currents, digital twin can simulate the three-phase stator voltages, the induced rotor currents, the generated electromagnetic torque, and all the parameters necessary for the Field Oriented Control (FOC).

Looking to its electromagnetic capability, digital twin can estimate torque and current density with high reliability. How is showed in the Fig.5.7, the electromagnetic torque estimated by it is compared with FEM estimation and the torque measured directly from the torquemeter. As can be observed, the estimate of the digital twin is equal to that of the FEM, which means that the reduced order model, obtained with MOR, has been well designed. The measurement differs slightly from the estimates because the torque in the shaft is smaller due to the mechanical losses.

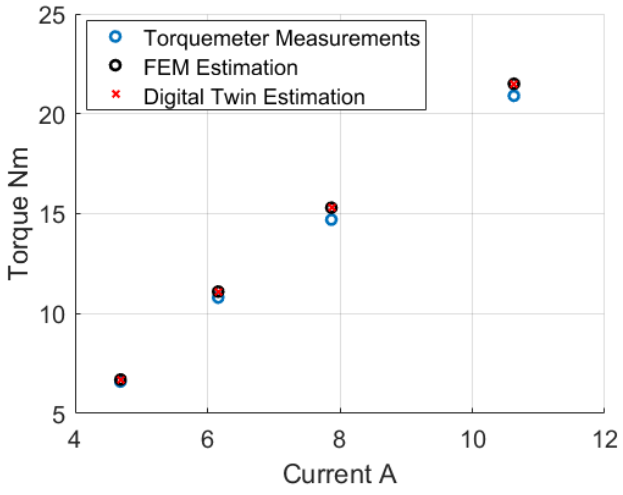

Figure 5.7: Electromagnetic torque estimation

The Fig.5.8 shows the estimated current density of the IM at a certain time during a steady-state operating condition. A real-time torque and current estimates can have multiple uses, and with FEM it is not possible to obtain real-time predictions.

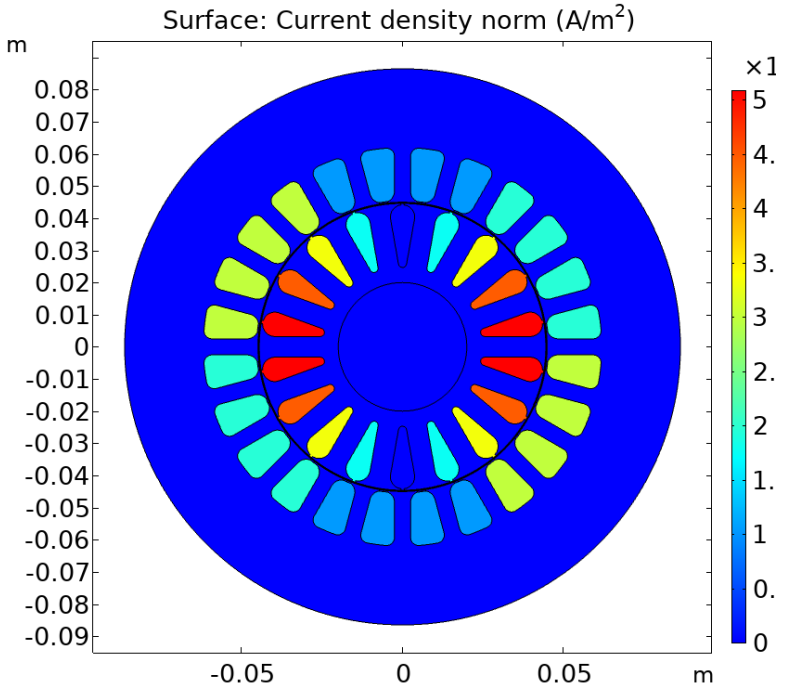

Figure 5.8: Stator and rotor current density estimation

Thermal analysis is very important because of the high temperatures can increase the probability of efficiency problems, failures and profit reduction. However, it is often not easy to measure or even estimate the temperature of EMs in general, especially in real-time. Digital Twin model can overcome this problem with a highly accurate temperature estimation of the IM, similarly to having a thermal imaging camera that can estimate temperature un real-time and also predict thermal dynamics.

Looking to the Fig.5.9, the 3D FEM model, where four temperature sensors, two in the rotor and two in the stator, are implemented to study the thermal behaviour of the IM. This figure is obtained feeding the motor for 500 seconds, and after switched off and start to cool down. It is worth noting that the estimate of the digital twin is almost identical to the one obtained by FEM, and, thanks to its reduced order model, it can predict in a few seconds the thermal behaviour of the IM over several hours of operating conditions. This feature has multiple advantages, for example, it is possible to predict the temperature of each individual rotor

point and use this information to efficiently manage the cooling system, which is generally overused because the rotor temperature is unknown, but this drastically compromises the efficiency of the IM.

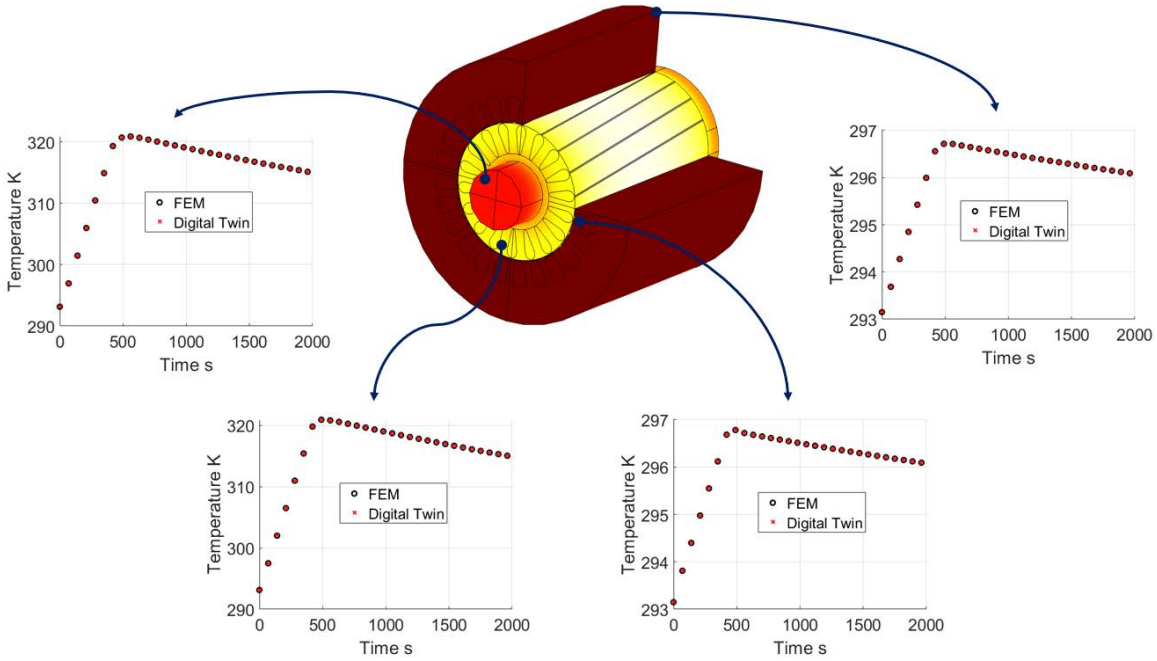

Figure 5.9: Comparison of the predictions of the thermal dynamics between FEM and Digital Twin models.

Real-time implementation capability is an important feature of digital twin concept. Looking to the Tab.1.1, the calculation time requires for an execution of 2000 seconds temperature behaviour is completely different for the FEM and the Reduced Order Model (ROM).

	Time	DoF
FEM	300 s	100000
ROM	0.1 s	11

Table 1.1: Comparison of execution time between FEM and ROM models.

In addition, the numbers of Degrees of Freedom (DoF) of FEM and ROM are sensitively different. It is evident how ROM is particularly performing thanks to its limited number of values, without any loss of accuracy.

CONCLUSION

As expected, adopting a Digital Twin parameters estimation allowed to obtain a more performing and reliable drive response, which is able to adapt to the estimated motor's parameters value step by step. In addition to improving control performance, the FOC control condition is always guaranteed, allowing to follow better the different load torque and speed requirements in any circumstance of the motor parameters.

Even if these circumstances are always guaranteed with constant values, a more performing system behaviour can be obtained by adopting the Digital Twin estimated values. Looking at the currents trend, the absorbed current in the estimated values is lower than in the constant cases, with a better adaptive drive response. In this way, a saving of the absorbed power can be achieved also getting a cost reduction and a lower stress of the electrical components.

Looking to the chapter 4.4, the demanding flux is always guaranteed and maintained constant without any ripple. This is possible thanks to the i_d current that adapts to different dynamics in every moment. Moreover, the i_q current average value is higher with variable parameter than in the constant case, due to better fitting system response.

In the chapter 4.5, it is strongly visible the potential of the Predictive Twin, making it possible either to predict the future system conditions or to improve the fault detection system by comparing real and estimated motor trends.

By observing the practical test, the reliability of the Digital Twin values estimation is absolutely guaranteed and it is true to the values estimated by FEM software. This allows us to highlight the advantages of using the Digital Twin parameters estimation used in the electric drive behaviour, getting a more reliable and secure system response to the different working conditions with the assurance of the accuracy of the estimate made by the Digital Twin.

Appendices

A. Symbols table

Quantities	Symbol	Unit of measure
Time	t	s
Frequency	f	Hz
Current	I	A
Voltage	u	V
Resistance	R	Ω
Inductance	L	H
Imaginary operator	j	-
Impedance	Z	Ω
Reactance	X	Ω
Magnetic voltage	A	AS
Magnetic field	H	AS/m
Magnetic induction	B	Wb/m
Magnetic permeability	μ	H/m
Angular speed	ω	rad el/s, rad/s
Angular speed	n	rpm
Angular position	ϑ	rad
Concatenated flux	λ	Vs
Slip	s	-
Force	F	N

Torque	m	Nm
Friction coefficient	B	Nms
Inertia coefficient	J	Nms^2

B. Superscript and subscript

Symbol	**Meaning**
a, b, c	a, b, c phase
α, β	α, β axis
d, q	d, q axis
me	Electromechanical
s	Stator
r	Rotor
i	Current
λ	Flux
0	Empty condition
el	Elemental
,s	at slip frequency
rs	Rotor to stator

Bibliography

[1] S. Bolognani, "*Appunti di Azionamenti elettrici, Capitolo 7 - Motori a Induzione"* (14/01/2014)

[2] S. Bolognani, "*Appunti di Azionamenti elettrici, Capitolo 8 - Azionamenti con motore a Induzione"* (01/01/2015)

[3] S. Bolognani, "*Appendice A - Vettori spaziali per lo studio dei sistemi trifase"* (11/10/2015)

[4] M. Guarnieri and A. Stella, "*Principi ed applicazioni di elettrotecnica*", Privo volume III edizione, Ed. Progetto Padova (2004)

[5] A. Rasheed, O. San and T. Kvamsdal, "*Digital Twin: Values, Challenges and Enablers from a Modelling Perspective*" in *IEEE Access*, vol. 8, pp. 21980-22012, 2020, doi: 10.1109/ACCESS.2020.2970143.

[6] D. Hartmann, M. Herz and U. Wever, "*Model Order Reduction, a Key Technology for Digital Twins*" in ResearchGate, doi: 10.1007/978-3-319-75319-5_8.

[7] H. Brandtstaedter, C. Ludwig, L. Hübner, E. Tsouchnika, A. Jungiewicz and U. Wever, "*Digital Twins for large electric drive trains*" *2018 Petroleum and Chemical Industry Conference Europe (PCIC Europe)*, Antwerp, 2018, pp.1-5, doi: 10.23919/PCICEurope.2018.8491413.

[8] K. Zhou, J. Pries and H. Hofmann, "*Computationally Efficient 3-D Finite-Element-Based Dynamic Thermal Models of Electric Machines*," in IEEE Transactions on Transportation Electrification, vol. 1, no. 2, pp. 138-149, Aug. 2015, doi: 10.1109/TTE.2015.2456429.

[9] F. Toso, A Favato, R. Torchio, M. Carbonieri, M. De Soricellis, P. Alotto, S. Bolognani, "*Digital Twin Software for Electrical Machines*", www.hexadrivengineering.com

[10] P. Rocco, "*Dispense di Automatica – Regolatori PID*"

[11] W. Schilders, "*Introduction to Model Order Reduction*" in ResearchGate, doi: 10.1007/978-3-540-78841-6_1.

Colgo l’occasione per ringraziare tutti coloro che mi hanno supportato, sopportato e motivato durante questi anni di università, caratterizzati da un insieme di grandi soddisfazioni e delusioni, ma sicuramente molto importanti per le innumerevoli lezioni di vita imparate.
Per la realizzazione di questa tesi ringrazio il Professore Silverio Bolognani, il correlatore Francesco Toso e i dottorandi Paolo Gherardo Carlet e Andrea Favato per la pazienza e costante disponibilità per comprendere ogni mia perplessità.